



Title: Analysis of accidental iceberg impacts with membrane tank LNG carriers	Delivered: June 14, 2010
	Availability: Open
Student: Stine Aas Myhre	Number of pages: 62

Abstract:

The probability of ship-iceberg impacts are increasing due to increasing production and due to more transportation routes near arctic areas. The first part of this thesis is an introduction to Liquefied Natural Gas (LNG) and the LNG carriers, particularly LNG carriers with membrane type cargo containment system.

Some theory regarding the principles of Non Linear Finite Element Analysis (NLFEA) and ship-iceberg collision is briefly described.

A detailed finite element model of the cargo tank is created. For Finite Element Modelling MSC Patran is used. Choice of element and element size is described. Boundary conditions are introduced to compensate for the non-analysed part of the structure. Two different iceberg models are included and the explicit NLFEA solver LS-DYNA is used for the integrated analysis. Seven different collision points are checked for the two different iceberg models.

Deformation of the inner hull is explored and checked against design criteria. Figures and graphs are included to illustrate this. Accelerations, velocity and deflection is found for some critical nodes in inner and outer hull and checked for critical values.

Keyword:

LNG carriers
Ship-iceberg collision
Finite Element Analysis, LS-DYNA

Advisor:

Professor Jørgen Amdahl



MASTER THESIS SPRING 2010

for

Stud. Techn. Stine Aas Myhre

Analysis of accidental iceberg impacts with membrane tank LNG carriers

Analyse av ylykkesstøt fra små isfjell mot LNG skip med membrantanker

The expected increase of exploitation of gas fields in Northern regions will precipitate the development of arctic LNG shipping. LNG ships carry huge amount of energy and it is vital that these ships possess adequate resistance to ice actions, so as to keep the risk of catastrophic events sufficiently low. A potentially severe risk is associated collision small icebergs (bergy bits/growlers). Large icebergs are very likely to be observed by radars installed aboard the ship or by airborne radars, but smaller icebergs may avoid detection. This implies that rare (accidental) events cannot be disregarded and must be considered in the design.

For accidental iceberg collisions use of ship classification design rules may yield overly conservative design. The rules are typically based upon elastic or plastic bending failure modes of stiffeners and plates implying small deformations. For accidental/abnormal iceberg impacts some degree of damage to the structure (side shell/frames) may be accepted, but the integrity of the cargo tank should impair, causing gas leakage to the environment and possible ignition. In the Accidental Limit State the resistance may be assessed by non-linear methods of analysis; the structure may undergo yielding, buckling and large permanent deformations on member and sub-structure level. This can only be assessed accurately if both the ship and the ice are modelled, and the interaction between the two structures is accounted for.

When dealing with numerical simulations of ship-ice interaction, there is always a search for the best suitable models for such investigations. Generally, it could be categorized as Discrete Element modelling (DE), e.g. Matlock (1971), Matlock (1969), Daley (1990), Sayed (1997) and Finite Element modelling (FE), e.g. Varsta (1983), Xiao (1991), Derradji-Aouat (2005), Gagnon (2007), Gürtner (2008). Nevertheless, it is not possible to find a conventional method to simulate the ice behavior due to complicated ice properties, which mainly depend on temperature, salinity and strain rate. A PhD-student at department of marine technology – Zhenhui Liu - approaches the ship-iceberg collision problem numerically by using the Tsai-Wu based ice material



model by an Explicit FE code. In the study, the Tsai-Wu material model turned out to be a promising candidate for calculating the ice impact loads.

Recently the Gas Transport /Technigas (GTT) cargo containment system (CCS) – the membrane tank - has become popular. The membrane tank consists of a cryogenic liner directly supported by the ship inner hull. The primary and secondary insulation system consists of 0.7 mm nickel–steel alloy carried by prefabricated plywood boxes filled with expanded perlite.

It has been maintained that the support of membrane tank directly on the inner hull as well as the smaller space between the cargo tank and the side shell make these concepts more vulnerable to iceberg collisions than e.g. carriers with spherical tanks. Further, in some Korean numerical studies very large accelerations have been reported (up to 2000g). The findings are not discussed in detail, but the magnitude of the accelerations have caused some concern that iceberg collisions may cause failure in the cargo containment system far away from the contact area, in addition the local hull damage. If this should be correct, it represents a significant drawback of membrane tanks.

The purpose of the work is to study the behaviour and resistance of Arctic LNG carriers with the membrane tank system subjected to accidental impacts. The work is proposed carried out in the following steps:

- 1) Describe the structural configuration of an LNG carrier with the membrane type CCS including the containment system itself. Acceptance criteria for the CCS shall be reviewed.
- 2) Perform a review of previous work carried out on ship-ice berg collisions with special emphasis on membrane–type CCS.
- 3) Discuss relevant impact scenarios: among others impact geometry, speed of vessel and iceberg, size and shape of iceberg.
- 4) Perform a brief review of the ice mechanics model developed by Zhenhui Liu and discuss relevant ice properties to be used in the simulations. Establish characteristic the ice–pressure relationships produced by the model
- 5) Develop a finite element model of an LNG ship structure and the iceberg for the selected impact scenario(s). The finite element model for the ship and the ice shall be sufficiently fine to capture the governing deformation mechanisms of



the ice, but still meet requirements with respect to acceptable CPU consumption.

- 6) Perform integrated analysis of internal mechanics. The kinematical/boundary conditions adopted for the study shall be discussed with respect to physical relevance. The damage and energy dissipation in the ship and the iceberg shall be documented. The displacements and acceleration levels at critical locations shall be discussed and checked against acceptance criteria established in pt 1.
- 7) The damage caused by the design impact event shall be assessed. In this context the external mechanics shall be accounted for using the algorithm developed by Zhenhui Liu. Alternatively, the critical scenarios (ice berg size, speed of vessel) causing leakage of cargo tank shall be estimated.
- 8) Conclusions and recommendation for further work.

Literature studies of specific topics relevant to the thesis work may be included.

The work scope may prove to be larger than initially anticipated. Subject to approval from the supervisors, topics may be deleted from the list above or reduced in extent.

In the thesis the candidate shall present his personal contribution to the resolution of problems within the scope of the thesis work.

Theories and conclusions should be based on mathematical derivations and/or logic reasoning identifying the various steps in the deduction.

The candidate should utilise the existing possibilities for obtaining relevant literature.

Thesis format

The thesis should be organised in a rational manner to give a clear exposition of results, assessments, and conclusions. The text should be brief and to the point, with a clear language. Telegraphic language should be avoided.

The thesis shall contain the following elements: A text defining the scope, preface, list of contents, summary, main body of thesis, conclusions with recommendations for further work, list of symbols and acronyms, references and (optional) appendices. All figures, tables and equations shall be numerated.

The supervisors may require that the candidate, in an early stage of the work, presents a written plan for the completion of the work. The plan should include a budget for the use



of computer and laboratory resources which will be charged to the department. Overruns shall be reported to the supervisors.

The original contribution of the candidate and material taken from other sources shall be clearly defined. Work from other sources shall be properly referenced using an acknowledged referencing system.

The report shall be submitted in two copies:

- Signed by the candidate
- The text defining the scope included
- In bound volume(s)
- Drawings and/or computer prints which cannot be bound should be organised in a separate folder.

Ownership

NTNU has according to the present rules the ownership of the thesis. Any use of the thesis has to be approved by NTNU (or external partner when this applies). The department has the right to use the thesis as if the work was carried out by a NTNU employee, if nothing else has been agreed in advance.

Thesis supervisors

Prof. Jørgen Amdahl
(Prof. Sveinung Løset)

Contact person at Det norske Veritas.

Håvard Nyseth

Deadline: June 14th, 2010

Trondheim, January 16, 2010

Jørgen Amdahl



Summary

Northern areas contain some of the largest natural gas fields in the world and the production is assumed to increase the following years. The gas produced in these areas can be transported by ship to gas terminals all over the world. The transportation is done by Liquefied Natural Gas (LNG) carriers with a LNG cargo containment system. LNG ships carry huge amount of energy and it is important that tanks and the ship's hull have an adequate resistance to sloshing forces and external accidental loads as iceberg impact. Bergy bits and growlers (iceberg <1000 tonnes) are the most critical as they are not displayed on at the radar and might not be observed by the ship's crew. For accidental iceberg impacts some damage to the structure can be accepted, but the integrity of the cargo tanks should not be damaged. This can potentially cause gas leakage with huge environmental impact.

In previous work done on LNG carriers-iceberg impact the conclusions are that an impact would not cause severe damage to the inner hull and potentially cause leakage. However, some of the accelerations detected are large and a concern is that these accelerations could make damage to the cargo containment system far away from the contact point.

Different iceberg geometry simplifications are suggested by DNV and a spherical shape is used to simulate an iceberg in this thesis. The collision point is assumed to be in the middle of a cargo tank, perpendicular to the side of the ship.

A finite element model of a ship side has been created and analysed for 7 different impact locations with two different iceberg models. The final number of elements for the ship structure is more than 256 000, with an element size of 250 mm. The two investigated iceberg have a radius of 5 and 10 meter, and a mass of 470 and 3800 tonnes respectively. The iceberg models used for analyses are a hemisphere with solid elements. The element size is 50*50*50mm for the smallest and 100*100*100mm for the largest model.



A prescribed displacement of 2000 mm in 0.5s is added to achieve a wanted deflection, but at the same time save some computational time.

Inner hull deflection is checked for twelve different collision scenarios and the energy dissipated as strain energy in the ship is found. The inner hull deformations found in collisions with the smallest iceberg were not large enough to exceed the established design criteria. For the largest iceberg the critical inner hull deflection could be reached. However, this would be in a collision point higher than the waterline and in a collision speed larger than a realistic value for side collision. An inner hull deflection exceeding the critical limit would not happen if the assumptions in this thesis are assumed.

Accelerations are found for some critical nodes in inner and outer hull and a node in the side far away from the collision point. The accelerations are found to reach a high level in the outer hull, but only for a very short duration. The change in the corresponding displacement curves could be neglected. The oscillations created in the impact are assumed to be small and will not cause failure in other parts than the impact point of the CCS.



Preface

This report is the result of the Master Thesis conducted by stud.techn. Stine Aas Myhre spring 2010 at the Norwegian University of Science and Technology (NTNU).

The topic is slightly changed from the topic of the Project Thesis which had a greater focus on icebergs and 2D calculations. Only a minor part of this Thesis is based on the information retrieved in the Project.

My knowledge of LNG carriers was limited and the first part of the thesis is related to information about LNG and LNG carriers.

A big part of the Thesis was to make a FE model to use in the analyses. I had never used MSC Patran before and my knowledge in other FE modelling software was limited. Frank Klæbo at Marintek was a great help, giving me “crash course” and always responding quickly on e-mail or telephone. I started in March with a simple wall and finished in middle of April a ship tank section to use in the analyses. The final ship section had more than 250 000 elements before the iceberg structure was included.

To do the pre-processing and analyses, LS-Prepost and LS-DYNA were used. I had been introduced to the programs in the Project, but the main understanding is learned for this Thesis. Ph.D. candidate Zhenhui Liu has been a great help with this and has also provided the two models for the icebergs due to lack of program feature on my own computer.

The analyses have been run on total 8 CPUs. For the analyses including the smallest iceberg the CPU hours were around 140, giving a calculation time of around 18 clock hours. For the analyses that included the biggest iceberg the approximately CPU hours were only 70. This is due to the small size of the elements on the smallest iceberg (50*50*50mm).



The work with the Thesis has been challenging, frustrating and very informative. Starting the semester with little knowledge about LNG Carriers and FE modelling software, I now feel that I have the knowledge to continue to work with similar tasks after graduation and that I have the knowledge to learn other FE modelling software quickly. In the beginning of the semester the Thesis workload looked big, but I feel that I have answered all the steps in the Thesis description well and I am pleased with my final result of the Thesis.

Besides Frank Klæbo and Zhenhui Liu, I would like to thank my Master Thesis supervisor Professor Jørgen Amdahl for good discussions and guidance during the semester and Håvard Nyseth at DNV for providing LNGC scantlings and data.

Tyholt, Trondheim, June 14, 2010

Stine Aas Myhre



Table of contents

SUMMARY	V
PREFACE	VII
1 INTRODUCTION	1
2 LNG AND LNG CARRIERS	2
2.1 LNG VALUE CHAIN	2
2.2 LNG CARRIERS.....	3
2.3 LNG CARRIER WITH MEMBRANE TYPE CCS.....	6
2.3.1 TYPES OF MEMBRANE SYSTEM.....	6
2.3.2 NO96 MEMBRANE SYSTEM.....	6
2.3.3 MARK III SYSTEM.....	7
2.4 DESIGN CRITERIA	8
3 SHIP-ICEBERG COLLISION, PREVIOUS WORK	9
3.1 ARTICLE 1	9
3.2 ARTICLE 2	11
3.3 ARTICLE 3.....	14
4 INTEGRATED ANALYSES FOR SHIP ICEBERG COLLISION	17
5 SHIP IMPACT SCENARIOS	21
5.1 ICEBERG SHAPE	21
5.2 ICEBERG CHARACTERISTICS	21
5.3 SHIP IMPACT GEOMETRY	22
6 ICE MECHANICS	23
6.1 PRESSURE-AREA CURVES.....	26
7 NON LINEAR FINITE ELEMENT	28
7.1 SOLUTION METHODS.....	28
7.2 SOFTWARE	29
7.2.1 MSC PATRAN.....	29
7.2.2 LS-DYNA	29
8 NLFEA MODELLING	32
8.1 MODEL	32
8.1.1 GEOMETRY MODEL.....	33



8.1.2	ELEMENTS	35
8.1.3	ICEBERG MODEL	36
8.2	PRE-PROCESSING	37
8.2.1	MATERIAL	38
8.2.2	BOUNDARY CONDITIONS	39
8.2.3	PRESCRIBED DISPLACEMENT	40
8.2.4	CONTACT	41
8.2.5	TERMINATION TIME.....	41
9	LS-DYNA SIMULATION RESULTS	42
9.1	DEFORMATION	42
9.2	CRUSHING OF ICEBERG	47
9.3	ACCELERATIONS.....	50
9.4	ENERGY DISSIPATION	52
10	PREDICTED DAMAGE.....	54
11	DISCUSSION/CONCLUSION	57
12	RECOMMENDATIONS FOR FURTHER WORK	59
	REFERENCES	61



List of Figures

FIGURE 1 LNG VALUE CHAIN	2
FIGURE 2 LNG CARGO CONTAINMENT SYSTEMS DISTRIBUTION	4
FIGURE 3 NO 96 MEMBRANE SYSTEM (LEFT) AND MARK III MEMBRANE SYSTEM (RIGHT)	6
FIGURE 4 NO 96 MEMBRANE SYSTEM	7
FIGURE 5 MARK III MEMBRANE SYSTEM	8
FIGURE 6 MATERIAL PROPERTIES FOR INSULATION PANEL - CCS	10
FIGURE 7 STRESS WAVE PROPAGATION DUE TO BOW (LEFT) AND SIDE COLLISION	10
FIGURE 8 STRAIN ENERGY/INNER HULL DISPLACEMENT OF TANK1 (LEFT) AND COFFERDAM (RIGHT)	12
FIGURE 9 ICEBERG SHAPE AND SIZES	12
FIGURE 10 STRAIN ENERGY IN ICEBERG COLLISION WITH TANK 1 (TOP) AND COFFERDAM.	13
FIGURE 11 MAXIMUM RESPONSES FROM ICEBERG COLLISION AT TANK 1	13
FIGURE 12 COLLISION SCENARIO	15
FIGURE 13 ACCELERATION AND DEFORMATION FOR SOME COLLISION SCENARIOS.....	15
FIGURE 14 ENERGY DISSIPATIONS FOR STRENGTH, DUCTILE AND SHARED-ENERGY DESIGN (NORSOK N-004).....	17
FIGURE 15 COLLISION BETWEEN TWO ROUGH BODIES (STRONGE).....	18
FIGURE 16 TSAI-WU CRITERIA PLOTTED FOR DIFFERENT CONSTANTS IN $P - J_2$ SPACE.....	24
FIGURE 17 PRESSURE-AREA CURVE, ICEBERG 1	26
FIGURE 18 PRESSURE-AREA CURVE, ICEBERG 2	27
FIGURE 19 TIME INTEGRATION LOOP IN LS-DYNA	30
FIGURE 20 GENERAL ARRANGEMENT MEMBRANE TYPE LNGC.....	33
FIGURE 21 MIDSHIP SECTION	33
FIGURE 22 FIRST PART OF 3D MODELLING/MESHING	34
FIGURE 23 FINISHED TANK GEOMETRY.....	34
FIGURE 24 QUAD4 ISOMESH, SIDE AND BOTTOM PART OF STRUCTURE.....	35
FIGURE 25 QUAD4 PAVER MESH	36
FIGURE 26 ICEBERG MODEL.....	37
FIGURE 27 ANALYSES OUTLINE.....	42
FIGURE 28 GLOBAL X-DEFORMATION OF A SHIP SIDE	43
FIGURE 29 DEFLECTION OF SHIP SIDE AND VON MISES STRESS DISTRIBUTION IN DIFFERENT COLLISION POINTS, ICEBERG 1.....	44
FIGURE 30 DEFLECTION OF SHIP SIDE AND VON MISES STRESS DISTRIBUTION IN DIFFERENT COLLISION POINTS, ICEBERG 2.....	45
FIGURE 31 ICEBERG CRUSHING - ICEBERG 1	48
FIGURE 32 ICEBERG CRUSHING - ICEBERG 2	49
FIGURE 33 ACCELERATION IN NODE AT OUTER HULL, COLLISION POINT 5 - ICEBERG 2	50
FIGURE 34 ACCELERATION, VELOCITY AND DISPLACEMENT CURVES - INNER HULL NODE	51
FIGURE 35 DISSIPATED ENERGY - ICEBERG 1 IMPACT	52
FIGURE 36 DISSIPATED ENERGY - ICEBERG 2 IMPACT	52
FIGURE 37 DEMANDED ENERGY FOR DISSIPATION - ICEBERG 1 COLLISION	55
FIGURE 38 DEMANDED ENERGY FOR DISSIPATION - ICEBERG 2 COLLISION	55
FIGURE 39 MOST CRITICAL NODE IN INNER HULL, IN COLLISION WITH ICEBERG 1 (LEFT) AND ICEBERG 2(RIGHT).....	56



List of Tables

TABLE 1 DIFFERENT LNG CARRIER DESIGN.....	5
TABLE 2 ICEBERG SIZE CLASSIFICATION (IIP)	21
TABLE 3 ICEBERG SHAPE AND SIZE	22
TABLE 4 INPUT PARAMETERS FOR ICEBERG MATERIAL MODEL	23
TABLE 5 ICE MATERIAL PROPERTIES	25
TABLE 6 MAIN SHIP DIMENSIONS.....	32
TABLE 7 ICEBERG GEOMETRY	37
TABLE 8 STEEL MATERIAL PROPERTIES.....	38
TABLE 9 RIGID MATERIAL PROPERTIES.....	39
TABLE 10 BOUNDARY CONDITIONS	40
TABLE 11 COLLISION POINT COORDINATES	43
TABLE 12 INNER AND OUTER HULL DEFLECTION AND COLLISION POINT	46
TABLE 13 DISSIPATED ENERGY CALCULATIONS	54



Abbreviations

ABS	American Bureau of Shipping
AIR	Air Analysis Technique
ALS	Accidental Limit State
CCS	Cargo Containment System
COG	Centre Of Gravity
CPU	Central Processing Unit
DNV	Det Norske Veritas
FE(A)	Finite Element (Analysis)
FR	Fully Refrigerated
FSI	Fluid-structure Interaction
GT&T	Gaz Transport & Technigaz
GTT	Gaz Transport/Technigas
LNG	Liquefied Natural Gas
LNGC	Liquefied Natural Gas Carrier
LPG	Liquefied Petroleum Gas
MCOL	Rigid Ship Motion Program
mm	Millimetre [mm]
m	Meter [m]
ms	Millisecond [ms]
MPa	Mega Pascal [Mpa]
NTNU	Norwegian University of Science and Technology
NORSOK	Norsk sokkels konkurranseposisjon
s	Second [s]
V _r	Ship speed



1 Introduction

Arctic, sub-arctic regions of Russia and other Northern areas contain some of the largest natural gas fields in the world. The gas produced in these areas could be transported by ship to gas terminals all over the world. The transportation is done by Liquefied Natural Gas (LNG) carriers with a LNG cargo containment system. LNG ships carry huge amount of energy and it is important that the tanks and the ship's hull have an adequate resistance to sloshing forces and external accidental loads as ice actions.

A potentially severe risk is collision with icebergs of the size of bergy bits and growlers (< 1000 tonnes). Bigger icebergs are usually observed on radar or visually seen from the ship and can easily be avoided. The International Ice Patrol monitors all big icebergs in the world and collisions rarely happen. Small icebergs can make huge damage to the ship's hull. For accidental iceberg impacts some damage to the structure can be accepted, but the integrity of the cargo tanks should not be damaged. This could potentially lead to gas leakage and huge environmental damage.

Scope of work

The main part of this thesis is to study the behaviour and resistance of a LNG carrier subjected to an accidental limit load, as iceberg impact. A FE model of a ship structure will be made and analysed for different impact locations. The inner hull deformation will be checked against design criteria to locate any leakage possibilities.

Previous work has been done on LNG ships colliding with iceberg and large accelerations are found. Accelerations in critical nodes will be investigated and compared to deflection and velocity at the same nodes to see if the oscillating waves are large enough to injure other part of the structure.



2 LNG and LNG carriers

2.1 LNG value chain

A LNG carrier is a Fully Refrigerated (FR) ship, constructed to carry cargo under atmospheric pressure at a very low temperature. The value chain, found in [2], of the gas is showed in Figure 1.



Figure 1 LNG value chain

Production:

Gas is found both onshore and offshore. The gas can be found in oil reservoir as associated gas or alone in a reservoir as non-associated gas. The non-associated gas is dryer and contains nearly pure methane. The gas is transported from the production area to the liquefaction plant in pipelines. There are some units that can both produce and liquefy the gas.

Liquefaction:

Before the gas arrive at the liquefaction plant some heavier hydrocarbons has to be removed. The gas is treated and carbon dioxide, sulphur, mercury and water are removed from the gas. Only methane and some light hydrocarbons are left. Condensate and Liquefied Petroleum Gas (LPG) removed from the gas can be shipped and sold separately. When the quality of the natural gas is saleable for the marked the gas is cooled to a liquid state by compressors. At a temperature around minus 162°C the gas becomes a liquid at atmospheric pressure [3]. The volume of the liquefied gas is 1/614 of the non liquefied gas.

Shipping:

After liquefaction and storage at the plant the LNG is loaded in to a LNG carrier. This is a cost efficient way to transport LNG over long distances. LNG carriers are more described in Chapter 2.2.

*Regasification terminals:*

In the costumer country, the LNG cargo is regasified at regasification terminals (import terminals). The LNG is then moved to a pipeline system or tanker trucks for road delivery.

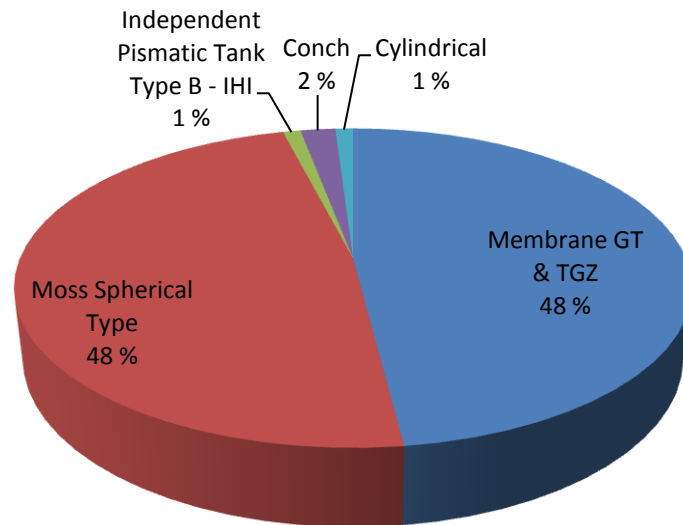
Market:

LNG is usually sold on a long-term basis. The costumer is typically a large gas or a power company, who sell the natural gas to industry or private houses. In private houses the gas is used as a power source both to provide heat and to cook. The gas can be used in transportation or to produce other minerals as hydrogen. Natural gas can be used in the manufacturing of steel, glass, fabrics and paint.

2.2 LNG carriers

In 1915 the first patent for transporting liquefied natural gas was approved for a river barge [2] but the concept was not in use before 1951 in Mississippi, USA. However, American Bureau of Shipping (ABS) refused to class the barge. The first LNG tanker was the converted tanker Methane Pioneer. This ship had its maiden voyage filled with LNG cargo in 1959. After that the LNG ship and containment systems have developed and today there are more than 185 LNG carriers in service. There are two main containment systems that have been developed, a self-supported system and membrane types. The self-supported system can be box shaped or spherical, as Moss spherical tank design. Membrane tanks are box shaped and supported directly on the ship's inner hull. The distribution of the different cargo containment types is showed in Figure 2.

The safety of LNG ships is very good and there have never been an accident that led to spill or losses of LNG cargo.



Total number of LNG ships - 185



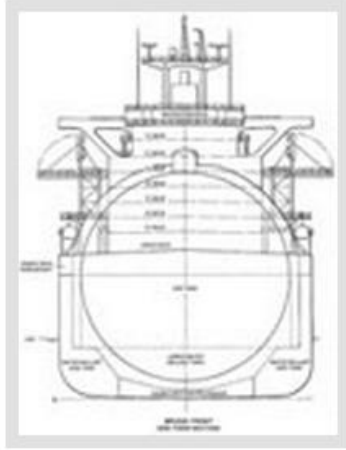
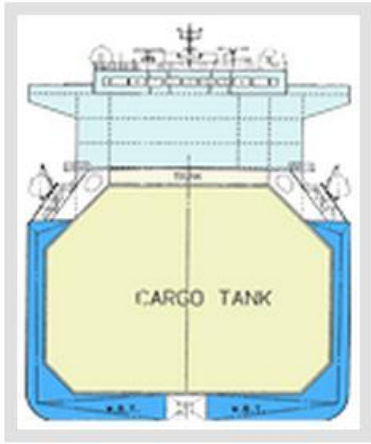
Figure 2 LNG cargo containment systems distribution

There are technical and commercial advantages and drawbacks on all designs; some are presented in Table 1 for the membrane system and spherical Moss design. The table is found in ref. [2].

For iceberg impact membrane type CCS is assumed to be the most critical and is the one which is investigated in this thesis.



Table 1 Different LNG carrier design

Containment types	Moss Spherical Tank 	Membrane Tanks 
Advantages	<p><i>Most proven of all second-generation containments</i></p> <p><i>Excellent operating hours</i></p> <p><i>No tank-filling restrictions</i></p> <p><i>No slosh damage potential</i></p> <p><i>95% of welding is automatic (reducing defects probability during construction)</i></p>	<p><i>Lower fuel consumption than for Moss</i></p> <p><i>Lower canal charges(smaller gross tonnage)</i></p> <p><i>Maximum usage of hold's volume for cargo</i></p> <p><i>Primary barrier has first-class history</i></p> <p><i>Unrestricted navigation visibility (flat continuous deck)</i></p> <p><i>Good manoeuvrability</i></p> <p><i>Low wheelhouse and cargo control room air drafts</i></p>
Drawbacks	<p><i>Larger-dimensional ships (for the same carrying capacity than the others)</i></p> <p><i>Less manoeuvrability (high wind area)</i></p> <p><i>More affected by weather and poor navigational visibility</i></p> <p><i>Higher canal charges (40% higher gross tonnage than for membrane ships)</i></p> <p><i>Slightly higher fuel consumptions</i></p> <p><i>Most difficult deck access and maintenance</i></p>	<p><i>Potential slosh damage problems due to cargo tanks</i></p> <p><i>Membrane fatigue life is difficult to measure</i></p> <p><i>Difficult accessibility to containment system</i></p> <p><i>Labour intensive during construction – increased probability of defects.</i></p>
Containment Sections and Profiles		



2.3 LNG carrier with membrane type CCS

2.3.1 Types of membrane system

The first LNG carrier with membrane type Cargo Containment System (CCS) was built in 1965 and named the Phytagore. The membrane tanks were designed by Technigaz. In 1994, Technigaz merged with a company with competing design, Gaz Transport. Now, Gaz Transport & Technigaz (GT&T) is the leader in the CCS marked with two main design, NO96 membrane system and Mark III system. A third system called The Combined System- 1 (CS-1) is a hybrid of the Mark III and the NO96 containment. The first CS-1 containment was built in 2004 but the success was short since it appears to be a problematic design. The NO96 and Mark III CCS are described in the following.

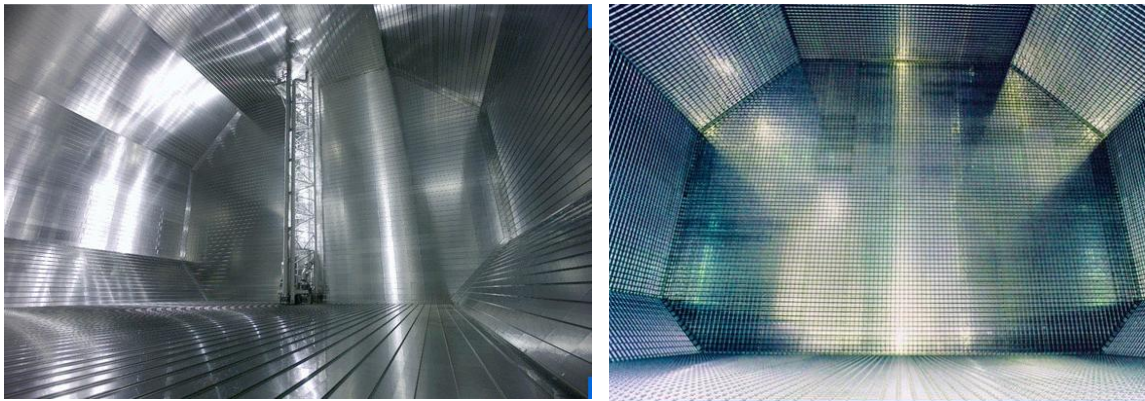


Figure 3 NO 96 membrane system (left) and Mark III membrane system (right)

2.3.2 NO96 membrane system

NO96 membrane [4] system has been improved and used since 1969 and was originally a tank designed by Gaz Transport's. The isolating layers are directly supported by the ship's inner hull. The cryogenic liner consists of two identical layers of invar membrane and thermal insulation, illustrated in Figure 4. The primary layer of membrane contains the LNG cargo and the secondary layer ensures redundancy in case of leakage. The thermal insulation layers consist in a load bearing system made of plywood boxes filled with perlite. The area of the boxes is 1 m x 1.2 m. The thickness of the primary layer (closest to the LNG cargo) is adjustable from 170 mm to 250 mm and the secondary layer is 300 mm thick. Both boxes are fixed to the inner hull by coupler assembly (see highlighted box in Figure 4).

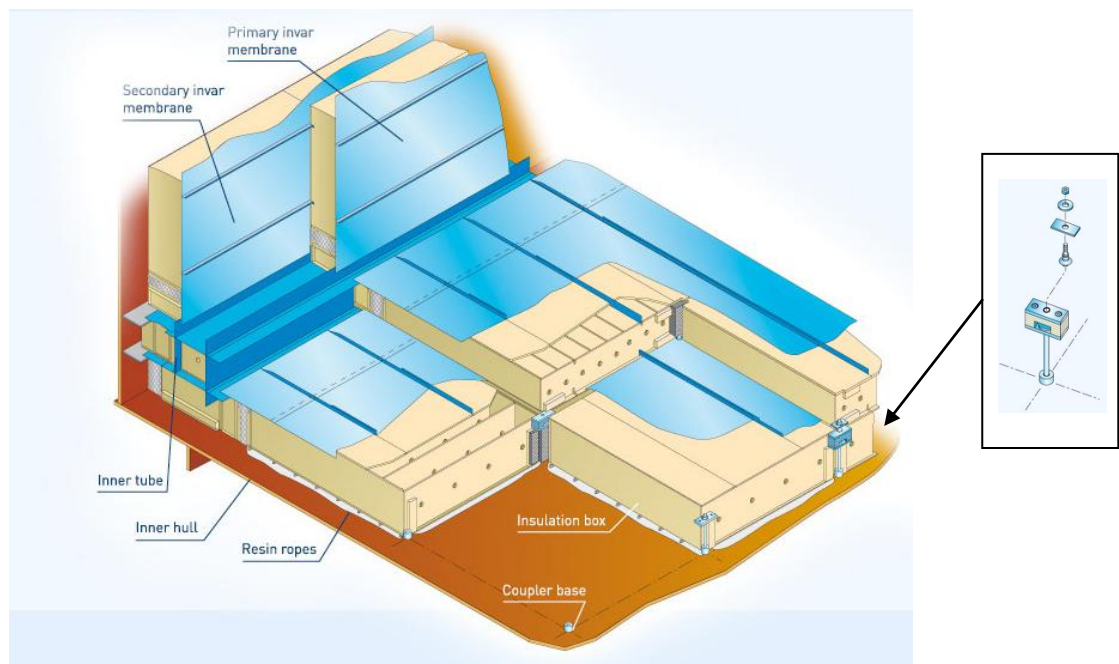


Figure 4 NO 96 membrane system

The invar membrane offers an extremely low thermal contraction coefficient. All dynamic and thermal loads are directly and uniformly transferred to the steel structure. The boxes are designed to absorb the energy from liquid motion and withstand high impact pressure.

2.3.3 Mark III system

The Mark III system [5] has been improved and used since 1967 and was originally Technigaz's design. As the NO 96 membrane system, the Mark III membrane system is directly supported by the inner hull. The cryogenic liner consists of primary membrane, insulation panel and secondary membrane. The primary stainless steel membrane is directly supported and fixed to the insulation layer. Standard area size is 3mx1m with thickness 1.2 mm. The secondary triplex membrane is a composited laminated material positioned inside the two insulation layers. The primary and secondary insulation layers are both made of prefabricated panels in reinforced polyurethane foam. The area of the panels is 3mx1m with a thickness adjustable from 250 mm to 350 mm. The panels are bonded to the inner hull by resin ropes, for anchoring and spreading the loads. Fiberglass in the polyurethane gives high mechanical properties and the high density foam and plywood allow the insulation to absorb the energy resulting from liquid motion and withstand high impact pressure.

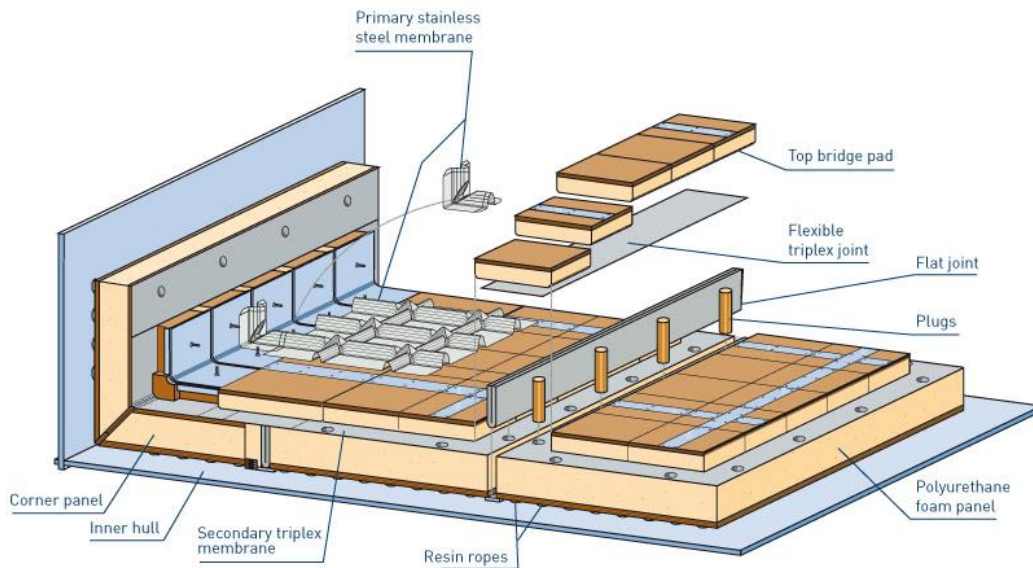


Figure 5 Mark III membrane system

2.4 Design criteria

There are two limiting design states, the operational and survival limit. The operational limit is the maximum deflection you can have in daily/operational basis which will not affect or damage the membrane tanks. The survival limit is the most serious state where the consequence could be large damage of the membrane tanks and leakage of LNG.

A risk analysis has been performed for the NO96 membrane type, [13] and the survival criteria for critical impacts have been developed.

The invar membrane performs well in elongation, and the elongation limit is up to 40%. However, this cannot be used as the survival limit because the limiting areas are could be the welded joints in the ends.

Given from GTT the membrane survival limit is 40 mm/m in longitudinal direction. Based on this survival limit, deformation from a specific grounding scenario and the limit state of the hull structure, the survival criterion is defined as the state where the deformation of the inner hull reaches 70 cm. For the Mark III CCS the survival limit is assumed to be higher than for the GTT NO96 CCS.

The survival criteria for GTT NO96 membrane type tanker is 70 cm deflection of inner hull.



3 Ship-iceberg collision, previous work

Previous work has been carried out to investigate the consequences in a ship-iceberg collision. In this chapter some articles have been reviewed and a short summary of the main content are made in the following chapters.

3.1 Article 1

“Safety of membrane type cargo containment system in LNG carrier under accidental iceberg collision” [12]

For the simulations in this article a bergy bit with the shape of a cube is considered. The size of the cube is 20 meters in each direction with a sail height above waterline of 2 meters and keel depth of 18 meters.

Two different scenarios are considered. Scenario 1 is a bow collision in full design speed, 19.5 knots. Scenario 2 is side collision under a sharp turning of the ship. The radial ship speed is assumed to be 10% of design speed, 1.95 knots. For both scenarios the drifting speed the iceberg is assumed to be 2 knots.

For simulation a global analysis is first performed. A FE model is made for the entire ship and critical regions for local analysis are selected by screening analysis. The structural components of CCS are assumed to have single material property. The element density of the bow model should be sufficient to transmit impact forces to the hull and deformation and collapse of the bulb, and an element size of 100*100mm is used. For the side collision the mesh density is less sensitive because the collapse and deformation are limited to a small area.

As a second step, a local analysis is performed. A detailed FE model is made for critical regions to define the composite structures of CCS more precisely. Nodal velocities from the global analysis are used to excite the local model. All composites structures of the panel are analyzed.



For the hull structure an elastic-plastic steel material is considered with fracture at 20% of total strain. Iceberg material is assumed to be elastic-plastic with yield stress of 3.5 MPa with little hardening modulus. The material properties of the insulation panels are showed in Figure 6.

Material	Property	Young's modulus (MPa)	Poisson's Ratio	Thickness (mm)	Density (kg/m ³)
Membrane		200000	0.27	1.2	7850
Top Plywood		8200	0.17	12	710
Top R-PUF		131	0.2	120	125
Triplex		13133	0.3	2	2500
Bottom R-PUF		131	0.2	150	125
Bottom Plywood		8200	0.17	9	710
Mastics		2877	0.3	12.5	1500

Figure 6 Material properties for insulation panel - CCS

A nonlinear impact simulation is carried out for a 0.3 second period for both impact scenarios. For the bow impact the stress waves reached the stern after 90 ms, see Figure 7. The maximum response in terms of accelerations and stress of CCS is found in the first bulkhead. For the side collision the stress wave reached the other side of the hull after 15 ms and reflected as illustrated to the right in Figure 7. Maximum response of stress and acceleration of CCS was found in inner hull near contact point.

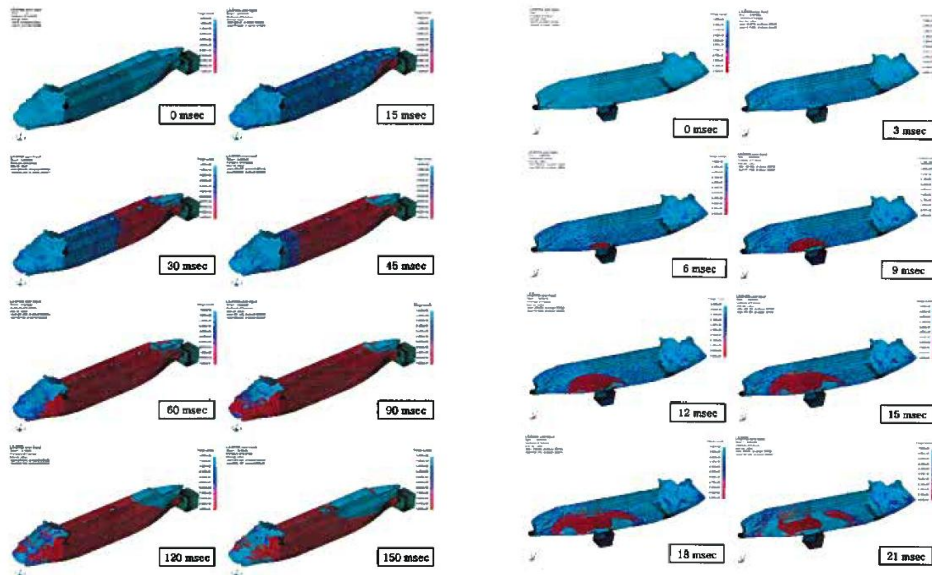


Figure 7 Stress wave propagation due to bow (left) and side collision

Time history is recorded and found that for a side collision the iceberg starts rebounding from the side hull at 0.9 s. They are completely separated at 0.18 s. For the bow collision the contact remains during the simulation.



The stress results for the bow collision are low and it is assumed that the CCS may not suffer critical damages in collision. For the side collision some of the layers in the insulation panels may reach a critical stress level and possible damage in some parts. The conclusion is that because of the short distance from the collision location to the LNG CCS, the structural response of LNG CCS was more significant in case of the side collision.

3.2 Article 2

“Structural risk analysis of an NO96 membrane-type liquefied natural gas carrier in Baltic ice operations” [13]

This report covers a structural risk analysis for a 170 000 m³ LNGC with GTT NO96 membrane type system and Finnish maritime Administration Ica Class 1A. The ship’s trade route is from the Baltic to Canada, an area with different ice hazards. In the Baltic the risks are related to level ice, ice ridge, small ice floe and stuck-in-ice hazards. These conclusions are not covered in this thesis and are not considered in my report.

The GTT NO96 membrane system is placed directly on the inner hull and fixed by couplers in the four corners. This makes the membrane tanks flexible and capable to absorb deflection from ballast tanks. The invar membrane performs excellent in elongation. In transverse and longitudinal direction the edges are welded and these welds are thought to be the most critical areas.

A serious consequence for the vessel would be damage to the membrane barriers which would cause a LNG leakage. The survival limit for the allowable inner hull deflection is calculated based on longitudinal elongation limit of 40 mm/m. This gives the maximum lateral deflection of 6417mm. This deflection appears not to occur, because the hull is expected to collapse before the invar membrane reaches the tensile limit state.

For the ship-iceberg collision, Tank 1 and cofferdam bulkhead are the main target areas. Pressure loading was applied to these contact areas until the maximum deflection of the inner hull reached 1 m. For the study, an inner hull deflection of 70 cm is used as a survival limit. The results can be seen in Figure 8.

The ice-ship collision is determined as:

-ice classification; icebergs and other ice hazards

-ice height above sea level; 2 m

-ship speed: 19.5 knots (forward) with various incident angels

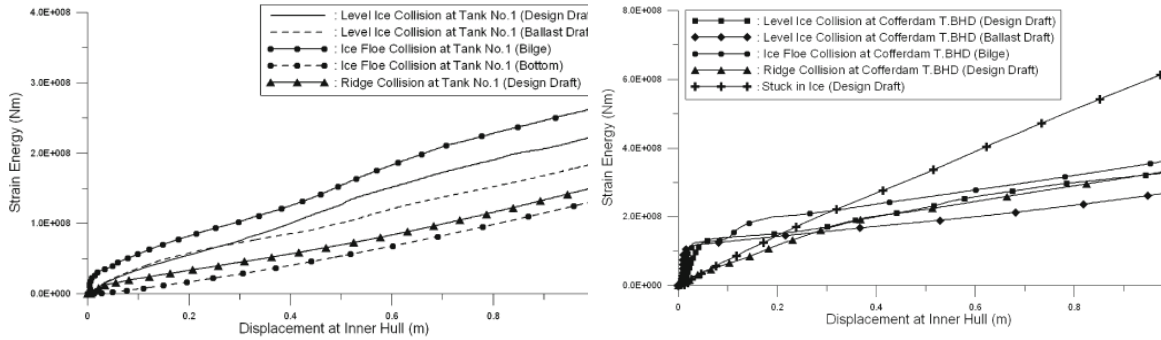


Figure 8 Strain energy/inner hull displacement of tank1 (left) and Cofferdam (right)

As expected the transverse bulkhead area are stiff and resist higher external loading than the middle part of the membrane tank.

Different iceberg shapes and size have been investigated, see Figure 9. A bell shape is added to increase the contact area between ship and iceberg.

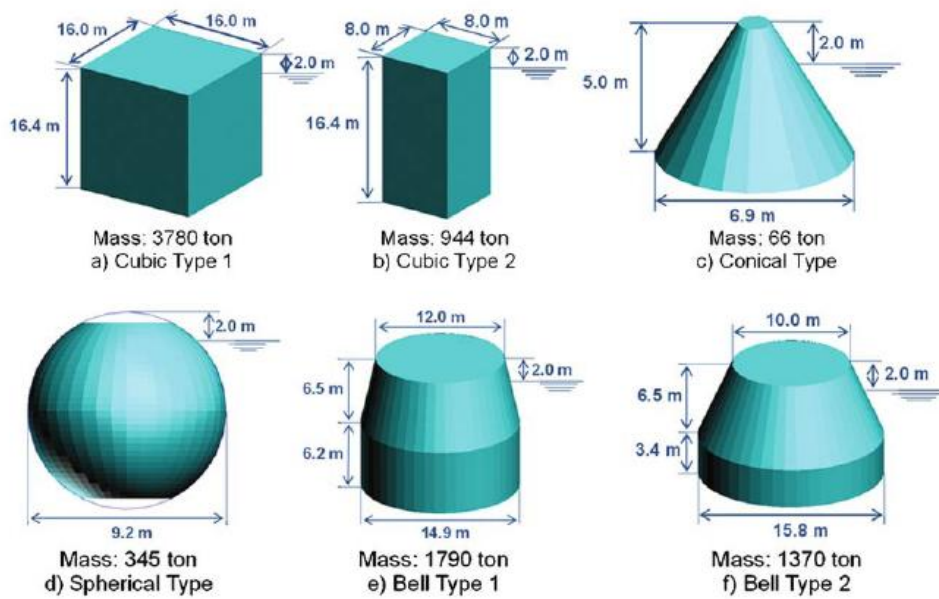


Figure 9 Iceberg shape and sizes

In the analysis the icebergs are postulated to move towards the ship at a forward speed at 19.5 knots. The iceberg will collide with the ship at an angle of 15° at a tide of 2.6 m/s in normal direction to the ship. Results can be seen in Figure 10.



Iceberg collision		Initial kinetic energy of ice (Nm)	Struck ship (LNGC)		Absorption rate*
			Strain energy (Nm)	Kinetic energy (Nm)	
Cubic	Type 1	1.90×10^8	8.40×10^6	1.34×10^6	4.4%
	Type 2	4.74×10^7	1.63×10^6	7.66×10^5	3.4%
Conical		3.31×10^6	9.71×10^5	8.27×10^4	2.9%
Spherical		1.73×10^7	8.66×10^7	3.56×10^5	5.0%
Bell	Type 1	8.99×10^7	1.51×10^6	6.12×10^5	16.8%
	Type 2	6.89×10^7	7.53×10^6	8.86×10^5	10.9%

*(LNGC strain energy)/(ice initial kinetic energy).

Iceberg collision		Initial kinetic energy of ice (Nm)	Struck ship (LNGC)		Absorption rate*
			Strain energy (Nm)	Kinetic energy (Nm)	
Cubic	Type 1	1.90×10^8	6.77×10^6	1.41×10^6	3.6%
	Type 2	4.74×10^7	1.55×10^6	7.45×10^5	3.3%
Conical		3.31×10^6	8.47×10^4	6.77×10^4	2.4%
Spherical		1.73×10^7	7.96×10^5	2.16×10^5	4.6%
Bell	Type 1	8.99×10^7	1.02×10^7	3.56×10^5	11.4%
	Type 2	6.89×10^7	4.66×10^6	6.03×10^5	6.8%

JEMEI18 © IMechE 2008

Proc. IMechE Vol. 222 Part M: J. Engineering for the Maritime Environment

Figure 10 Strain energy in iceberg collision with Tank 1 (top) and Cofferdam.

The capacity of the vessel is defined as the maximum internal strain absorbed by the hull before it reaches a critical limit. This is numerical calculated by MSC/DYTRAN. The kinetic energy of the ice is transmitted to the hull, the strain energy stored in the hull after collision is used as the demand. Maximum responses from the iceberg collision with tank 1 are showed in Figure 11.

Iceberg collision		Side shell		Web frames		Inner hull	
		Maximum stress (MPa)	Plastic strain	Maximum stress (MPa)	Plastic strain	Maximum stress (MPa)	Maximum displacement (mm)
Cubic	Type 1	237	0.011	253	0.027	89	6.0
	Type 2	237	0.003	239	0.007	61	4.2
Conical		136	—	142	—	18	1.6
Spherical		237	0.002	236	0.008	36	2.5
Bell	Type 1	248	0.026	356	0.15	92	8.8
	Type 2	241	0.015	289	0.088	85	8.0

Figure 11 Maximum responses from iceberg collision at tank 1

Based on iceberg-hull interactions the survival limit of the inner hull is a maximum deflection of 70 cm. The operational limit is 4.6 mm lateral deflection on 1 m. From the collision analysis the maximum deflection was detected to be less than the operational limit and the conclusion for the report is that the ship can operate in the proposed areas, route from Baltic Canada, without any risk of leakage.



3.3 Article 3

“Structural Safety Assessment in Membrane-type CCS in LNGC under Iceberg Collision” [14]

An important safety criterion for a LNG carrier under iceberg collision would be to resist leakage of LNG from damaged membrane tanks. In previous articles allowable deformation have been investigated for GTT NO96 membrane type, in this article Mark III membrane system is examined. A full scale iceberg-ship collision is considered with surrounding water and fine FE mesh. A local zooming technique is used for the critical areas, areas with maximum deformation.

First a suitable ice material model is found. Under compressive stress crushing is the dominant ice failure and it is important that the material model have the right characteristics. Two types of elasto-plastic materials are tested, both experimental with fresh water ice and by using simulations, and found fairly good concerning the crushing failure. One elastic material and one ice material are used in the analyses. Different analyses are done to investigate the ice failure strain, failure stress, failure tensile stress, young's modulus and iceberg mesh size. Increased failure strains are found to result in greater collision response values and crushing strength. The failure stress, failure tensile stress and Young's modulus had a very small (no) influence. The iceberg elements mesh size, on the other hand, have a great influence on the crushing strength and collision response of the inner hull.

For the analyses in this article a cubic iceberg of 20mx20mx20m is considered. Three different analyse techniques are used, respectively Fluid-Structure Interaction (FSI), Rigid Ship Motion Program (MCOL) and traditional in the air (AIR) analysis technique. Different mesh sizes, ship velocities and attack angels were examined for different techniques. The collision scenario is illustrated in Figure 12.

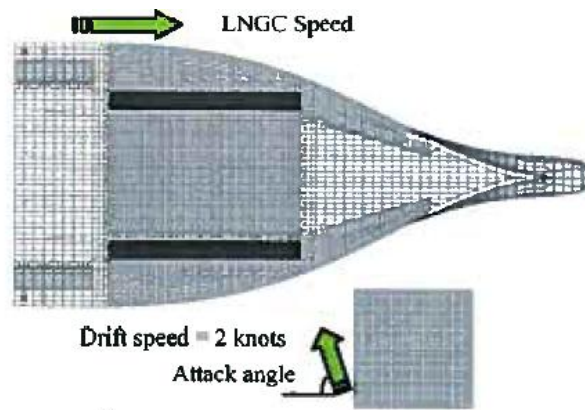


Figure 12 Collision scenario

The FSI analysis technique was found to give the most realistic and reasonable collision responses. The elastic iceberg caused much greater damage to the inner hull than the iceberg material.

Different attach angels, icebergs size and LNGC speed were also considered. Increasing attack angel, iceberg size and ship speed had a big influence on the simulations and caused large deformations on the inner hull.

The damping effect of the inner fluid in the cargo tank was found not to have a great influence on the damage of the side structure, but it did affect the inner hull deformation and acceleration responses.

Case	Iceberg material	Analysis technique	Collision force (MN)	LNGC Absorbed energy (MJ)	Iceberg Absorbed energy (MJ)	Vertical displ. (m)
1	elastic	AIR	84.11	364.45	-	0.00
2		MCOL	94.07	712.94	-	2.69
3		FSI	145.02	992.38	-	2.49
4	ice	AIR	89.33	431.59	6.23	0.00
5		MCOL	75.13	600.71	6.05	7.52
6		FSI	81.07	571.13	8.05	7.21

Case	Iceberg size (m)	Attack angle	Collision force (MN)	LNGC Absorbed energy (MJ)	Iceberg Absorbed energy (MJ)	Vertical displ. (m)
7	20×20×20	45°	28.59	24.10	4.22	3.61
6		70°	81.07	571.13	8.05	7.21
8	30×30×30	90°	75.69	336.89	6.01	10.32
9		70°	100.90	841.45	9.83	4.55
10	30×30×30	90°	85.59	625.64	8.23	6.06
6		70°	81.07	571.13	8.05	7.21
9	30×30×30	90°	100.90	841.45	9.83	4.55
8	20×20×20		75.69	336.89	6.01	10.32
10	30×30×30	85.59	625.64	8.23	6.06	

Case	Inner hull		Iceberg		
	Max. deform. (m)	Max. accel. (m/s ²)	Total number	Failure number	Ratio (%)
1	0.279	7,972.19	-	-	-
2	0.952	18,052.76	-	-	-
3	1.226	21,419.70	-	-	-
4	0.194	5,717.36	64,000	166	0.26
5	0.180	5,019.55	64,000	935	1.46
6	0.097	3,916.80	64,000	1,171	1.83

Case	Inner hull		Iceberg		
	Max. deform. (m)	Max. accel. (m/s ²)	Total number	Failure number	Ratio (%)
7	0.016	1,400.02	64,000	282	0.44
6	0.097	3,916.80	64,000	1,171	1.83
8	0.167	4,836.29	64,000	763	1.19
9	0.209	6,267.22	216,000	2,051	0.95
10	0.261	8,219.22	216,000	1,188	0.55
6	0.097	3,916.80	64,000	1,171	1.83
9	0.209	6,267.22	216,000	2,051	0.95
8	0.167	4,836.29	64,000	763	1.19
10	0.261	8,219.22	216,000	1,188	0.55

Figure 13 Acceleration and deformation for some collision scenarios

Some of the acceleration found in Figure 13 is relatively high, marked with a red circle, and a consequence could be damage other places in the hull than at the collision point.



For the structural safety assessment for Mark III membrane type a local zooming analysis were assumed for the most critical deformation points found in the global analyses.

The survival limit for the Mark III membrane system is assumed to be greater than the survival limit for the NO96 membrane type because a more flexible local deformation could be allowed. The deformation found in the analyses was found to be under the survival limit.



4 Integrated analyses for ship iceberg collision

In ship-ship collisions or iceberg-ship collisions the impact actions is characterised by kinetic energy, NORSOK [6]. A part of the kinetic energy will remain as kinetic energy after the collision and needs to be dissipated as strain energy in the colliding objects. There are three outcomes with respect to the dissipated strain energy; strength, ductility and shared energy design.

Strength design - the ship is strong enough to resist the collision force with minor deformation, this force the iceberg to deform and dissipate the major part of the collision energy.

Ductility design - the ship undergoes large, plastic deformations and dissipates the major part of the collision energy. This is often conservative with respect to structural damage.

Shared energy design - both the iceberg and the ship contributes to the energy dissipation and undergoes large deformations.

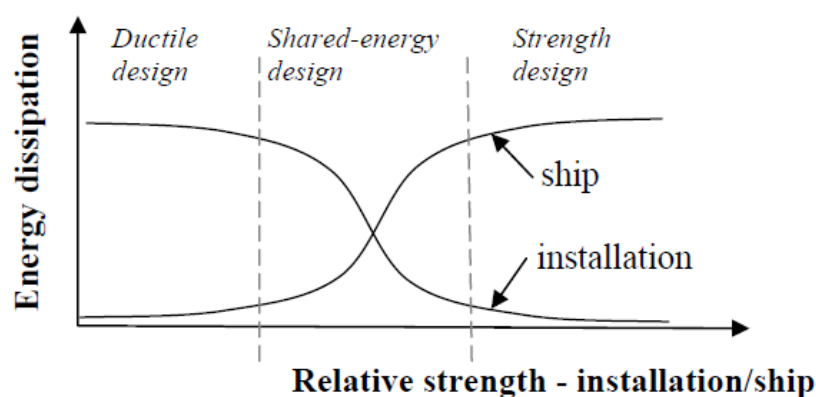


Figure 14 Energy dissipations for strength, ductile and shared-energy design (NORSOK N-004)

Since both the iceberg and the ship undergo large deformations, shared energy analysis and design is the most realistic choice for this case.



The analysis of a collision in accidental limit state (ALS) can be divided into two uncoupled processes; internal and external mechanics, [17]. The dissipated energy causing crushing and deformation of the colliding objects, is analysed in the internal mechanics. The external mechanics deals with the energy released for dissipation, the demand of dissipated energy to cause damage to the crushing objects. By using internal and external mechanic calculation the damage and deformations of the ship side can be calculated, this is done in Chapter 10.

The external mechanics calculations are based on Stronge's [18] impact mechanics, which have two assumptions;

- The impact duration is short and the impact force is large, all other external forces are neglected.
- The deformation is limited to a small area within the surface.

Two bodies are assumed to collide in point C. The bodies have no displacement constrains except that they are mutually impenetrable in C. A common normal vector n is perpendicular to the common tangent plane. Then n_1, n_2, n_3 are perpendicular unit vectors. The bodies have mass center G and G' , see Figure 15.

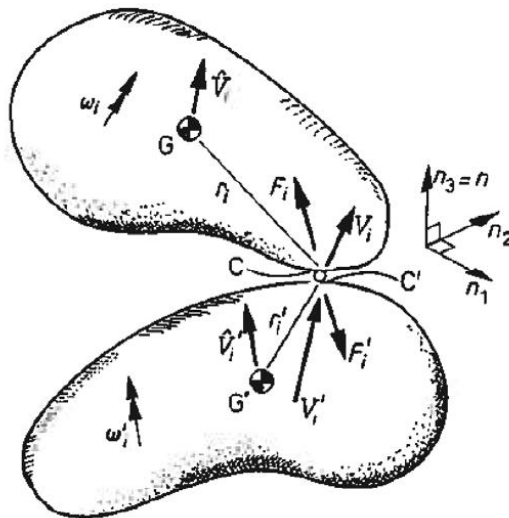


Figure 15 Collision between two rough bodies (Stronge)

The position vectors r_i and r'_i are between the mass point G and G' and C and C' respectively. The two bodies have mass M and M' , inertia tensors \hat{I}_{ij} and \hat{I}'_{ij} at G and G' . \hat{V}_i and \hat{V}'_i are the velocities in the center of the mass and ω_i and ω'_i are the corresponding velocities for the bodies in the reference frame n_i . At the contact points



C and C' the bodies are subjected to contact forces F_i and F'_i . These contact forces are reactions that apply in an impulse to each body. The impulses can be denoted as

$$dP_i = F_i dt \quad (1)$$

$$dP'_i = F'_i dt \quad (2)$$

The equation of motion can be expressed as

$$M d\hat{V}_i = dP_i \quad (3)$$

$$\hat{I}_{ij} d\omega_j = \varepsilon_{ijk} r_j dP_k \quad (4)$$

and

$$M' d\hat{V}'_i = dP'_i \quad (5)$$

$$\hat{I}'_{ij} d\omega'_j = \varepsilon_{ijk} r'_j dP'_k \quad (6)$$

The repeated index (e.g. j or k) indicates the summation and the permutation tensors. $\varepsilon_{ijk} = +1$ if the indices in a cyclic order, $\varepsilon_{ijk} = -1$ if anticyclonic and $\varepsilon_{ijk} = 0$ for repeated indices.

The velocity in each contact point, V_i and V'_i , can be obtained from the velocity of the respective center of mass and the relationship between velocities of two points on a rigid body. Respectively

$$V_i = \hat{V}_i + \varepsilon_{ijk} \omega_j r_k \quad (7)$$

$$V'_i = \hat{V}'_i + \varepsilon_{ijk} \omega'_j r'_k \quad (8)$$

The relative velocity is

$$v_i = V_i - V'_i \quad (9)$$

Any incremental change in reaction pulse acting on the rigid bodies is equal in magnitude but opposite in direction if the infinitesimally small deforming element's mass is negligible.

$$dp_i = dP_i - dP'_i \quad (10)$$

This gives the change in the velocity

$$dv_i = m_{ij}^{-1} dp_j \quad (11)$$

Where the elements of the inverse inertia matrix for C are given by

$$m'_{ij} \equiv \left(\frac{1}{M} + \frac{1}{M'} \right) \delta_{ij} + \varepsilon_{ikm} \varepsilon_{jln} (l_{kl}^{-1} r_m r_n + l'_{kl}{}^{-1} r'_m r'_n) \quad (12)$$



The inverse inertia matrix is symmetric, $m_{ij}^{-1} = m_{ji}^{-1}$. The following are representative elements:

$$m'_{11} = (M^{-1} + r_2^2 I_{33}^{-1} - 2r_2 r_3 I_{23}^{-1} + r_3^2 r_{22}^{-1}) + (M'^{-1} + r_2'^2 I_{33}'^{-1} - 2r_2' r_3' I_{23}'^{-1} + r_3'^2 I_{22}'^{-1})$$

$$m'_{12} = (r_1 r_3 I_{23}^{-1} - r_3^2 I_{21}^{-1} - r_1 r_2 I_{23}^{-1} + r_2 r_3 I_{31}^{-1}) + (r_1' r_3' I_{23}'^{-1} + r_3'^2 I_{21}'^{-1} - r_1' r_2' I_{33}'^{-1} + r_2' r_3' I_{31}'^{-1})$$

$$m'_{13} = (r_1 r_2 I_{32}^{-1} - r_2^2 I_{31}^{-1} - r_1 r_3 I_{22}^{-1} + r_2 r_3 I_{21}^{-1}) + (r_1' r_2' I_{32}'^{-1} + r_2'^2 I_{31}'^{-1} - r_1' r_3' I_{22}'^{-1} + r_2' r_3' I_{21}'^{-1})$$

The matrix I_{ij} of moments and products of inertia has an inverse which is denoted by I_{ij}^{-1} . E.g. $I_{21}^{-1} = (I_{12}I_{23} - I_{12}I_{33})/\det(I_{ij})$



5 Ship impact scenarios

5.1 Iceberg shape

Usually the icebergs breaks off from Glaziers around Greenland or in the Antarctic, this makes the shape different for each icebergs. The water density, ice density, temperature and origin might affect the size and how much of the ice that is above the water surface. Normally 7/8ths of the iceberg is under water level, but sometimes as much as 90 %. This is related to the mass density and the buoyancy.

The classification of different iceberg sizes are given in Table 2, in this thesis iceberg of the size of bergy bits and growlers and considered.

Table 2 Iceberg size classification (IIP)

	Height above sea level(m)	Length (m)	Approx. mass (tones)
Growler	< 1.5	<5	100
Bergy bit	1.5 – 5	5 – 15	1000
Small berg	5 – 15	15 – 60	100 000
Medium berg	15 – 50	60 – 120	2 000 000
Large berg	50 – 100	120 – 220	10 000 000
Very large berg	>100	> 220	> 10 000 000

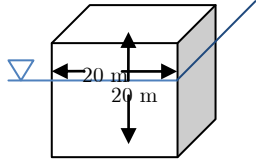
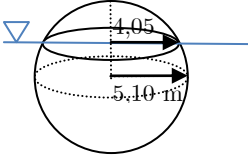
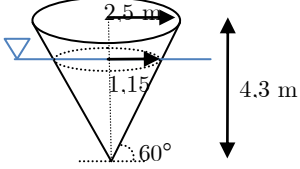
Some typical icebergs are listed in Appendix A.

5.2 Iceberg characteristics

Since the size and the outline of all icebergs are different some simplifications has to be made to do calculations. DNV has investigated some different impact scenarios, [1]. Three different iceberg shapes and sizes are considered, see Table 3. For all three cases the design size has been determined from a condition where the height above water surface should be 2.0 m.



Table 3 Iceberg shape and size

CUBE	SPHERE	CONE
Volume: 8000 m ³ Mass: 7200 tonnes 	Volume: 555 m ³ Mass: 500 tonnes 	Volume: 28 m ³ Mass: 25 tonnes 

DNV assume the drift velocity of the iceberg to be 2 knots (1 m/s).

5.3 Ship impact geometry

DNV consider three locations for the ship iceberg impact, [1].

Bow side

The bow side of the ship is where the impacts primarily will occur. If the iceberg is not observed before the impact, the iceberg will hit the bow area. This can happen from the stem to the bow shoulder. The ship speed (V_r) is considered to be the impact speed.

Midship

If the ship turns to try to avoid impact the impact can happen at the midship area. This is the worst case for impact considering the external energy. For a midship collision the transverse ship speed is assumed $0.1 \cdot V_r$.

Bottom

If the ship run over a bergy bit or grounds with an iceberg stuck at the seabed you would have impact with the ship's bottom area. For a bottom impact the ship speed would be equal the impact speed and the acting force would be equal the buoyancy of the iceberg.



6 Ice mechanics

Ph.D. student Zhenhui Liu has developed a relevant ice mechanics model for collision scenarios, [7]. Ice material model for Finite Element Modelling is previously not well established, but in Liu's paper a simple plastic model is proposed which seems to describe the ice material model well. His model does not take into account fracture or crack propagation in the ship shell plating.

Ice is in a triaxial stress state, since ice particles in the centre are extensively confined from neighbouring particles. Several scientist have developed yield surface formulas, one is the Tsai-Wu yield surface. This yield surface has been used for years, but has not been applied to FEM simulations for ship-iceberg impacts. This can be rewritten to an elliptical yield surface;

$$f(p, J_2) = J_2 - (a_0 + a_1 p + a_2 p^2) = 0 \quad (13)$$

Where the hydrostatic pressure $p = \frac{\sigma_{kk}}{3} = \frac{I_1}{3}$ and deviatoric stress $q = \sqrt{3J_2} = \sqrt{\frac{3}{2}s_{ij}s_{ij}}$.

The constants a_0 , a_1 and a_2 are based on different analysts recommended inputs, given in Table 4 and plotted in $p - J_2$ in Figure 16.

Table 4 Input parameters for iceberg material model

	Derradji-Aouat (2000)	Kierkegaard (1993)	Riska 1 (1987)	Riska 2 (1987)
Constant a_0	22.93	2.588	1.60	3.1
Constant a_1	2.06	8.63	4.26	9.20
Constant a_2	-0.023	-0.163	-0.62	-0.83

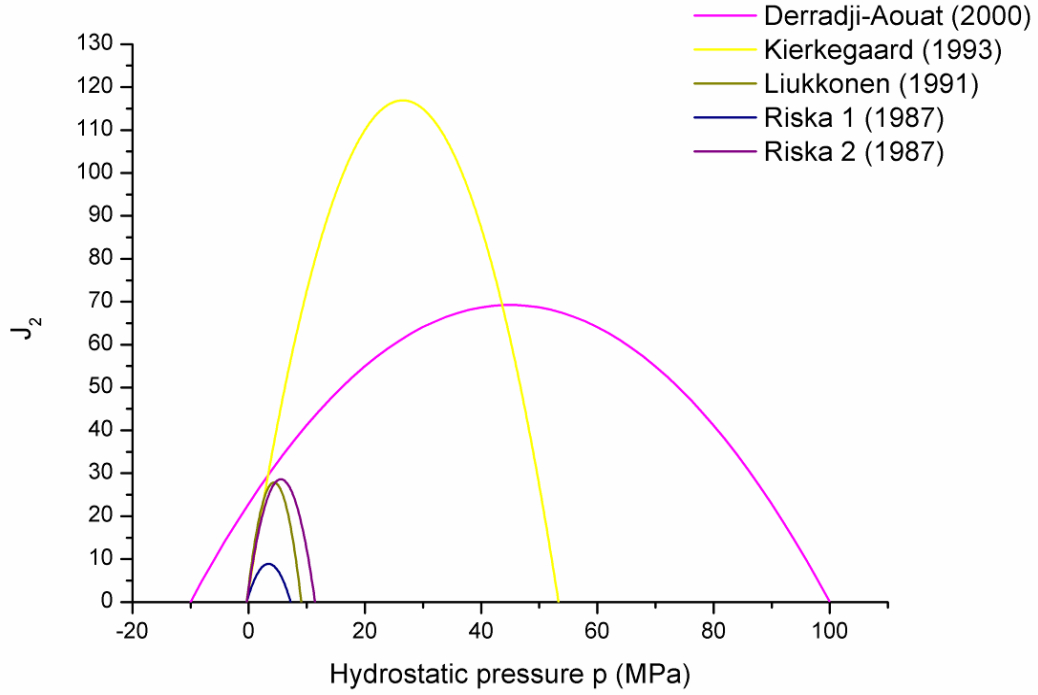


Figure 16 Tsai-Wu criteria plotted for different constants in $p - J_2$ space

Some analyses have been done on ice strength, but because of lack of experimental data on the strain rate effects, the strain rate dependence has not been included in Liu's material model. Instead a yield envelope for high strain rates is used in the simulations.

An *empirical* failure criterion is proposed and included in the material model. This is based on the effective plastic strain and the hydrostatic pressure.

The equivalent plastic stress;

$$\varepsilon_{eq}^p = \sqrt{\frac{2}{3} \varepsilon_{ij}^p \varepsilon_{ij}^p} \quad (14)$$

Failure strain;

$$\varepsilon_f = \varepsilon_0 + \left(\frac{p}{p_2} - 0.5\right)^2 \quad (15)$$

Where ε_{ij}^p is the plastic strain tensor, ε_0 is the initial failure strain and p_2 is the larger root in the yield function.

Different numerical simulations were performed to investigate the behaviour of the proposed material. The model is found to give good results, it undergoes mesh convergence and the computational time is acceptable. Ice properties used can be seen in Table 5.

**Table 5 Ice material properties**

Initial failure strain ϵ_0	1 %
Density [t/m ³]	0.9
Poisson's ratio Poisson's ratio[-]	0.3
Elastic modulus [GPa]	9.5
Cut-off pressure, tensile strength[MPa]	-2
Strain rate [s ⁻¹]	10 ⁻³

In the simulations pressure –area curves were made and a mesh size of 50mmx50mmx50mm was concluded to be appropriate for the ice model.

In a collision the dissipated energy is the coupling between the external and internal mechanics. A new formulation for calculating the maximum dissipated energy in a ship-iceberg collision is proposed:

$$E_o = \frac{1}{2} M_{iceberg} \hat{v}_{ship}^2 \frac{\left(1 - \frac{\hat{v}_{ice}}{\hat{v}_{ship}}\right)^2}{1 + \frac{M_{iceberg}}{M_{ship}}} \quad (16)$$

Where \hat{v}_{ice} and \hat{v}_{ship} is the velocities and $M_{iceberg}$ and M_{ship} is the mass properties of the ship and iceberg, respectively.

The material model is successfully applied to a ship-iceberg collision and the dissipated energy during the impact is calculated. The results prove that the model is optimistic for use in ALS calculations in ship-iceberg collision.



6.1 Pressure-area curves

Pressure area curves have been made for two different iceberg sizes, the iceberg shape and sizes are discussed later in Chapter 8.1.3. The icebergs are given a prescribed displacement of 2000 m in 0.5 s and are colliding with a rigid wall, 8 mm thick. The two iceberg models are provided by Ph.D. candidate Zhenhui Liu.

CASE 1 – small iceberg

First case a hemispherical shaped iceberg, with radius 5 m and an element size of 50*50*50 mm is colliding with a wall of 10*10m and an element size of 100*100mm.

The interface pressure for the two icebergs are found in LS-DYNA is shown in Appendix B.

By using eye measurement a pressure-area curve were plotted. Since the area of the maximum pressure is more than 1 m² the pressure for the smaller areas are just assumed and showed by a stippled line. The curve is plotted in Figure 17.

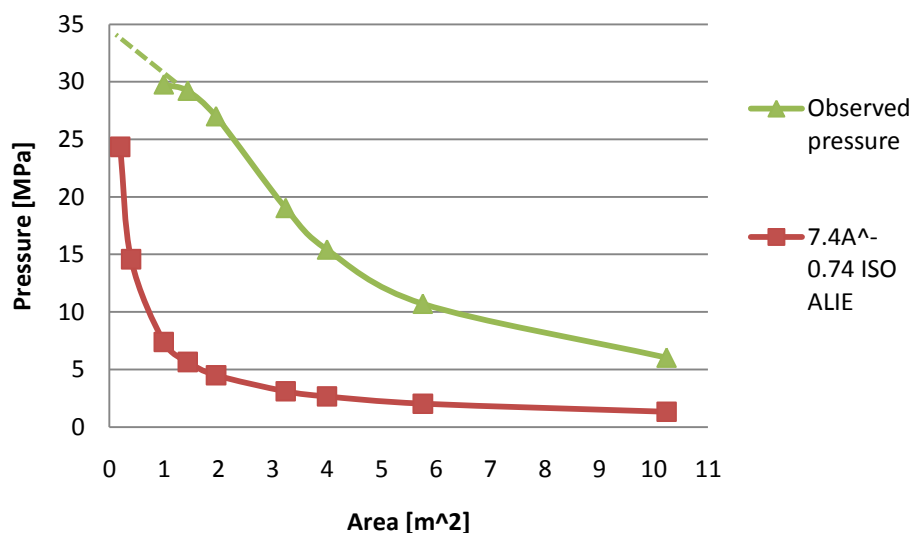


Figure 17 Pressure-area curve, Iceberg 1

CASE 2 – big iceberg

The next iceberg tested is a hemisphere with radius of 10 m. The element size of the hemisphere is 50*50*50 mm. The wall size is 20*20m with an element size of 200*200mm.

The pressure area-curve is plotted in the same way as for the small iceberg, included the assumed pressure for the smallest areas plotted as a stippled line. The graph is showed in Figure 18.

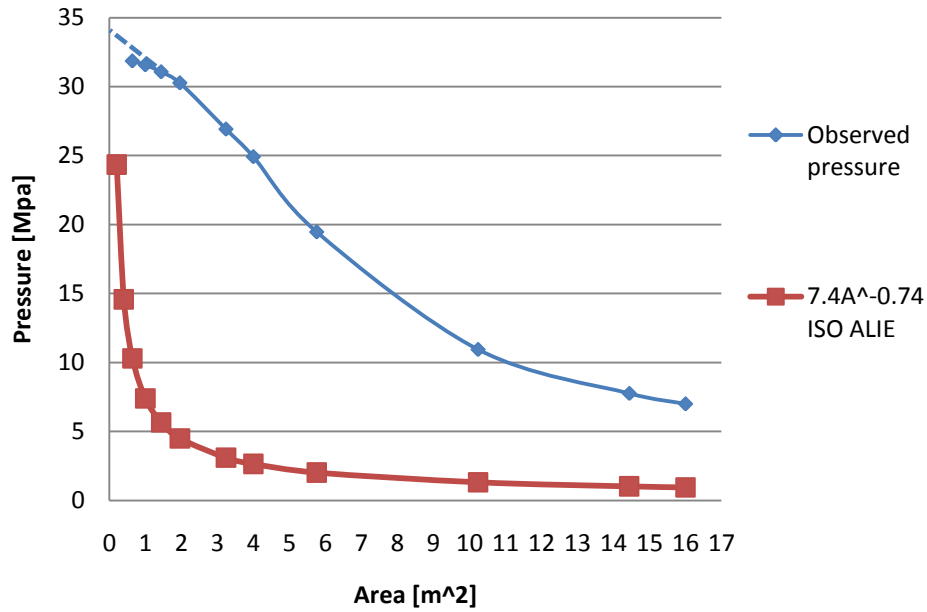


Figure 18 Pressure-area curve, Iceberg 2

For both pressure area curves the pressure is high. Compared to ISO pressure-area curve for ice the iceberg model might produce too high pressure and the iceberg model could then be a bit too stiff. Since the iceberg models are provided by Ph.D. candidate Zhenhui Liu they are assumed to be reliable for the later analyses.



7 Non Linear Finite Element

In structural analyse, nonlinearity can be divided into material, geometrical and boundary nonlinearity, [10].

Geometrical nonlinearity – Deformations in the geometry is allowed to be large compared to linear theory and the equilibrium equation must be written with the respect of the deformed structural geometry.

Material nonlinearity – Where the material is a function of the state of stress or strain. Hook's law is important. The modulus of elasticity is allowed to change, which will make the strain-stress relationship change.

Boundary/contact nonlinearity – In a collision/impact the contact force changes and the force-displacement curve is no longer linear. There could also be sliding force with frictional forces.

7.1 Solution methods

Both static and dynamic solution methods can be used to solve nonlinear problems. Static solution method could be used if you are interested in the long-term response of a structure subjected to an applied load that varies little with time, [9] and [10]. However, if the duration of the applied load is short or the loading is dynamic, a dynamic solution is preferred. For ship-iceberg impacts, the interaction is short and dynamic analysis is used.

Direct integration is calculations of response history using step-by-step integration time. The structural response from time $t=0$ to $t=T$ is divided into equal time step Δt and the structure displacement can be found in each step. Direct integration methods are classified into explicit and implicit methods. In explicit methods the displacement at one time step is directly obtained from the equilibrium conditions at that time step. This requires many step but low cost per time step. In implicit methods the displacement is obtained indirectly from the equilibrium conditions at the given time, including both current and later states. Implicit methods require fewer steps but higher cost per time step.



The CPU-cost can be calculated;

Explicit method: $\alpha \cdot \text{ndof}$

Implicit method: $\alpha \cdot \text{ndof}^3$

If the wave propagation problem is created by impact loading (short duration) an explicit method is preferred. Therefore, an explicit method is preferable for the thesis's ship-iceberg interaction.

7.2 Software

7.2.1 MSC Patran

For the finite element modelling MSC Patran is used. Detailed information is found in [15], but is briefly described here.

Patran is a widely used pre/post-processing tool, providing solid and shell modelling, meshing and analysis setup for LS-DYNA, Abaqus, ANSYS, MSC Nastran, Marc and Pam-Cash.

The software contains a large number of advanced geometry creation tools and the finite element modelling system permits the user to easily develop finite element meshes for surfaces and solids. The geometry contains intact in the original format and is imported into Patran database without any translation or modifications. Finite elements, loads, boundary conditions and material properties can be established and associated to the geometry in Patran. Analysis setup for the most popular FE solvers (mentioned above) is built in and minimizes the need to edit input decks.

7.2.2 LS-DYNA

The nonlinear finite element analysis is done in LS-DYNA. LS-DYNA is a tool to solve multi-physical problems, included solid mechanics, fluid mechanics and heat transfer. Full theory is described in the LS-DYNA theory manual [11] and some of the important factors are described below.

Time integration

LS-DYNA uses different integration tools. To decrease time cost without affecting the stability subcycling is used. Elements are sorted in groups based on their step size.

Constant length vectors are used as much as possible, even if that means that update the large elements incrementally with small time step size.



The time integration loop used in LS-DYNA is found in [11] and showed in Figure 19.

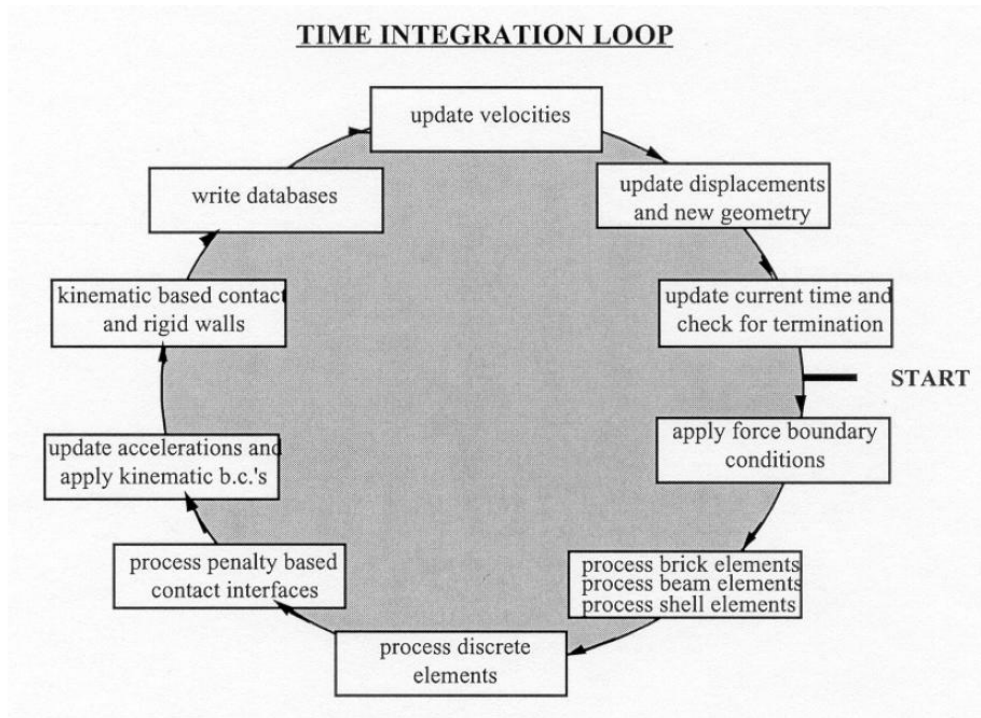


Figure 19 Time Integration loop in LS-DYNA

Time step control

For FEA the time cost is usually the governing factor. The time step size is limited by the smallest element in the finite element mesh. To fulfil the stability conditions the time step needs to be smaller than the time it takes the pressure wave from the impact to pass the element. If the time step is too large, the pressure wave will pass uncontrolled and cause the structure to become unstable.

For *shell elements* the critical time step size is given by;

$$\Delta t_c = \frac{L_s}{c} \quad (17)$$

where L_s is the characteristic length of an element and c is the sound speed in the material given by:

$$c = \sqrt{\frac{E}{\rho(1 - \nu^2)}} \quad (18)$$



where E is the Young's Modulus, ρ is the specific density of the material and ν is Poisson's ratio.

There are three ways to calculate the characteristic element length; default, conservative and non conservative. The default is the commonly used;

$$L_s = \frac{(1 + \beta)A_s}{\text{Max}(L_1, L_2, L_3, (1 - \beta)L_4)} \quad (19)$$

where $\beta = 0$ for quadrilateral and 1 for triangular elements, A_s is the area, and $L_i (i = 1, \dots, 4)$ is the length of the sides defining the material.

The critical time step for *solid shell elements* is;

$$\Delta t_e = \frac{v_e}{cA_{e_{max}}} \quad (20)$$

where v_e is the element volume, $A_{e_{max}}$ is the area of the largest side and c is the same as in Eq. (6).



8 NLFEA modelling

8.1 Model

The scantlings and ship data is provided by DNV. The ship is fictitious based on realistic dimensions and data from DNV software Nauticus, ref. [19]. Main dimensions for the LNGC is showed in Table 6.

Table 6 Main ship dimensions

L_{pp}	279 [m]
B	45.8[m]
D	26.5 [m]
T	11.95[m]
C_b	0.75 [-]
Tank length	50.4m
Cofferdam length (between tanks)	2.8 [m]

The centre of gravity of the ship is not given, but for later analyses the cog is assumed to be in the in the centre of the ship (in the middle of tank 3). A General Arrangement drawing of a similar membrane type tanker is showed in

Figure 20. A collision with iceberg would usually happen in the bow area and bow shoulder, but a collision in the side can happened if the ship starts to turn to avoid collision or waves and currents pushes the iceberg into the ship. For the later analyses the iceberg-ship impact is assumed to be perpendicular into the side of the ship, in the middle of Tank 2.

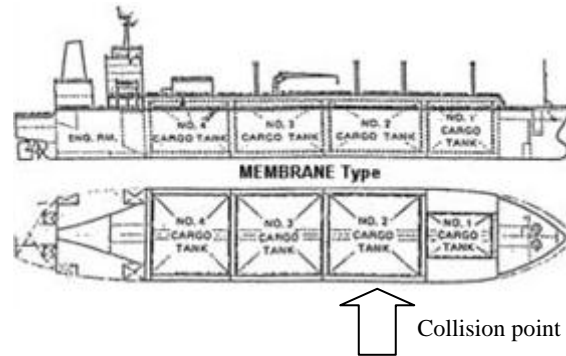


Figure 20 General Arrangement Membrane type LNGC

8.1.1 Geometry model

To reduce analyses time only the impacted tank is modelled. Boundary conditions are applied to simulate the end of the tanks and the symmetry around centre line, described in Chapter 8.2.2. Mid ship scantlings and node coordinates were provided by DNV, [18]. By using the node coordinates a 2D frame without stiffeners were made. Stiffener location and distance between the stiffeners were then used to include the stiffeners; the result can be seen in Figure 21.

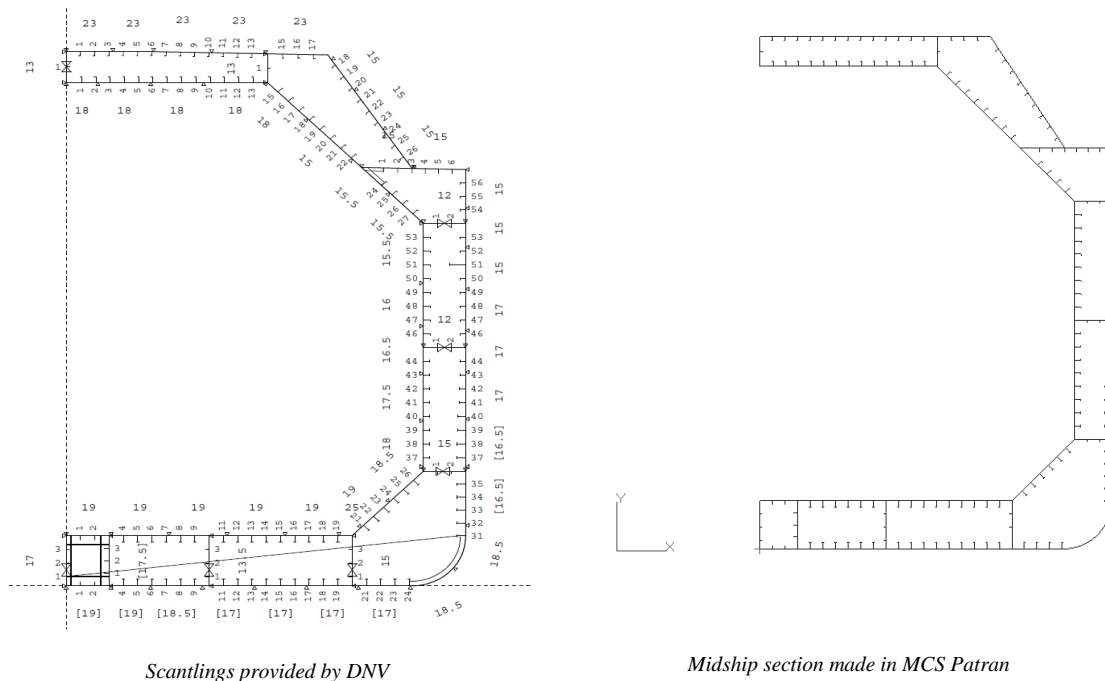


Figure 21 Midship section

To make the 3D section, all the parts in the 2D drawing were first extruded 3360 mm in z-direction. A transverse frame was added at the end of the section, see picture to



the left in Figure 22 . Each part were then divided in smaller pieces to simplify the meshing and then meshed by using automesh.

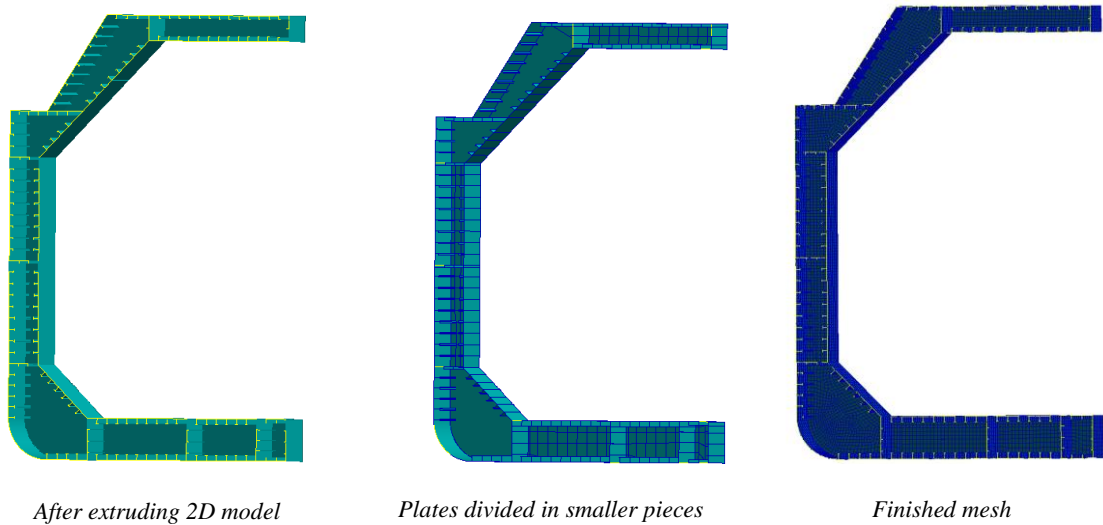


Figure 22 First part of 3D modelling/meshing

For the 3360 mm section 17331 elements were used. The element type and size is described in Chapter 8.1.2. The section were then copied and transformed 15 times in z-direction to make the total tank length of 50.4 m. The result can be seen in Figure 23.

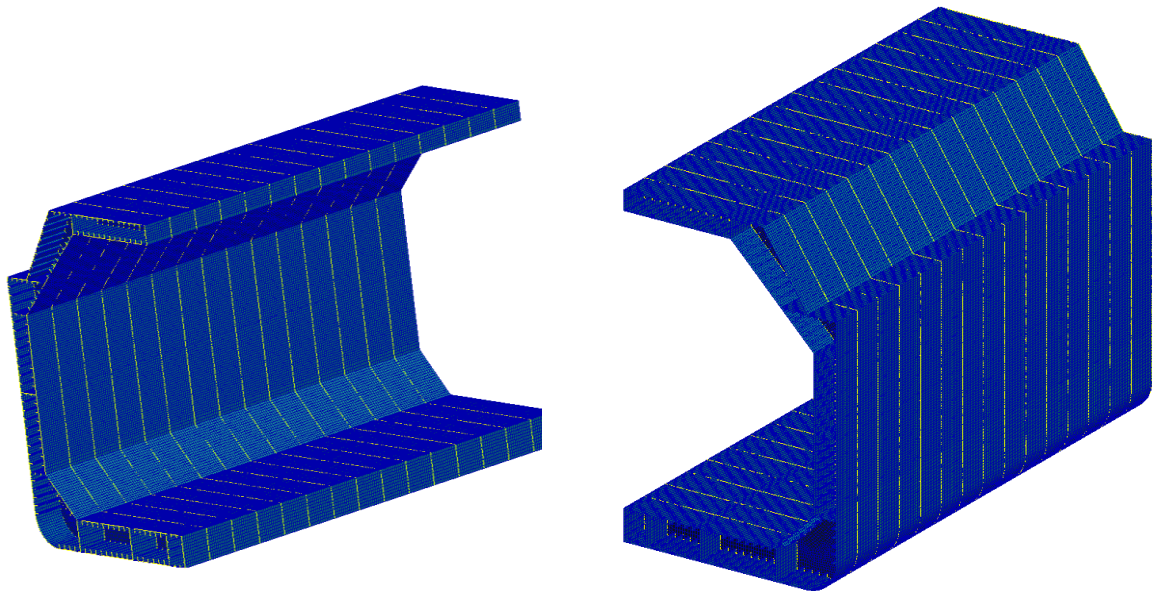


Figure 23 Finished tank geometry



8.1.2 Elements

The plates in the top, side and the bottom of the section in Figure 22 were divided in smaller pieces around the stiffeners to make the meshing simpler. For all these areas Quad4 shell elements are included by using isomesh. The elements seem to have a good aspect ratio, see Figure 24. An element size of 10 times the plate thickness is usually preferred and should for this structure be around the mean thickness of 15mm (150 mm mesh size). But because of the uncertainties of the total number of elements for both the structure and the iceberg, an element size of 250mm elements is used. The smallest elements are thought to be at the smallest stiffener's flange, with a 73 mm width.

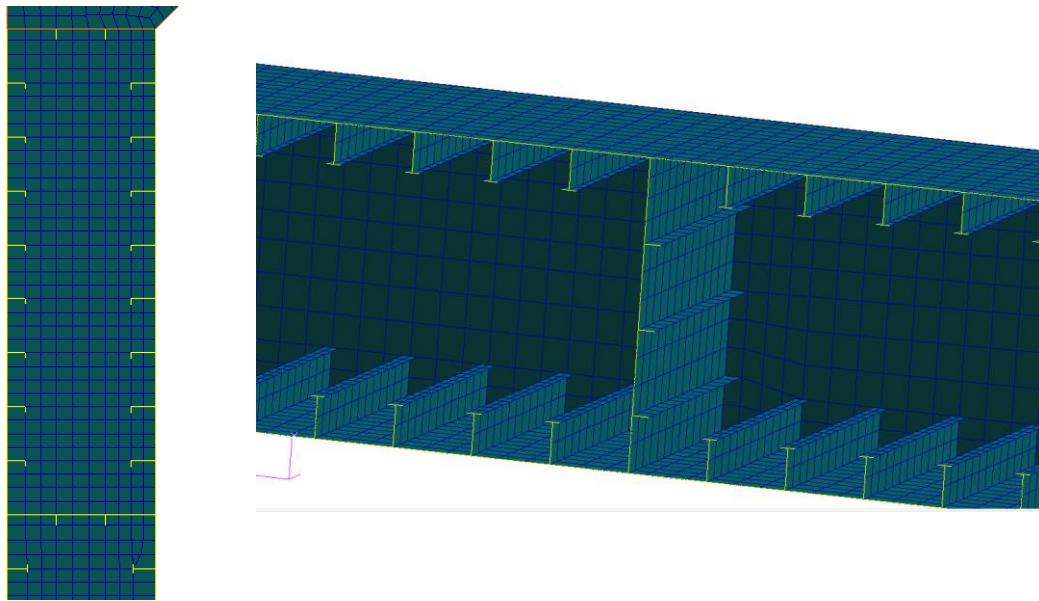


Figure 24 Quad4 isomesh, side and bottom part of structure

For the areas in the bilge plate and the sloping part of the tank top isomesh is not preferable and will not make an accepted mesh. Quad4 paver mesh is used together with mesh seeds on the edge to make the mesh consistent with the stiffener's mesh and the nodes on the side plates. The result of the paver mesh can be seen in Figure 25. For the paver mesh the same mesh size of 250mm is used.

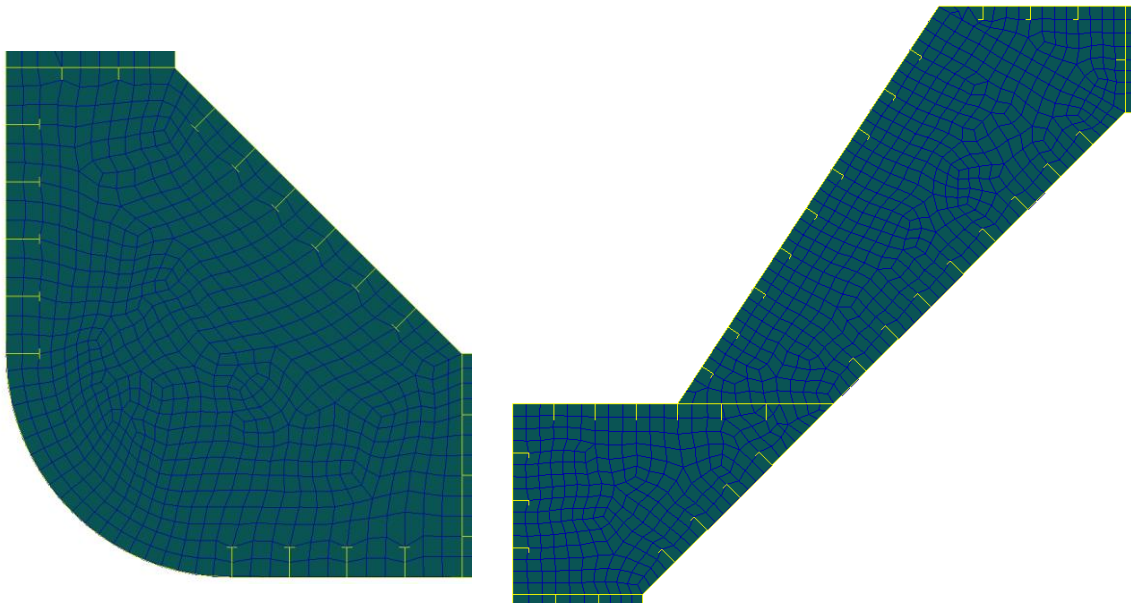


Figure 25 Quad4 paver mesh

The total number of elements in the ship structure reaches 256 873. Frank Klæbo at Marintek recommended that the total number of elements in the analysis should not exceed 500 000 elements due to long computational time. Since the iceberg is still not included in the final file for analysis, a total amount of elements of 256 000 is assumed to be sufficient to not reach the maximum number. The total number of nodes is 247873, all duplicate nodes are merged.

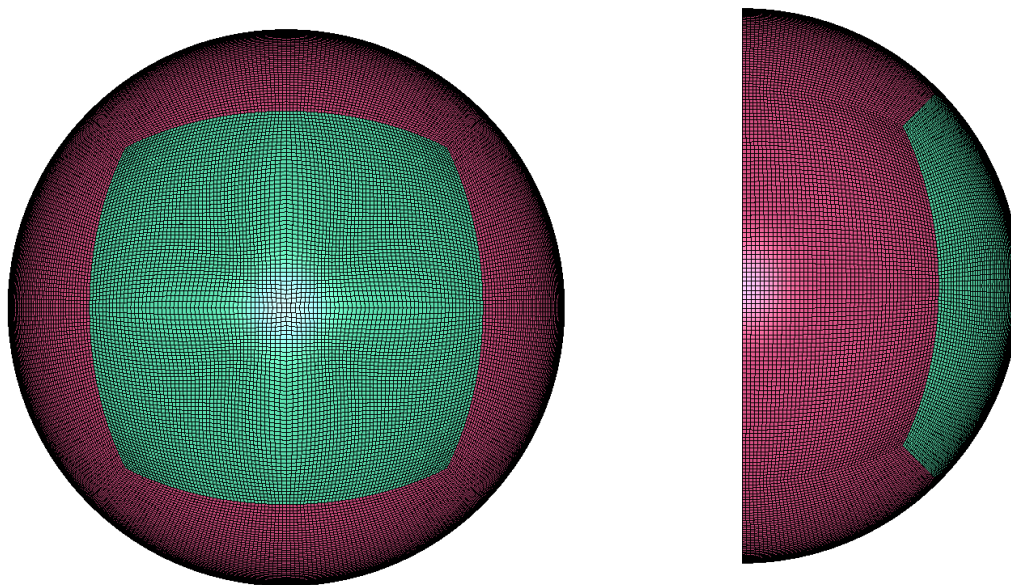
8.1.3 Iceberg model

Based on the shapes proposed by DNV in Chapter 5.2 sphere shaped iceberg models are assumed. Two different sizes are desirable. One with a radius of 5 meter as suggested by DNV for a sphere with a 2 meter sail height. To increase the mass of the iceberg, an iceberg model of 10 m radius is also proposed. The sail height for second iceberg is more than 2 meters, but is still used in the analyses. Due to lack in the provided software edition, two iceberg models are provided by Zhenhui Liu. Since only a small part of the iceberg will be in contact with the ship side, just half of the sphere is modelled. This will save computational time. The later analyses are done by giving the hemisphere prescribed displacement so the mass does not have any affect. The hemisphere is made of solid elements and divided in two, see Figure 26. The pink part of the hemisphere is assigned a rigid material and the green part a used defined iceberg material, see Chapter 8.2.1. For iceberg geometry definitions, see Table 7.

**Table 7 Iceberg geometry**

	Iceberg 1	Iceberg 2
Radius [mm]	5 000	10 000
Mass [tonnes]	471	3770
Mesh size [mm]	50	100

The mesh size of 100 mm is higher than what Liu has recommended in his material paper, but seen from the pressure-area curves in Chapter 6.1 the icebergs are acting similar in crushing and the maximum pressure is almost the same. The iceberg model could be a bit too stiff because of high interface pressure.

**Figure 26 Iceberg model**

8.2 Pre-processing

In LS-Prepost the pre-processing for the analyses is done. Material is added, contact area defined, boundary conditions introduced, prescribed displacement added and termination time given. Some of the different pre-processing actions are described under.



8.2.1 Material

In LS-Prepost several materials are defined. In the analyses three different materials are used. Elasto-plastic power law, rigid and user defined iceberg material. The material descriptions are found in LS-DYNA keyword manual, [16] and some of the main information is described below. Fracture or crack propagation in the ship shell plating is not accounted for.

SHIP SIDE

*MAT_POWER_LAW_PLASTICITY (MAT_18)

This material model provides elasto-plastic behaviour with isotropic power law hardening. The material is used both by Martin Storheim [8] and Zhenhui Liu and it sufficient to use for a ship structure made of mild steel.

The yield stress is a function of the plastic strain;

$$\sigma_y = k\varepsilon^n = k(\varepsilon_{yp} + \bar{\varepsilon}^p)^n \quad (21)$$

where $\bar{\varepsilon}^p$ is the effective plastic strain and the elastic strain at yield ε_{yp} is;

$$\varepsilon_{yp} = \left(\frac{E}{k}\right)^{\frac{1}{n-1}} \quad (22)$$

Strain rate is accounted for using a Cowper and Symonds model which scales the stress with the factor;

$$1 + \left(\frac{\dot{\varepsilon}}{C}\right)^{1/p} \quad (23)$$

where $\dot{\varepsilon}$ is the strain rate and C and p is strain rate parameters. Strain rate effects are neglected in the later analyses. The values used in Prepost can be seen in Table 8.

Table 8 Steel material properties

Density ρ [t/mm ³]	Young's Modulus [MPa]	Poisson's ratio [-]	Strength coefficient [MPa]	Hardening exponent[-]	Initial yield stress [MPa]
$7.89 \cdot 10^{-9}$	$2.1 \cdot 10^5$	0.3	740	0.24	275



RIGID

*MAT_RIGID (*MAT_20)

This material provides a convenient way to turn shell and solid elements to a rigid body. Rigid material is very cost efficient since no storage is allocated. For the analyses the pink part of Figure 26 is assumed to be rigid. This will lower the CPU time and have no affect on the final result. Another advantage is that the rigid part can be assigned prescribed displacement and then push the pink iceberg part into the ship side, described in Chapter 8.2.3.

Realistic values for Young's modulus, Poisson's ratio and density should be defined for the rigid material to get the sliding effect in the contact area. Unrealistic values may contribute to numerical problems therefore realistic values should be used. In the analyses mild steel properties have been included, see Table 9.

Table 9 Rigid material properties

Density ρ [t/mm ³]	Young's Modulus [MPa]	Poisson's ratio [-]
$7.89 \cdot 10^{-9}$	$2.1 \cdot 10^5$	0.3

ICEBERG

*MAT_USER_DEFINED_MATERIAL_MODELS

A user defined material has been provided by Zhenhui Liu based on his work with ice mechanics, Chapter 6. The material properties are assigned to the pink part of Figure 26 and run from a specific folder with LS-DYNA to get the right crushing and behaviour.

8.2.2 Boundary conditions

Only a part of the LNG tank is modelled and boundary conditions need to be introduced to compensate for the none-modelled ship structure. From Storheim's Master Thesis [8] it is found that the differences between inertia controlled and pinned boundary conditions is practically none-existing. The impact will happen in the centre of the tank and the deformation in the tank structure is assumed to be relatively small compared to the tank length. At the ends of the LNG tanks there is a transverse



bulkhead. Pinned boundary conditions are used for the analyses. To compensate for the stiffness of the bulkheads the tank ends are fixed in translation, but are allowed rotation. Around the centre line symmetry is assumed, this is conservative since there will not be a similar impact on the other side at the same time. The boundary conditions is discussed with Professor Jørgen Amdahl and Ph.D. candidate Zhenhui Liu and found reasonable. The boundary conditions adopted is presented in Table 10 and included in LS-Prepost with the command `*BOUNDARY_SPC_SET_ID` for the different areas.

Table 10 Boundary conditions

	Tx	Ty	Tz	Rx	Ry	Rz
Centre line	1	0	0	0	1	1
Left side	1	1	1	0	0	0
Right side	1	1	1	0	0	0

0 = free, 1 = fixed

8.2.3 Prescribed displacement

Instead of using initial velocity, prescribed displacement is added to the rigid (pink) part of Figure 26. Since the rigid part is behind the iceberg part (green) of the hemisphere, the rigid will push the iceberg part against the ship side simulating a collision forced by currents and transverse ship velocity. The hemisphere has x-translational degree of freedom and is moving in negative x-direction (towards the ship structure). From Chapter 5.3 the ship is assumed to have a transverse speed of $0.1 \cdot V_r$. Assuming a max speed of a LNG carrier to be 20 knots the transverse speed of the vessel is 2 knots. The drifting speed of the iceberg is in Chapter 5.2 assumed by DNV to be 2 knots. Thus, the collision velocity will be around 4 knots.

In LS-Prepost a curve scale factor is added and the prescribed displacement is given to be 2000 mm in 0.5s. This is equal to a collision speed of 4 m/s and some higher than the speed recommended by DNV. The speed is increased to have the wished displacement but at the same time decrease the computational time by decreasing the introduced deformation time. However, since strain rate is not included the impact speed would not affect the main result. The increased velocity could infect the buckling process and lower the ship structure's buckling load.

`*BOUNDARY_PRESCRIBED_MOTION_RIGID_ID` in LS-Prepost is used to give the rigid body the prescribed displacement.



8.2.4 Contact

Three different types of contact are defined. There is no need for a contact area between the rigid and the iceberg material part of the hemisphere because they are sharing nodes. One contact type had to be made for the contact between the iceberg and the ship side (master-slave) and two self contact types for each of the impact members. *CONTACT_ERODING_SURFACE_TO_SURFACE was used for the iceberg-ship contact area. For the self contact at the iceberg an eroding single surface was used and for the ship side an automatically single surface.

8.2.5 Termination time

The termination time is set to 0.5 second, same as when the prescribed deformation is reached. 20 output frames are included with a time interval of 0.025s .



9 LS-DYNA simulation results

9.1 Deformation

The iceberg is given a prescribed displacement and will try to move 2000 mm into the ship structure. The distance between the ship and the iceberg before the displacement start is 100mm. Because the iceberg is an eroding material the penetration in the outer hull could be less than the expected 1900 mm. The iceberg will crush and elements fail and if the size of the striking iceberg is small the ship structure will resist much of the deflection.

An example of the analysis outline is illustrated in Figure 27. This outline illustrates the smallest iceberg colliding in 12 meter height in the middle of the tank (collision point 2).

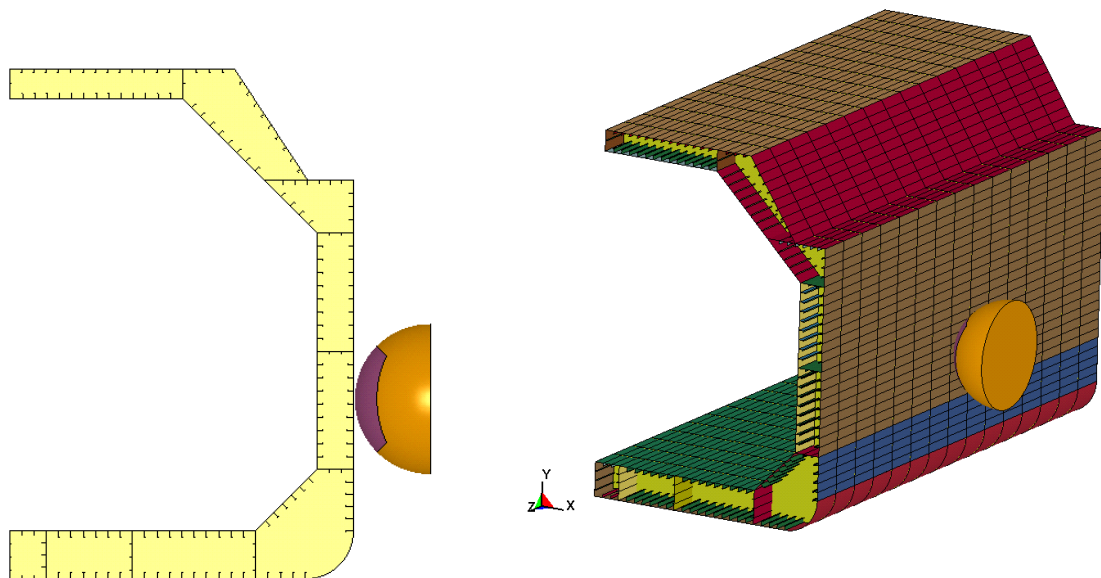


Figure 27 Analyses outline

Twelve different colliding cases are analysed. Six cases using an iceberg with diameter of 10 m (Iceberg 1) and six with a diameter of 20 m (Iceberg 2). The collision height on the ship side and the location in longitudinal direction is changing to see which parts of the tank structure that is most critical concerning iceberg impact.

The draft of the ship is 12 m, refer Chapter 8.1. Since the iceberg is assumed to have a sail height of 2 meters the actual collision point should be underneath 12 meters



assuming spherical shaped iceberg. But since the realistic shape of an iceberg is not spherical, and currents, waves and roll for the ship can affect the collision point on the ship side, different collision height is assumed. The result of the maximum deformations can be seen in Figure 29 and Figure 30 illustrated by von mises stress. To see how the von mises stress is distributed during a collision see Appendix C or videos attached in Appendix G.

The coordinates for the local collision points are indicated in Table 11. The origin of the coordinate system is in the end of the tank side at centre line.

Table 11 Collision Point coordinates

Collision Point	x-direction	y-direction	z-direction
1	23.0m	15.0m	25.2m
2	23.0m	12.0m	25.2m
3	23.0m	12.0m	24.0m
4	23.0m	12.0m	5.2m
5	23.0m	9.0m	25.2m
6	23.0m	9.0m	24.0m
7	23.0m	5.0m	25.2m

The maximum deflections in inner and outer hull are summaries in Table 12.

The global x-deformation of the ship side in collision point 2 is illustrated in Figure 28.

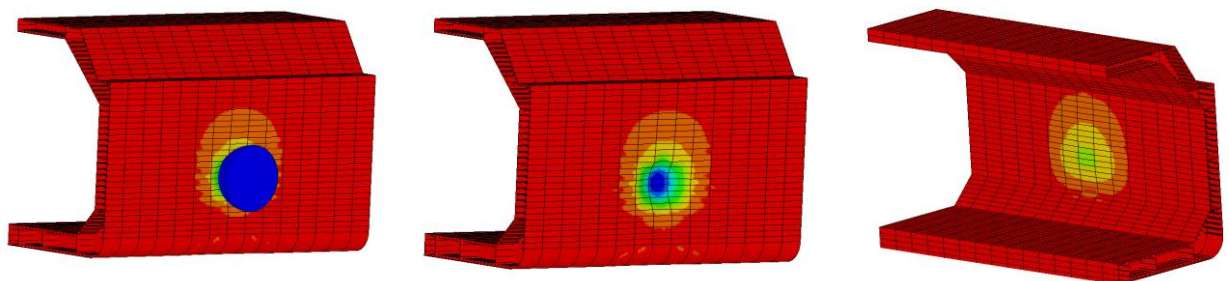


Figure 28 Global x-deformation of a ship side

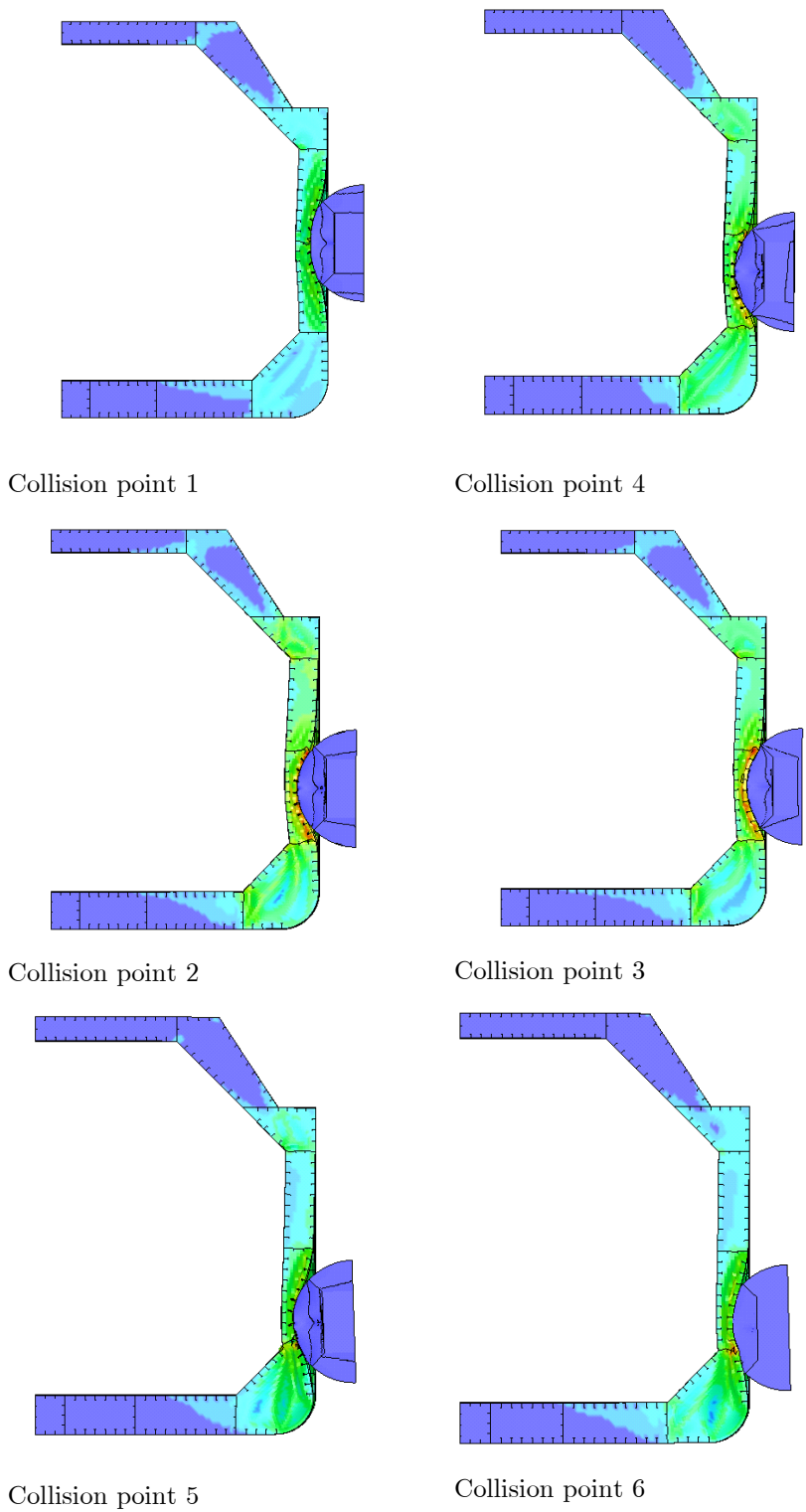


Figure 29 Deflection of ship side and von mises stress distribution in different collision points, Iceberg 1

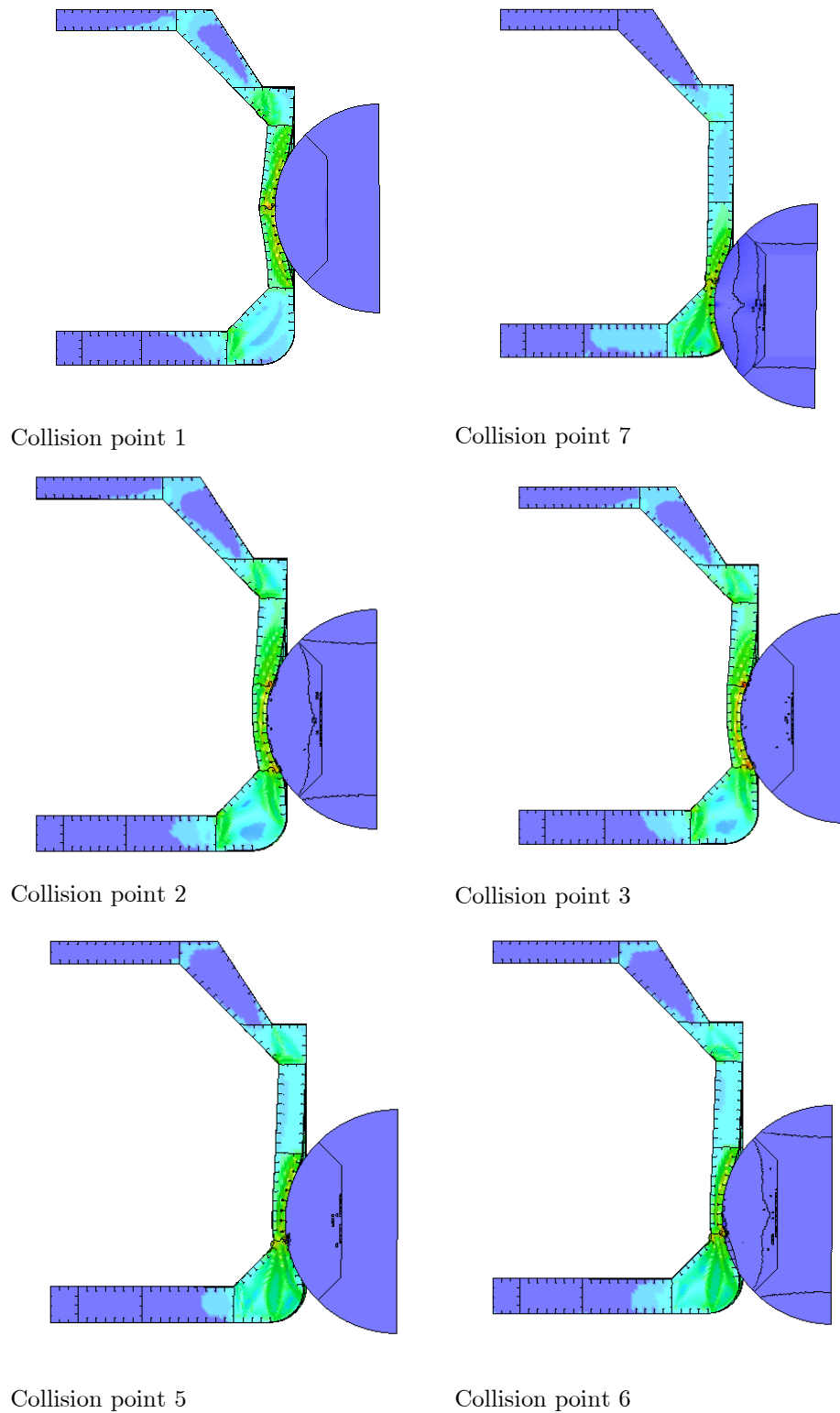


Figure 30 Deflection of ship side and von mises stress distribution in different collision points, Iceberg 2



Table 12 Inner and outer hull deflection and collision point

Collision point			Deflection, x-direction [mm]		
Nr.	y-direction	z-direction		Iceberg 1	Iceberg 2
1	15 m	25.2 m	Outer hull	1500	1900
			Inner hull	400	1050
2	12 m	25.2 m	Outer hull	1900	1900
			Inner hull	550	800
3	12 m	24 m	Outer hull	1700	1900
			Inner hull	400	750
4	12 m	5.2 m	Outer hull	1900	-
			Inner hull	530	-
5	9 m	25.2 m	Outer hull	1900	1900
			Inner hull	400	800
6	9m	24 m	Outer hull	1400	1900
			Inner hull	200	650
7	5 m	25.2 m	Outer hull	-	1900
			Inner hull	-	450

The design criteria discussed in Chapter 2.4 accept an inner hull deflection of 700 mm. For the smallest iceberg, Iceberg 1, there is no collision point reaching a maximum inner hull deflection of more than 700 mm and the probability for leakage is small/not existing. The deformations are as expected greater for the biggest iceberg collisions, Iceberg 2. The most critical collision is in 15 meter height, where the inner hull has a deflection of more than 1000 mm. All points except collision point 6 and 7 would give an inner hull deflection greater than 700 mm for the given assumptions.

There are some differences in the deflections for impacts happening in the same collision height but with different z-location. For collision in e.g. collision point 5 and 6, the collision at the middle of the tank (position 5) gives a greater deflection than the one 1.4 m closer to the side(position 6). This could be related to the fact that at 25.4 meter(middle of the tank) the collision point is between two transverse frames, but at 24 m the collision point is directly on a transverse frame.



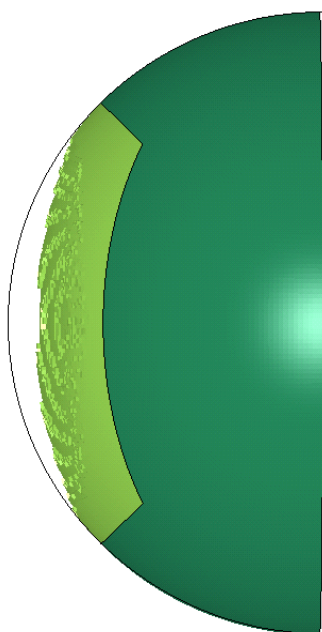
Collision point 1, 2, 3 and 4 are above or in the water line. These are the most uncertain colliding areas since the iceberg probably will collide somewhere under the water line where most of the iceberg mass is gathered. It is in point 5, 6 and 7 the collision most likely will happen, and these points give the smallest deflection of the inner hull.

Because of the crushing of the iceberg and stiffness in some parts of the ship side the outer hull deflection does not reach 1900 mm which is the prescribed deflection.

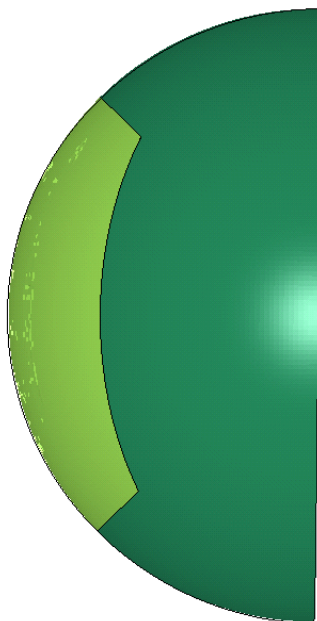
9.2 Crushing of iceberg

As found in the pressure–area curves in Chapter 6.1, the iceberg is relatively stiff and the crushing of the iceberg is not big. The deformation and crushing of the ice is illustrated for the two different icebergs in Figure 31 and Figure 32 . There is some crushing especially for Iceberg 1, this iceberg is small compared to the ship structure and the structure resists the movement and crushes the iceberg more compared to Iceberg 2.

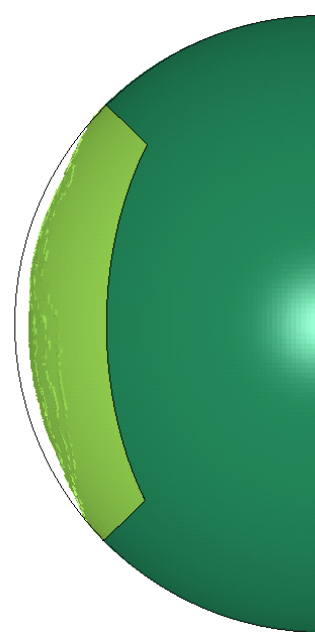
For the areas where the collision is at point where there is a stiffener or stringer the crushing of the iceberg is greater, e.g. collision point 1,3,5 and 6.



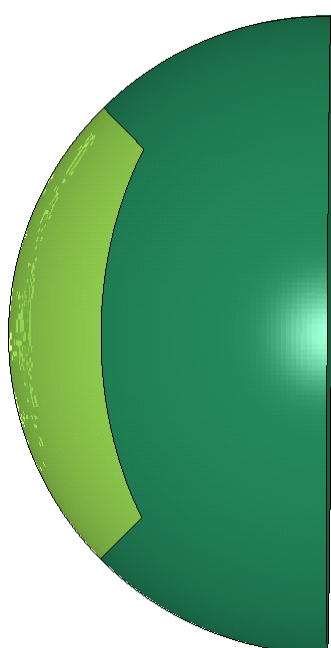
Collision point 1



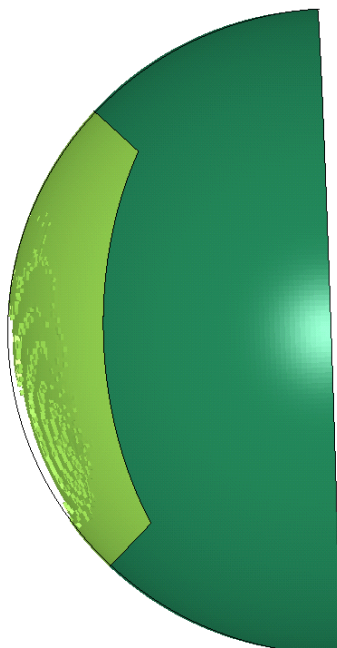
Collision point 2



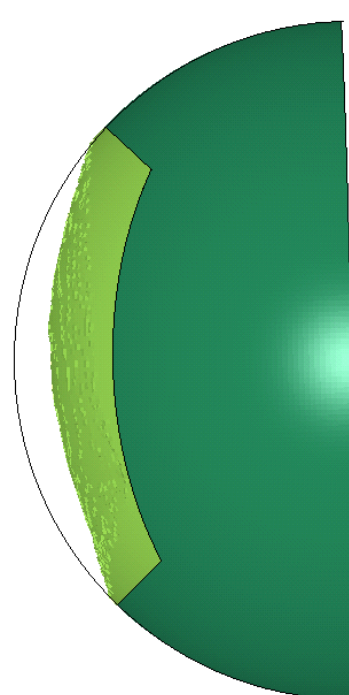
Collision point 3



Collision point 4

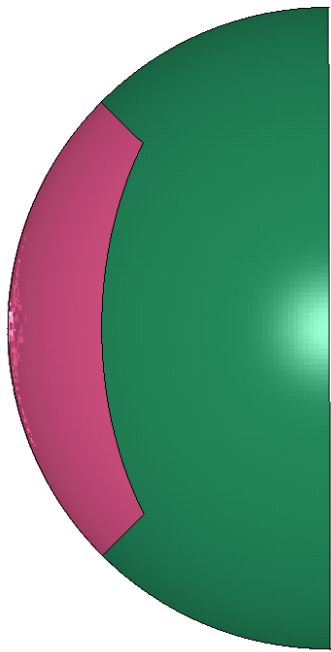


Collision point 5

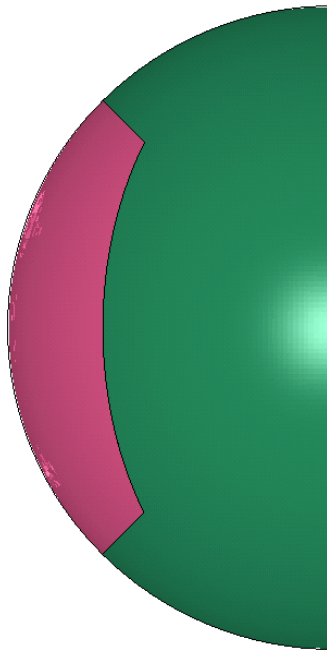


Collision point 6

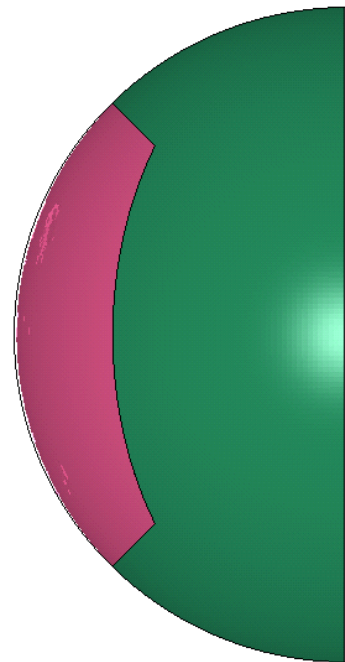
Figure 31 Iceberg crushing - Iceberg 1



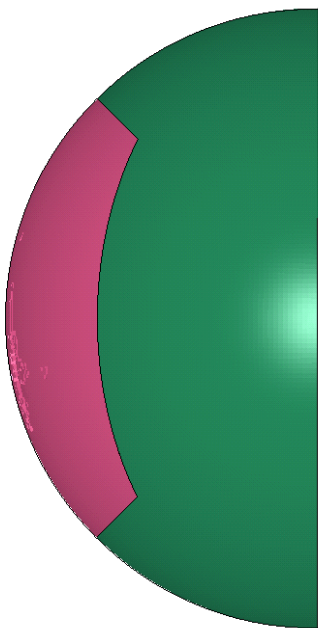
Collision point 1



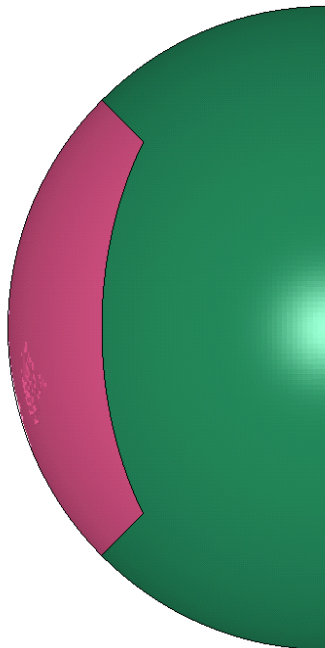
Collision point 2



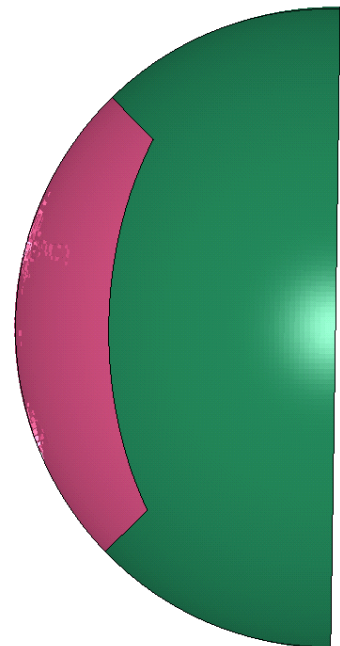
Collision point 3



Collision point 5



Collision point 6



Collision point 7

Figure 32 Iceberg crushing – iceberg 2



9.3 Accelerations

In the Korean reports in Chapter 3, some of the acceleration found is very high. For three different locations on the ship side; inner hull, outer hull and side, deflection, velocity and accelerations have been recorded with a time step of 0.1 ms at some the most critical nodes. Graphs from two different collision cases have been recorded, Iceberg 1 and 2 colliding in collision point 5 respectively. The outer and inner hull accelerations for collision with iceberg 1 are presented here, the rest of the graphs can be seen in Appendix D.

For the critical node in the outer hull the accelerations found are quite large, but as the graph in Figure 33 illustrates, the large acceleration is only for a short duration.

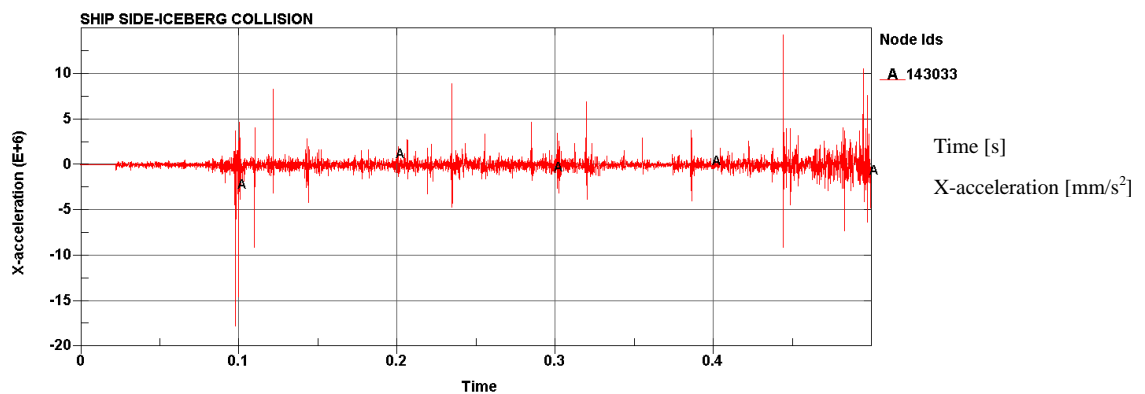


Figure 33 Acceleration in node at outer hull, Collision point 5 – Iceberg 2

For the inner hull the duration of the large acceleration is longer. Accelerations of 500 m/s^2 have duration of 10 ms, marked with a black circle in the upper plot in Figure 34. A consequence of this could be pertaining oscillations in the ship hull that could cause damage other places far away from the collision point. Oscillations could be noticed by the crew on the ship and if the oscillations are high they can harm people and consequently cause injuries.

The corresponding velocity and displacement curves are also showed in Figure 34. The displacement curve is quite smooth, only some small vibrations are noticed in the same time as the large acceleration. Hence, the accelerations do not need to be considered as a critical for this analysis.

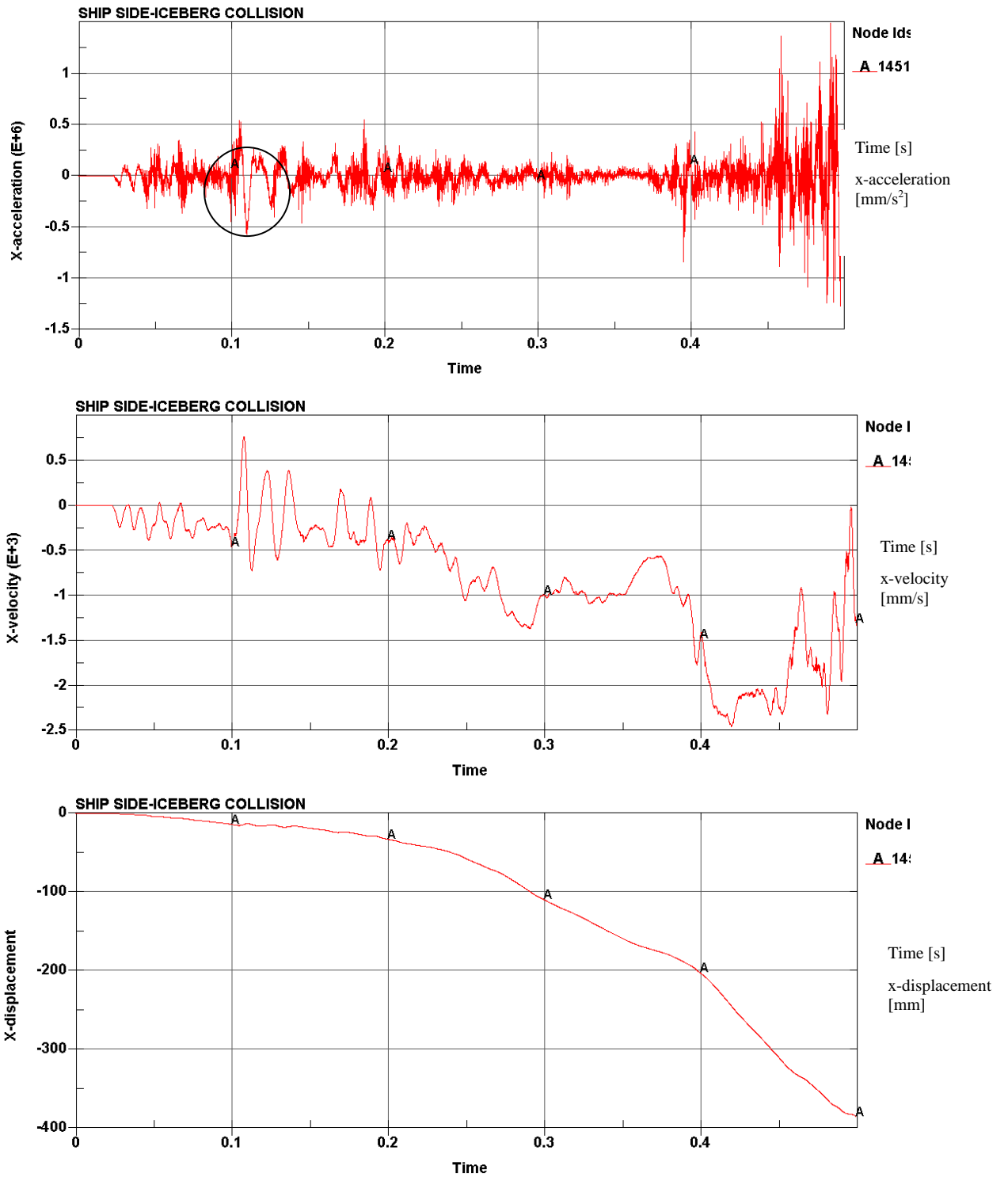


Figure 34 Acceleration, velocity and displacement curves – inner hull node



9.4 Energy dissipation

In Chapter 4 the principles of external and internal energy are introduced. The internal energy, the strain energy dissipated under crushing and deformation of the object under the impact, is plotted in a time-internal energy curve from LS-DYNA.

The dissipated energy from different collision scenarios with iceberg 1 and iceberg 2 is plotted in Figure 35 and Figure 36 respectively. The original curves from LS-DYNA can be seen in Appendix E.

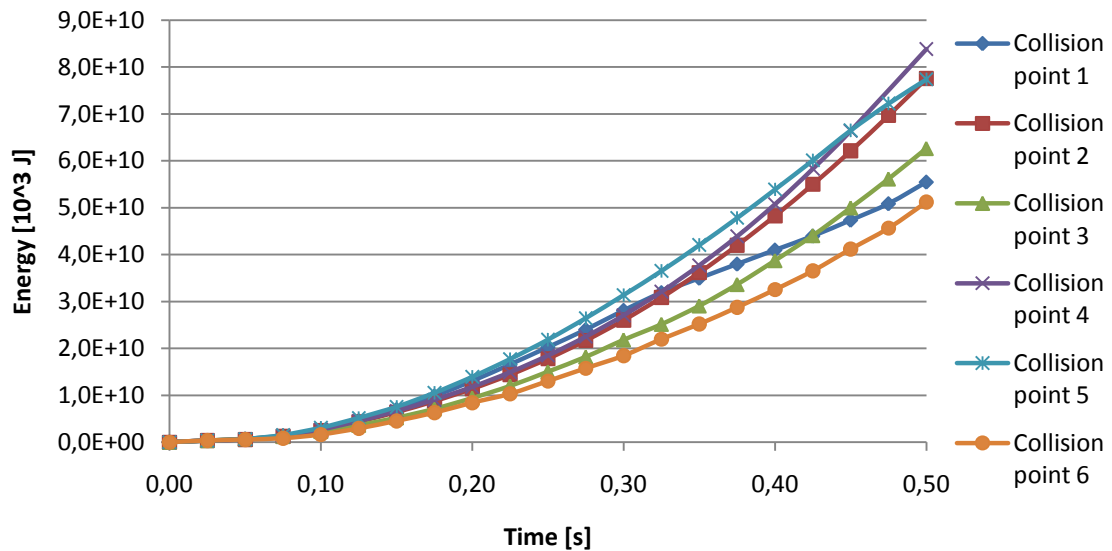


Figure 35 Dissipated energy – Iceberg 1 impact

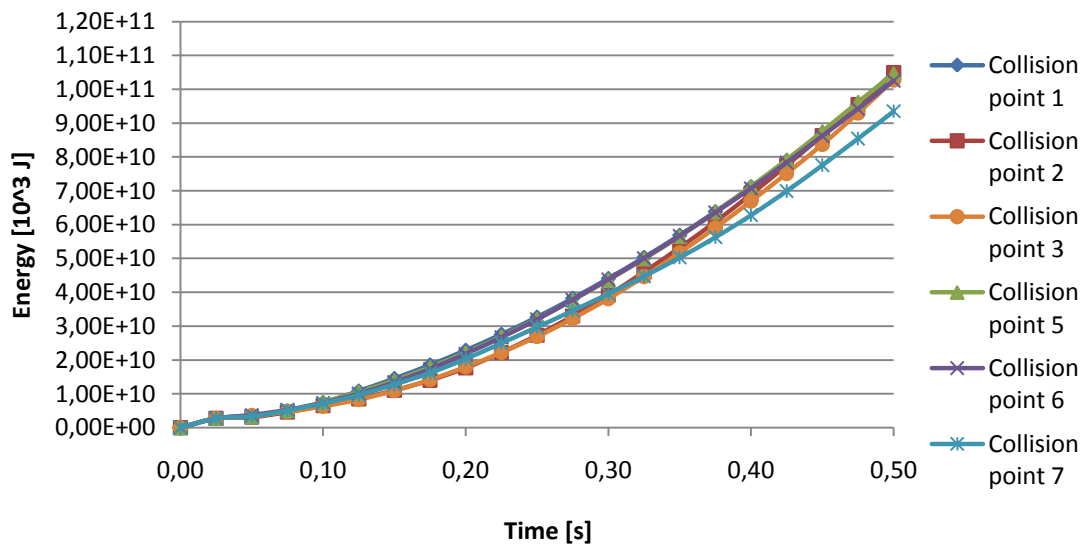


Figure 36 Dissipated energy – Iceberg 2 impact



The dissipated energy curves are slightly different for the different collision point for iceberg 1 compared to the ones for the iceberg 2 which is relatively similar. This is related to the different deflections for the hull in Chapter 9.1. For the graphs with the smallest values for dissipated energy the deflection of the ship's hull is smaller. Naturally, since the energy dissipated as strain energy is less. More of the energy is used in deformation of the iceberg.



10 Predicted damage

The method to do external energy calculations, the energy released for dissipation as strain energy, is presented in Chapter 9.4. To calculate the demanded energy Ph.D. candidate Liu has developed a MATLAB code. The code is based on Strong's impact mechanics and assume that the two colliding object have different coordinate system. For the analyses done in this thesis, the iceberg is colliding perpendicular to the ship side and the two object can be assumed to collide in the same coordinate system. The iceberg shape is spherical, which is simpler than the diamond-shaped iceberg Liu has presented in his work. Consequently, the MATLAB code has been modified for this case and attached in Appendix F. The dissipated energy calculations have been done for the 12 different collision points and the result can be se in Table 13. The global coordinate system is the coordinate system for the ship, where origin is in the centre of gravity found in Chapter 8.1. The collision velocity is 4 m/s as described in Chapter 8.2.3.

Table 13 Dissipated Energy Calculations

Collision point nr.	Collision point in global ship coordinate system [m]			Iceberg 1 [J]	Iceberg 2 [J]
1	50.4	22.9	2	5.60e+006	4.34e+007
2	50.4	22.9	-1	5.60e+006	4.34e+007
3	49.2	22.9	-1	5.61e+006	4.34e+007
4	30.4	22.9	-1	5.61e+006	-
5	50.4	22.9	-4	5.60e+006	4.33e+007
6	49.2	22.9	-4	5.60e+006	4.34e+007
7	50.4	22.9	-9	-	4.30e+007

The values from Table 13 are included in the graphs found in Chapter 9.4 and the pertaining time step is found. This is illustrated in Figure 37 and Figure 38. The demand for dissipated energy for the recommended collision velocity of 2m/s suggested by DNV is also included in the graphs to illustrate the difference.

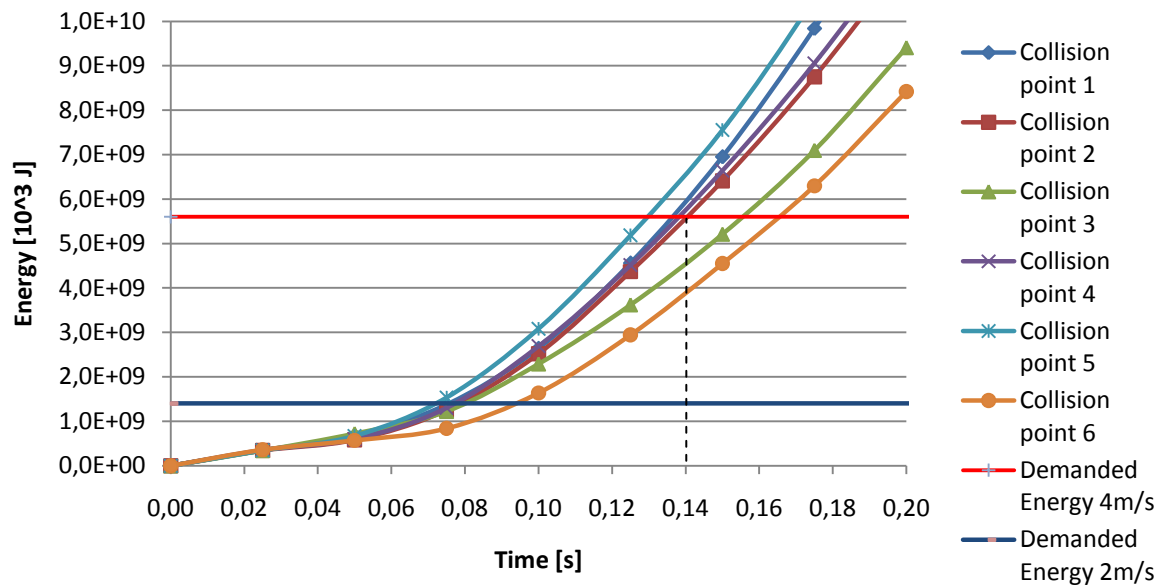


Figure 37 Demanded energy for dissipation – Iceberg 1 collision

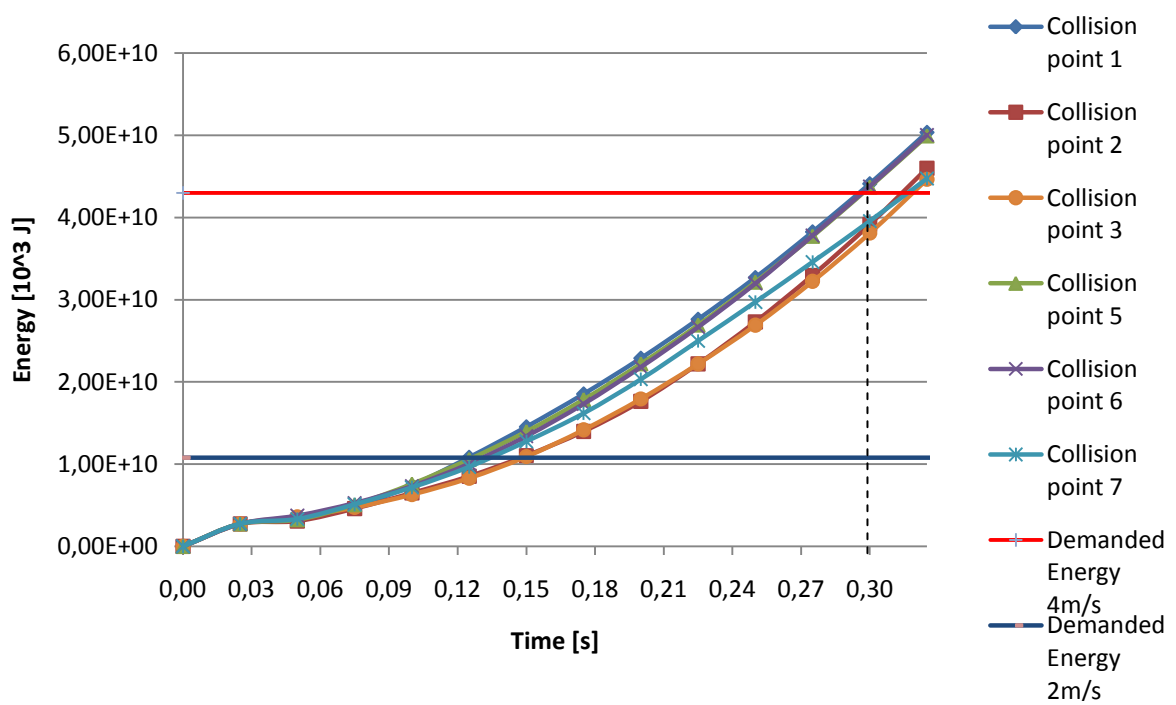


Figure 38 Demanded energy for dissipation – Iceberg 2 collision

From Figure 37 the demanded dissipated energy at 4m/s is reached at 0.14 s for the most critical collision point with iceberg 1, collision point 2. For collision with iceberg 2 at the most critical point, collision point 1, the demanded dissipated energy level is



reached at 0.3 s, illustrated in Figure 38. The x-displacement curves for relevant nodes in the critical scenarios are plotted in Figure 39.

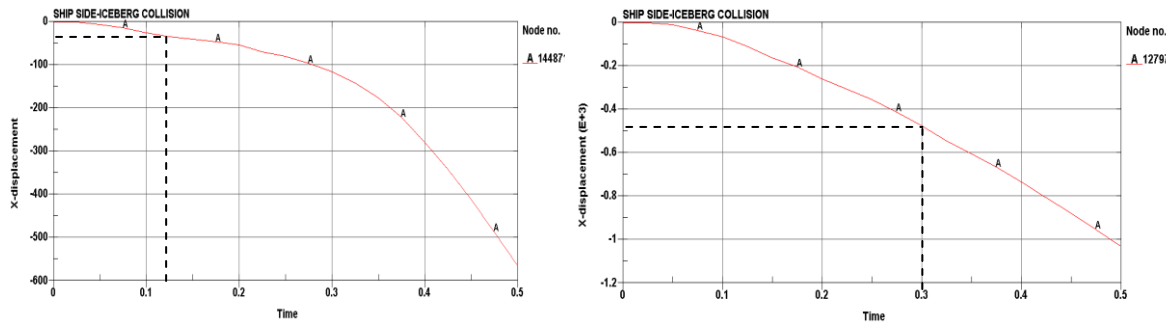


Figure 39 Most critical node in inner hull, in collision with iceberg 1 (left) and iceberg 2(right)

As detected in 9.1 the maximum deflection in a collision with iceberg 1 will never reach a critical level with the assumptions used in this thesis. From the graph seen in Figure 39, the x-displacement at 0.12 s is 50 mm and not critical for any leakage from the membrane tanks. The deflections are greater for Iceberg 2 and there could be some critical areas. For the given dissipated energy at 0.3 s, the x-deformation is around 450 mm and is not critical considering the design limit in Chapter 2.4., 700 mm deflection of inner hull. If the collision velocity of 2 m/s suggested by DNV were used the deflection would be even less, respectively 20 mm and 100 mm.

To reach 700 mm inner hull deflection for an impact with iceberg 2 in collision point 1, the dissipated energy level needs to be approximately 70 MJ. The dissipated energy level is increasing drastically with the collision speed. If the sideways velocity of the ship and the drifting speed of the iceberg together reaches 5 m/s the demand for dissipated energy is 67,7 MJ. A collision speed of above 5m/s could make a severe damage to the inner hull and potentially get leakage in the membrane.



11 Discussion/Conclusion

LNG carriers sailing in Northern areas will increase the following years due to increasing gas production. The increasing use of LNG carriers in these areas will increase the possibilities of iceberg impacts and with worst case consequences as leakage. The topic is highly relevant and the uncertainties of the consequences are important to investigate.

A ship side model has been created and analysed for 7 different impact locations with two different iceberg models. The total number of element of the ship structure is above 256 000. The element size is 250 mm and could be smaller to get a more accurate result. This is a topic for further work. The iceberg material and FE model are provided by Ph.D. candidate Zhenhui Liu and are not verified, but assumed to be reliable for the analyses done. In pressure-area curves the iceberg were found to give high pressure for large areas and the material could be a little too stiff. This could give an uncertain result for the deformation of the ship side.

The inner hull deformation found in collisions with the smallest iceberg was not large enough to exceed the established design criteria. For the largest iceberg the critical inner hull deflection could be reached, but in a collision point higher than the waterline and in a collision speed higher than a realistic value for side collision. An inner hull deflection exceeding the critical limit would not happen if the assumptions in this thesis are assumed.

A collision at a height of 9 meter, the bilge area, does not have a great influence of the inner hull deflection because stiffeners and plates are stiff and resist some of the deformation. But, the small deformation in the corner of the inner hull at the bilge could be critical because this is a point where it typically is a break in the membrane plates because of the changing angel. The critical limit for this area could be less than 700 mm. The design criteria/survival limit for the corner/bilge area of the tank is not established in this thesis and is a topic for further work.



In previous work established in Korea, the accelerations in the impact could reach very high levels. The accelerations are found for some critical nodes in inner and outer hull and a node in the side far away from the collision point. The accelerations do reach a high level in the outer hull but only for a very short duration. The change in the corresponding displacement curves could be neglected. The oscillations created in the impact are assumed to be small and will not cause failure in other parts than the impact point of the CCS.



12 Recommendations for further work

A FE model has been made with a mesh size of 250 mm. The mesh size should be around ten times the plate thickness and a mesh size of 150 would rather be preferable. Analyses with a finer mesh would take longer computational time but would give better accuracy in the results. For further work a model with finer mesh could be used.

By making only a small part of the ship structure, boundary conditions need to be introduced to represent the missing structure. This would make the structure relatively stiff and do not represent how the forces would develop to in the not modelled parts. Analyses introducing the whole ship structure could be investigated.

The collision speed assumed is used to get the wanted damage in the ship structure. Analyses could be done with different collision speeds.

All impacts analysed in this Thesis happens perpendicular to the ship side. Direct perpendicular collisions would rarely happen, even if the ship is turning, and different collision angels should be further investigated. Other collision points on the ship side as directly into the transverse bulkhead or in the cofferdam could be looked further into, together with collision in the bow area (bow shoulder) were the collision speed would be higher.

An impact happening directly in the bilge could be further investigated with a new design limit for this critical point.

The iceberg models are provided by PhD candidate Zhenhui Liu and not checked for accuracy. The knowledge of the given material models used in the analyses is limited and the models are assumed to be reliable. For later analyses more time could be spend on material and accuracy could be checked concerning the relatively stiff material found in the pressure-area curves in this thesis.

To simplify the geometry a spherical iceberg has been used for the analyses. Collision with other iceberg shapes could be checked. DNV recommends both spherical, cube and cone shaped.



The MATLAB code for the external mechanics is provided by Liu and rewritten the simpler analyses done in this thesis. Some uncertainties are related to the code and if for further work a simpler code could be made.



References

- [1] DNV Technical Report 2006-0672. *Ice Collision Scenario*. 2006
- [2] M.D. Tusiani and G. Shearer. *LNG – A nontechnical guide*. 2007
- [3] STATOIL ASA.
<http://www.statoil.com/no/TechnologyInnovation/gas/LiquefiedNaturalGasLNG/Pages/AboutLiquefiedNaturalGas.aspx>
- [4] Gaztransport & Technigaz. *No96 membrane system for LNG integrated tanks*.
- [5] Gaztransport & Technigaz. *Mark III system for LNG integrated tanks*.
- [6] NORSOK standards, N-004
- [7] Zhenhui Liu, Jørgen Amdahl and Sveinung Løseth. *Plasticity based material modelling of ice and its application to ship-iceberg*. Not yet accepted, 2010.
- [8] Martin Storheim. *Analysis of structural Damage of Tankers subjected to Collision*. Master thesis, NTNU, 2008.
- [9] Kjell Magne Mathisen, Lecture notes – *Solution of the Dynamic Equilibrium Equations by Explicit Direct Integration*
- [10] R.D.Cook, D.S.Malkus, M.E.Plesha, R.J.Witt. *Concepts and application of finite element analysis*. 2002
- [11] J.O. Hallquist. *LS-DYNA Theory Manual*. 2006
- [12] Hoonkyu Oh, Whasao Kim and J. Lee. *Safety of Membrane Type Cargo Containment System in LNG Carrier under Accidental Iceberg Collision*.
- [13] S. Han, J.Y. Lee, Y.I. Park, and J. Che. *Structural risk analysis of an NO96 membrane-type liquefied natural gas carrier in Baltic ice operation*. 2008
- [14] S.G. Lee, J.S. Lee, Y.H.Baek, J.K. Paik and B.J. Kim. *Structural Safety Assessment in Membrane-type CCS in LNGC under Iceberg Collision*.



[15] MCS Patran description.

<http://www.mscsoftware.com/Products/CAE-Tools/Patran.aspx>

[16] Livermore Software Technology Corporation(LSTC). *LS-DYNA –Keyword user’s manual*. 2007

[17] P.T.Pedersen and S.Zhang, *On impact mechanics in ship collision*. 1998

[18]W.J. Stronge. *Impact mechanics*. 2000

[19] Håvard Nyseth,DNV - personal correspondence. LNG carrier scantling from Nauticus.



List of Appendix

A.	ICEBERG SHAPES.....	II
B.	INTERFACE PRESSURE.....	IV
B.1	INTERFACE PRESSURE, ICEBERG 1	IV
B.2	INTERFACE PRESSURE, ICEBERG 2	IV
C.	COLLISION OF SHIP SIDE	V
D.	NODE ACCELERATION, VELOCITY AND DISPLACEMENT	VI
D.1	SMALL ICEBERG COLLISION.....	VI
D.1.1	<i>Outer hull node</i>	VI
D.1.2	<i>Inner hull node</i>	VII
D.1.3	<i>Side node</i>	VIII
D.2	BIG ICEBERG COLLISION	IX
D.2.1	<i>Outer hull node</i>	IX
D.2.2	<i>Inner hull node</i>	X
D.2.3	<i>Side node</i>	XI
E.	INTERNAL ENERGY PLOT FROM LS-DYNA	XII
E.1	SMAL ICEBERG COLLISION.....	XII
E.1.1	<i>Collision point 1</i>	XII
E.1.2	<i>Collision point 2</i>	XII
E.1.3	<i>Collision point 3</i>	XII
E.1.4	<i>Collision point 4</i>	XIII
E.1.5	<i>Collision point 5</i>	XIII
E.1.6	<i>Collision point 6</i>	XIII
E.2	BIGGEST ICEBERG COLLISIONS	XIV
E.2.1	<i>Collision point 1</i>	XIV
E.2.2	<i>Collision point 2</i>	XIV
E.2.3	<i>Collision point 3</i>	XIV
E.2.4	<i>Collision point 5</i>	XV
E.2.5	<i>Collision point 6</i>	XV
E.2.6	<i>Collision point 7</i>	XV
F.	MATLAB CODE.....	XVI
G.	MEMORY STICK	XIX



A. Iceberg shapes

TUBULAR:

A tubular iceberg has the shape of a table. Steep sides and a flat top. The length-to-height ratio is greater than 1:5.



NON-TUBULAR:

The non-tubular iceberg is an iceberg with an eroded surface. This makes it non-regular. Iceberg which cannot be put in a different category will be referred to as non-tubular iceberg.






BLOCK:

An ice block is a flat-topped iceberg with very steep hills.



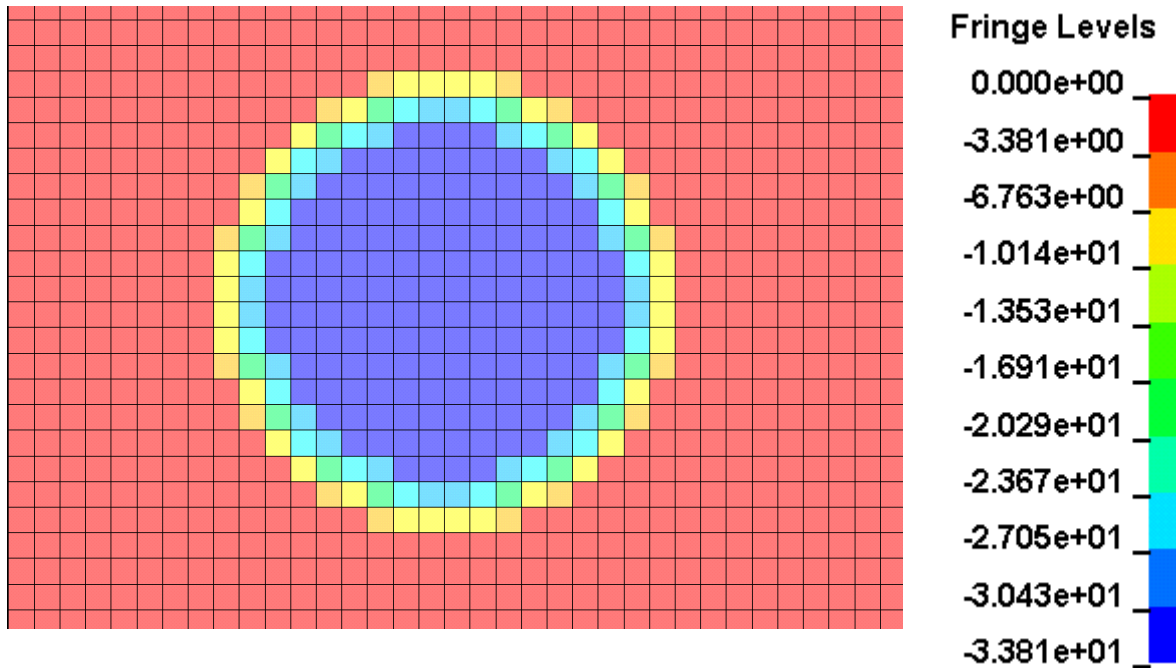


<p>DOME: A dome has a smooth and rounded top on the middle of the iceberg.</p>	
<p>PINNACLE: A pinnacle iceberg has one or more spires. It can also be formed as a very steep pyramid.</p>	
<p>WEDGE: An ice wedge has one side that will slope down into the waterline. The other side will be steep.</p>	

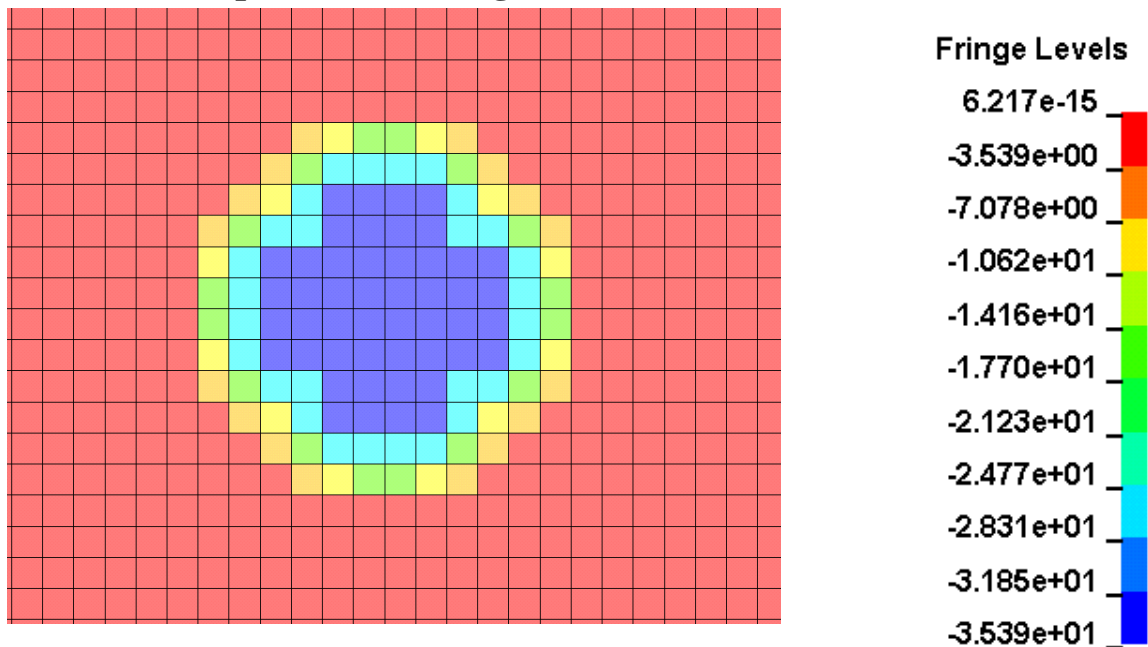


B. Interface pressure

B.1 Interface pressure, Iceberg 1



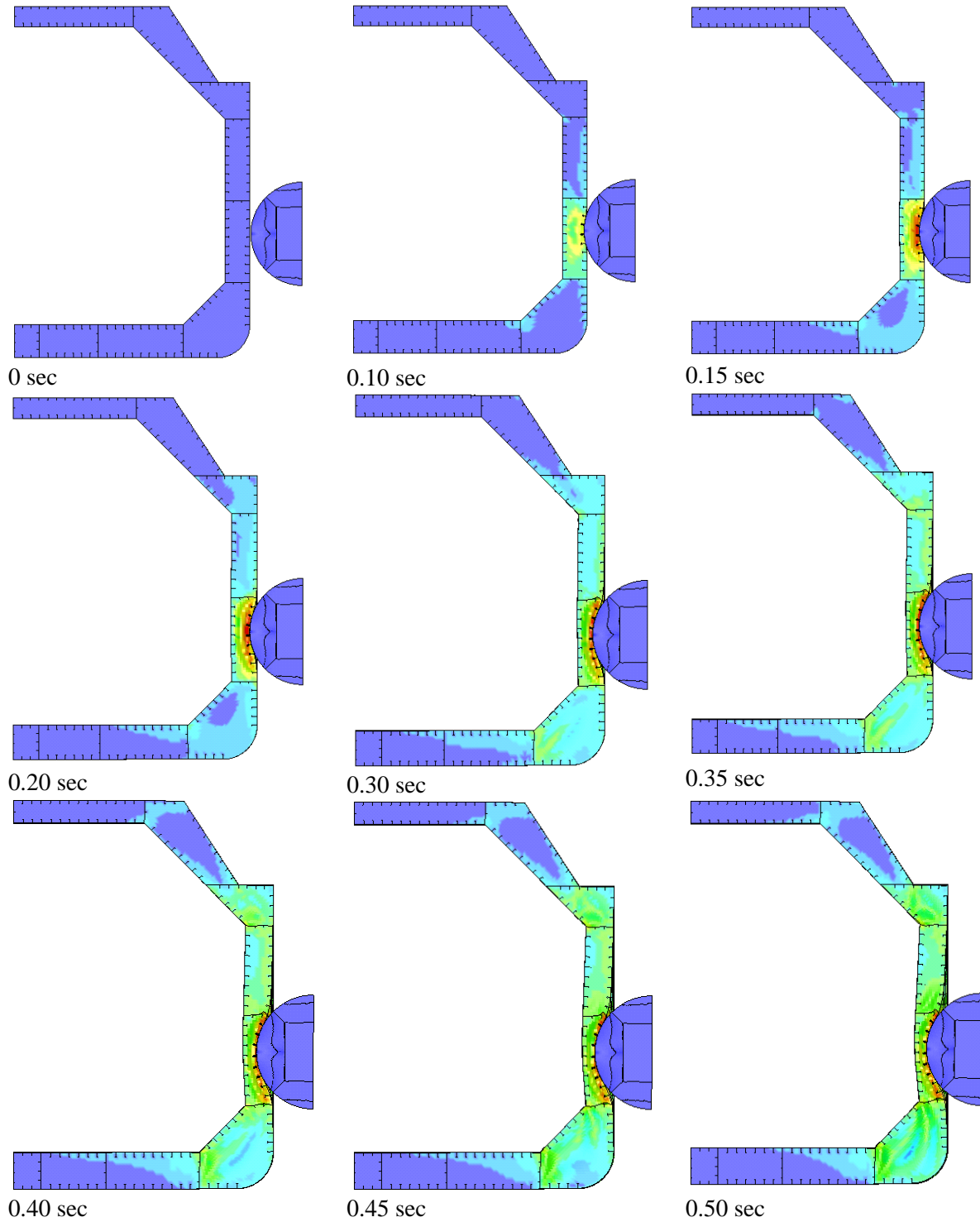
B.2 Interface pressure, Iceberg 2





C. Collision of ship side

The von mises stress distribution in the ship hull cross section during the impact. Collision scenario 2; colliding in the water line at 12 m, iceberg radius 5 m.

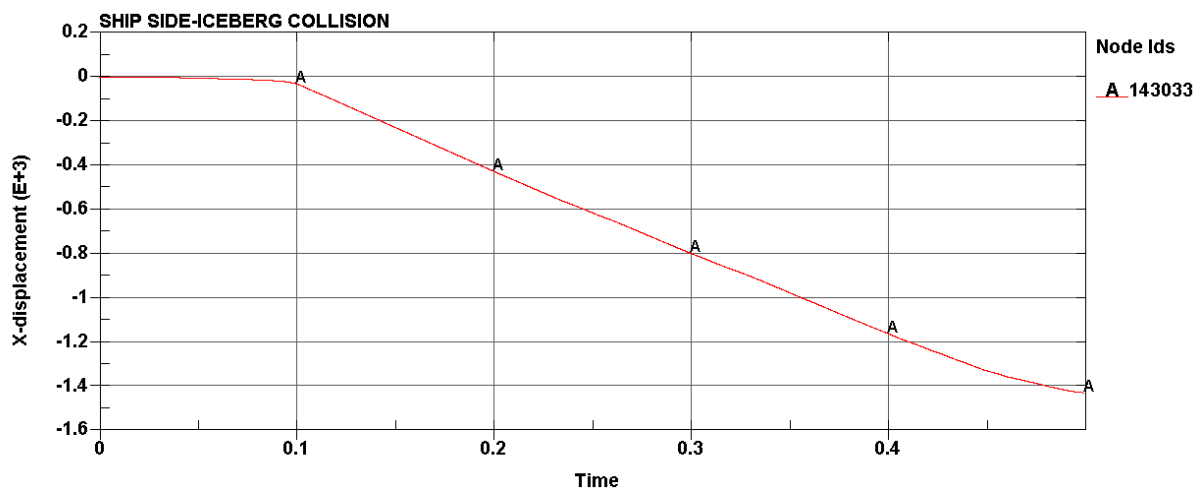
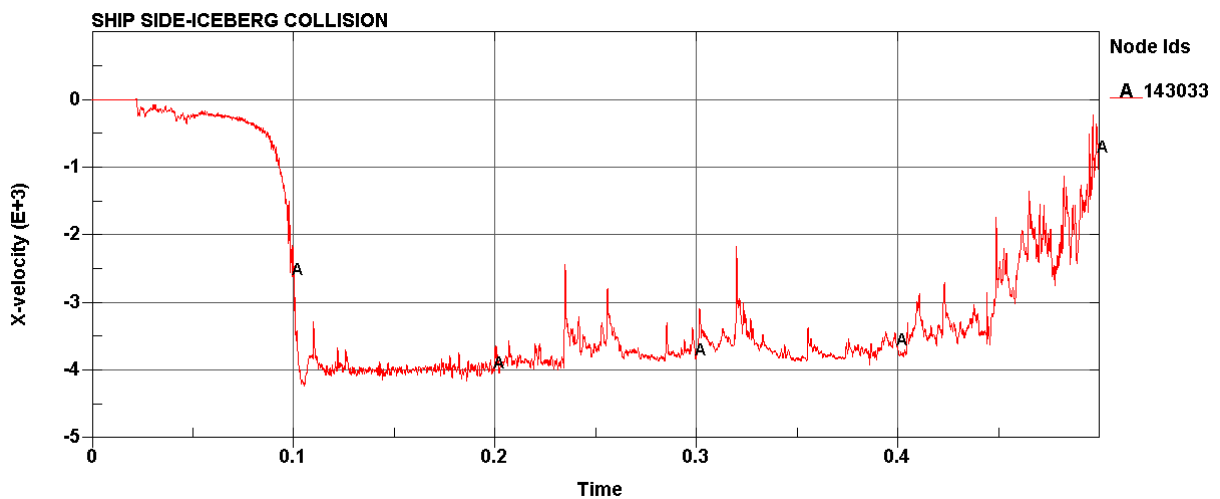
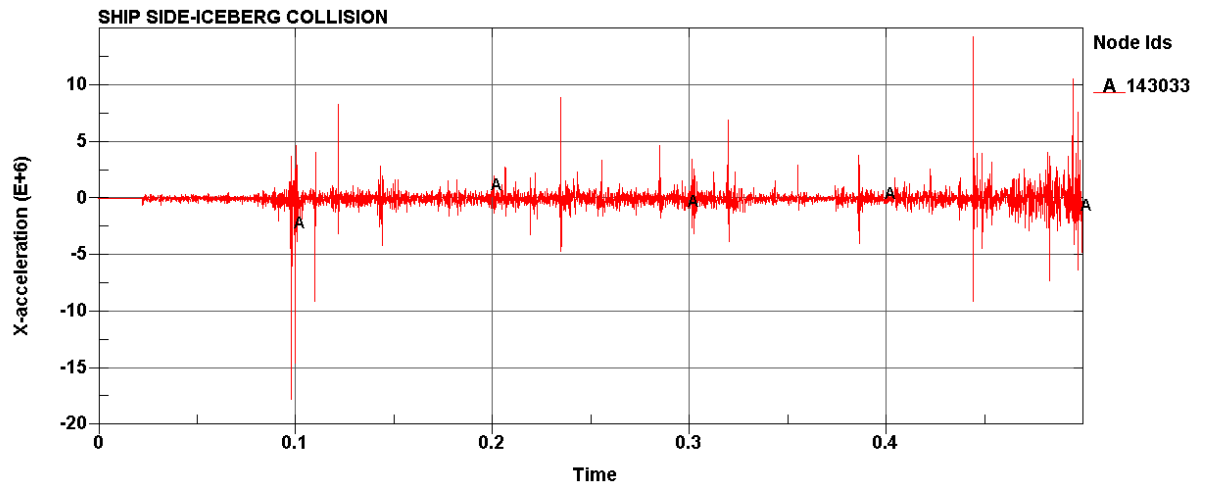




D. Node acceleration, velocity and displacement

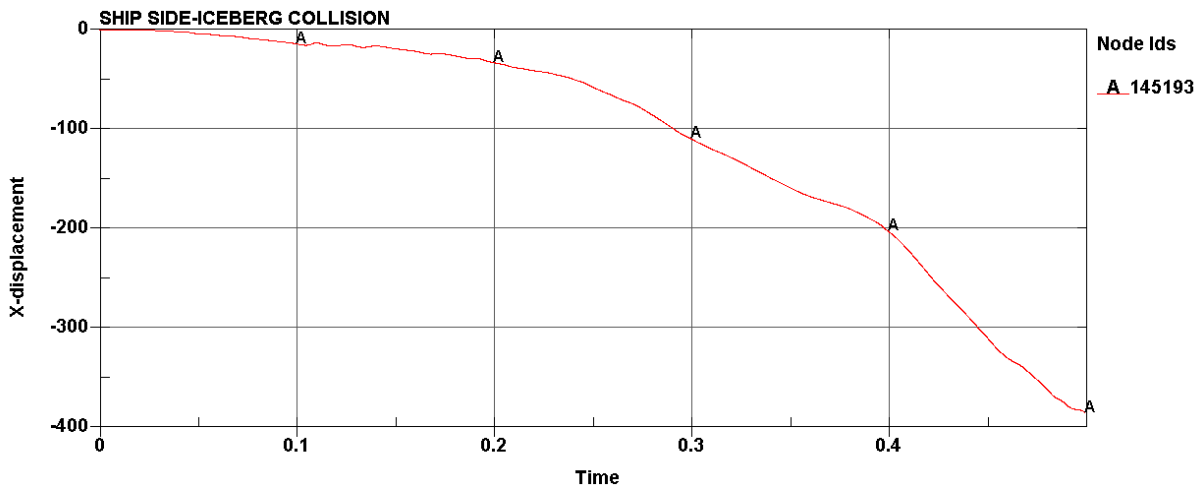
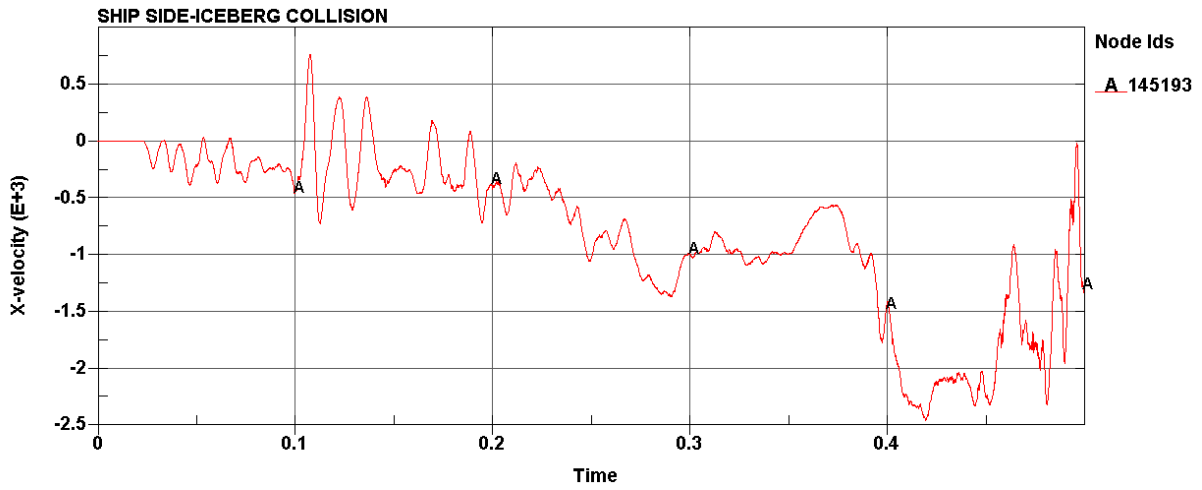
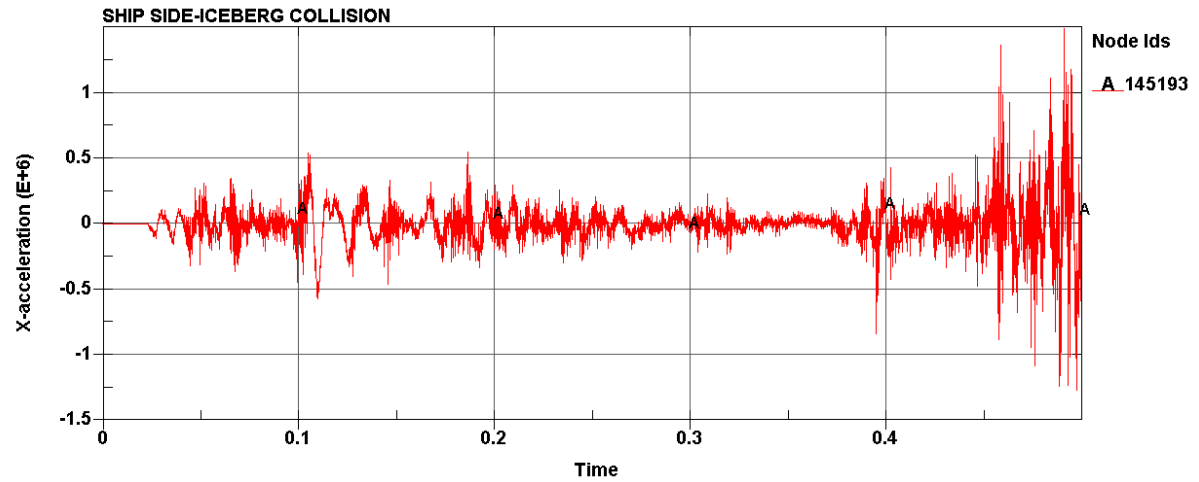
D.1 Small iceberg collision

D.1.1 Outer hull node



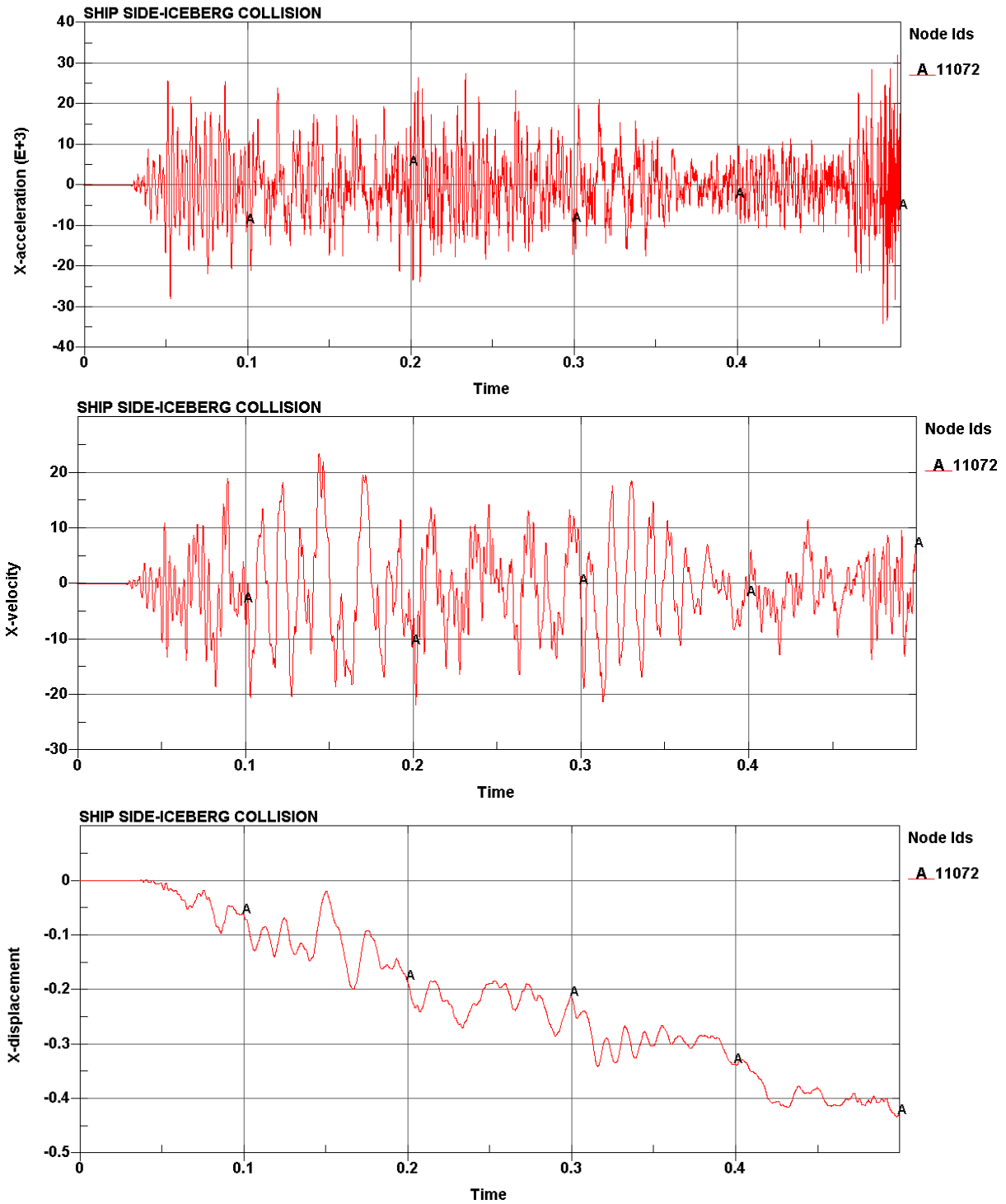


D.1.2 Inner hull node





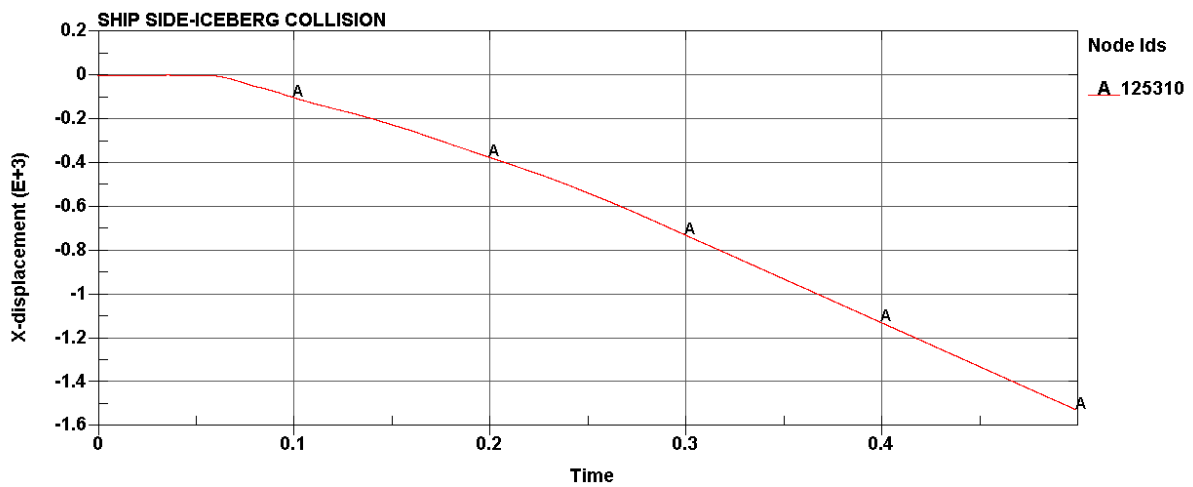
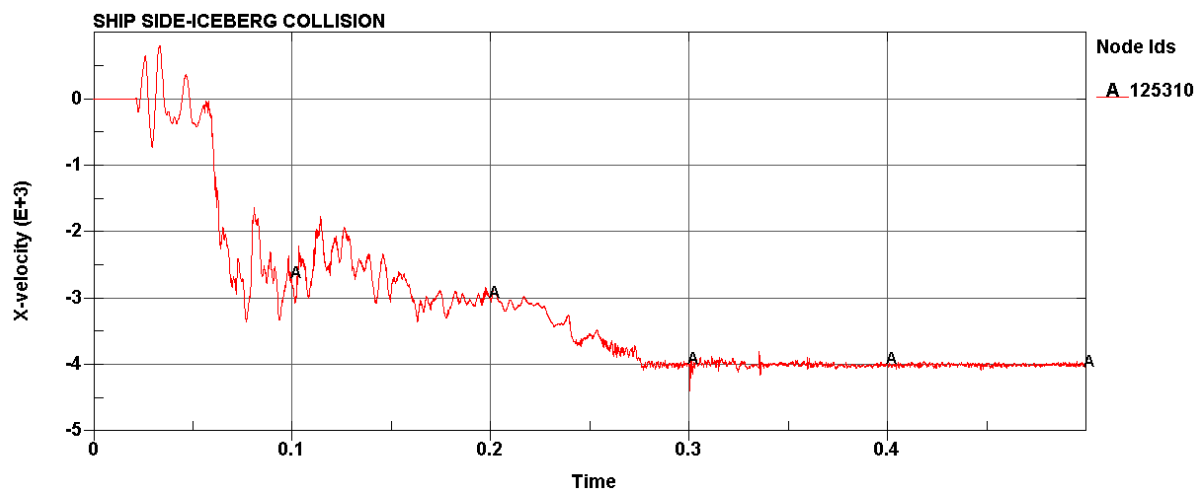
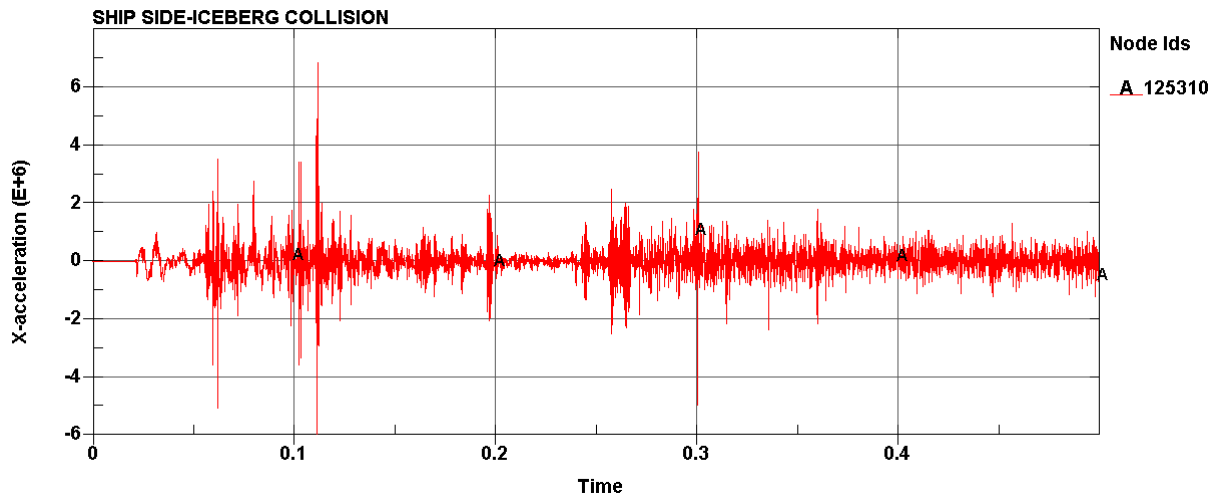
D.1.3 Side node





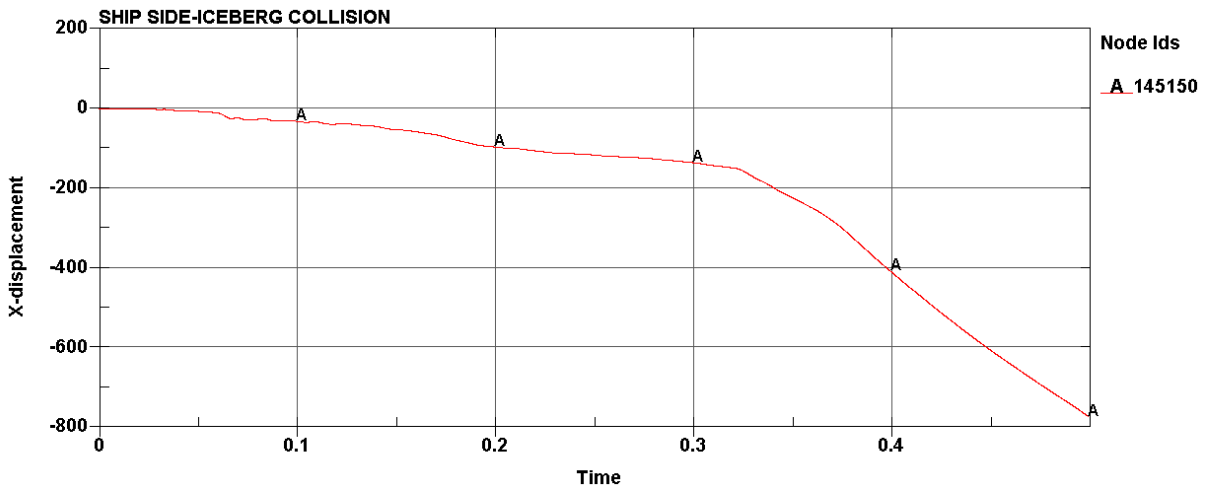
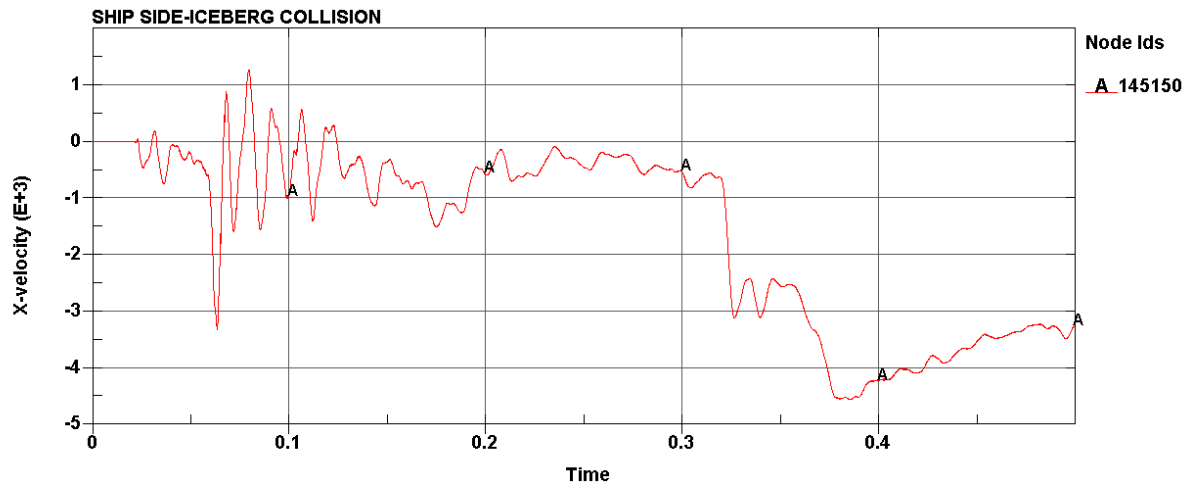
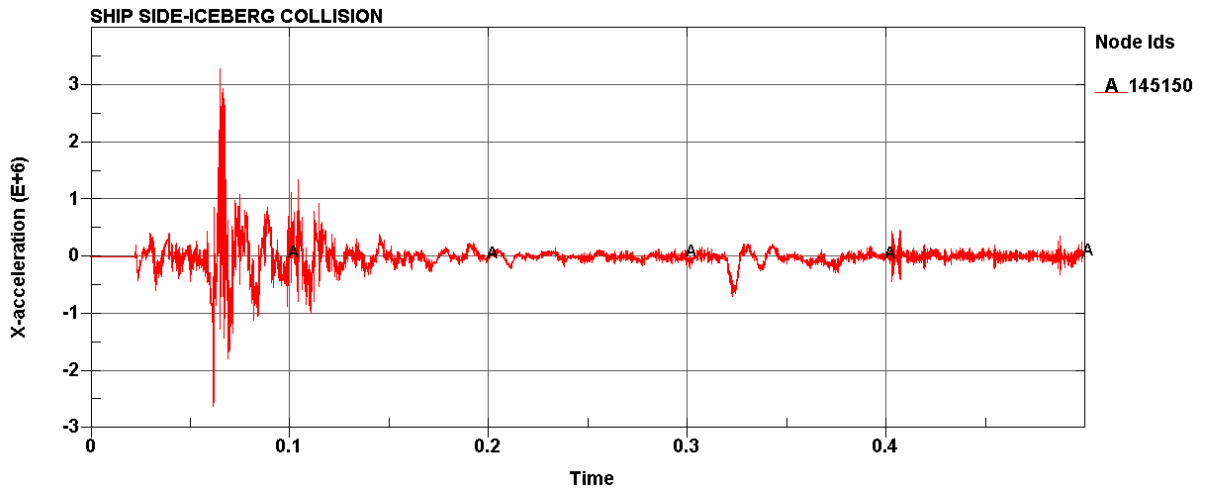
D.2 Big iceberg collision

D.2.1 Outer hull node



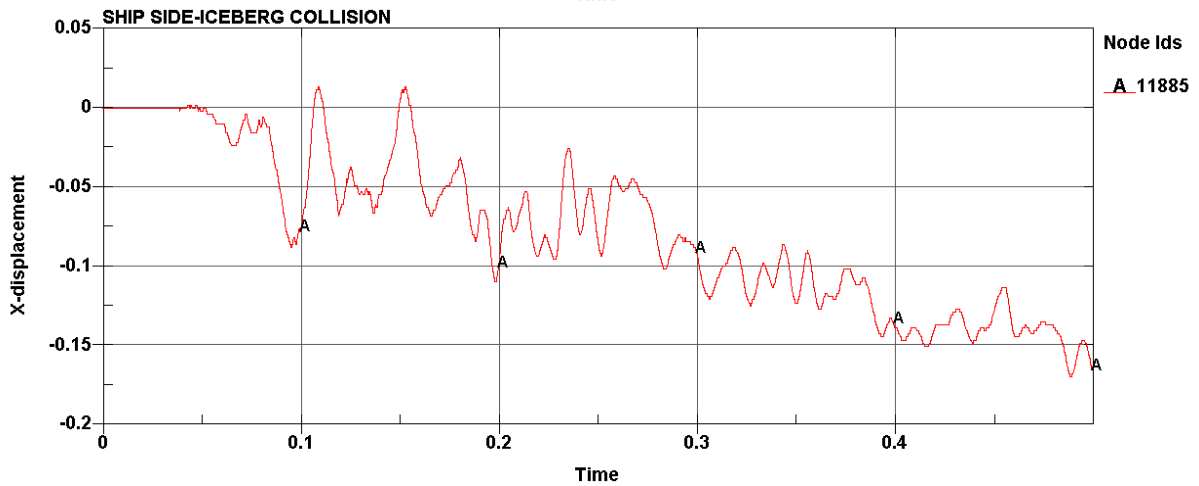
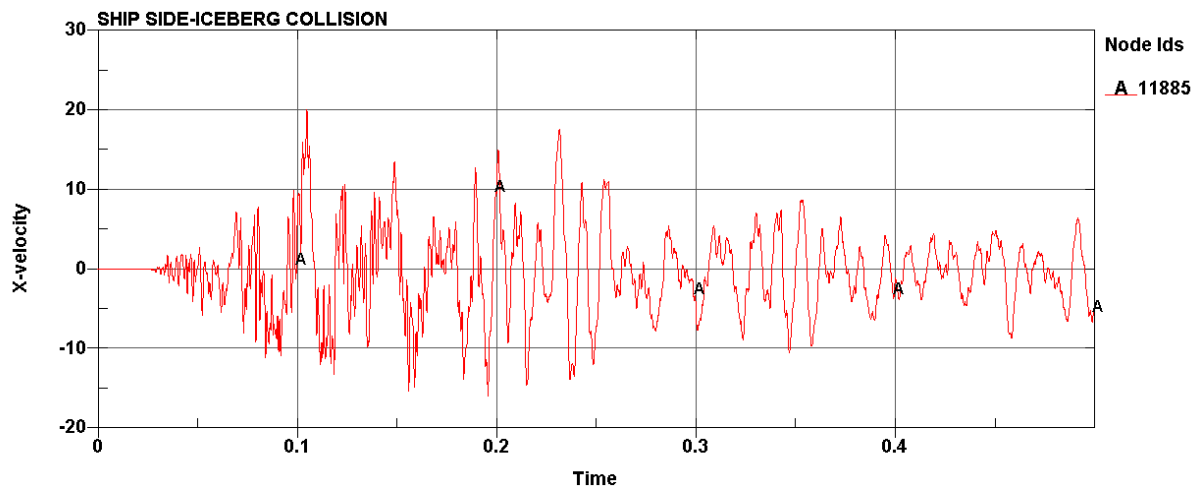
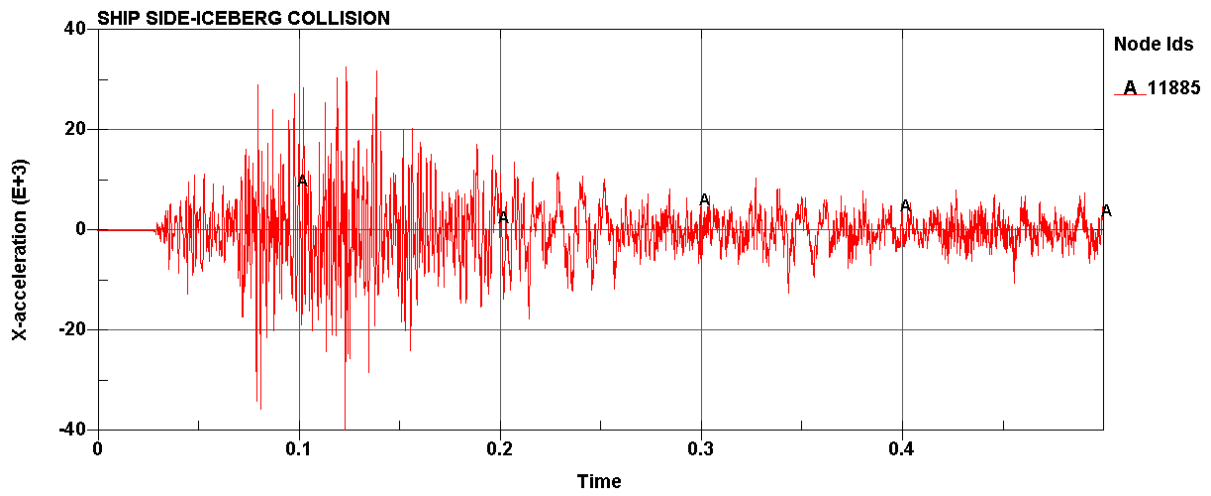


D.2.2 Inner hull node





D.2.3 Side node

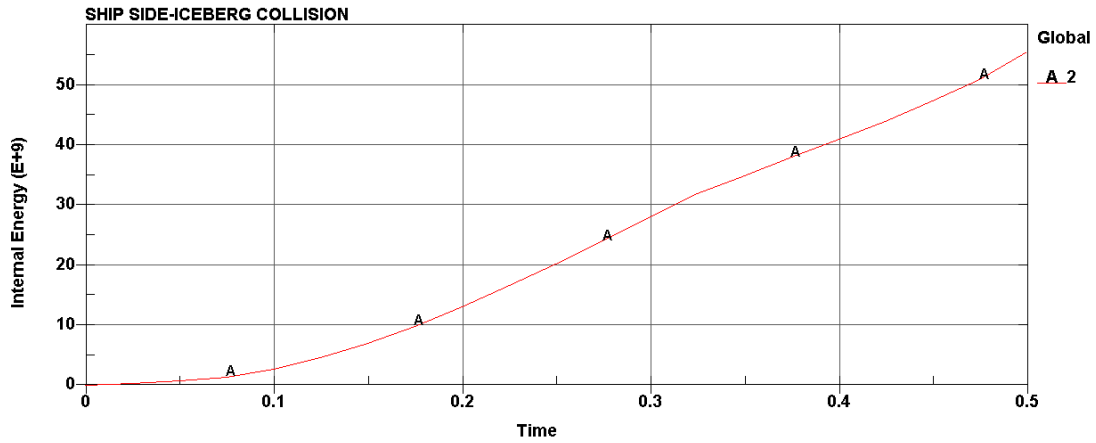




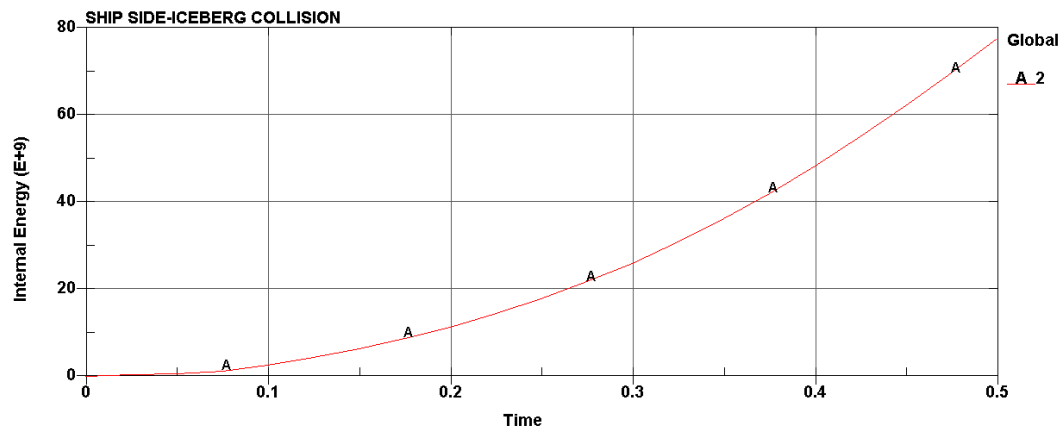
E. Internal energy plot from LS-DYNA

E.1 Smal iceberg collision

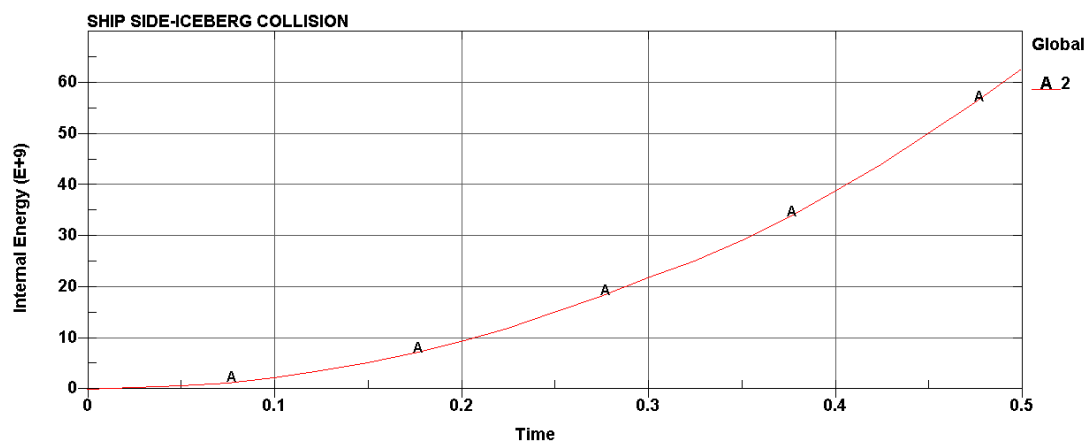
E.1.1 Collision point 1



E.1.2 Collision point 2

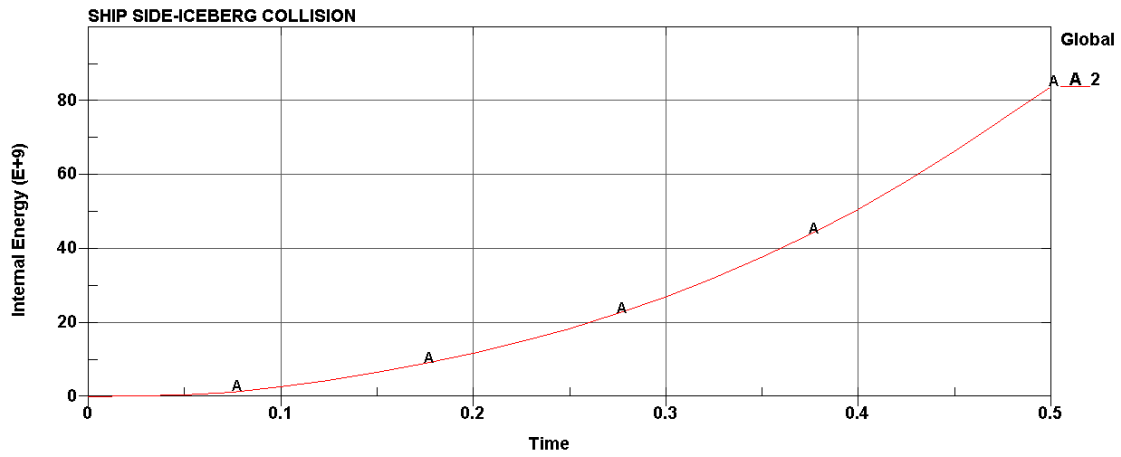


E.1.3 Collision point 3

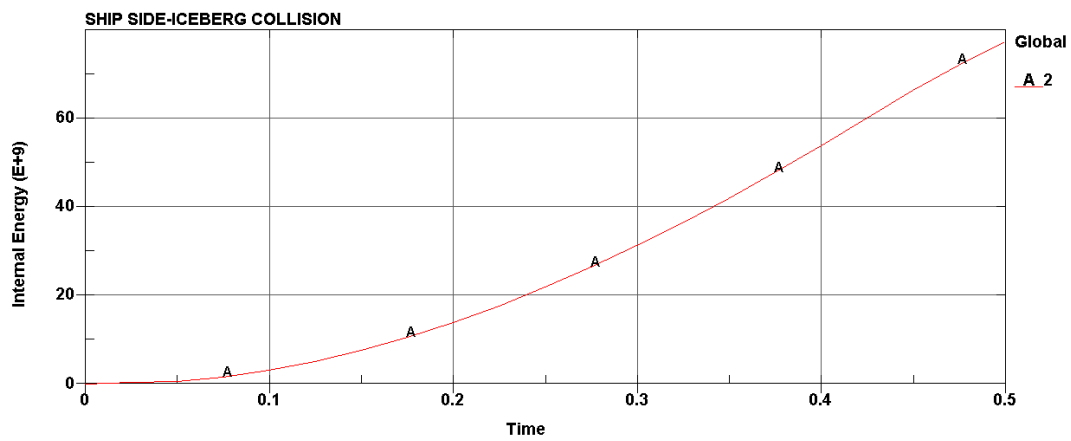




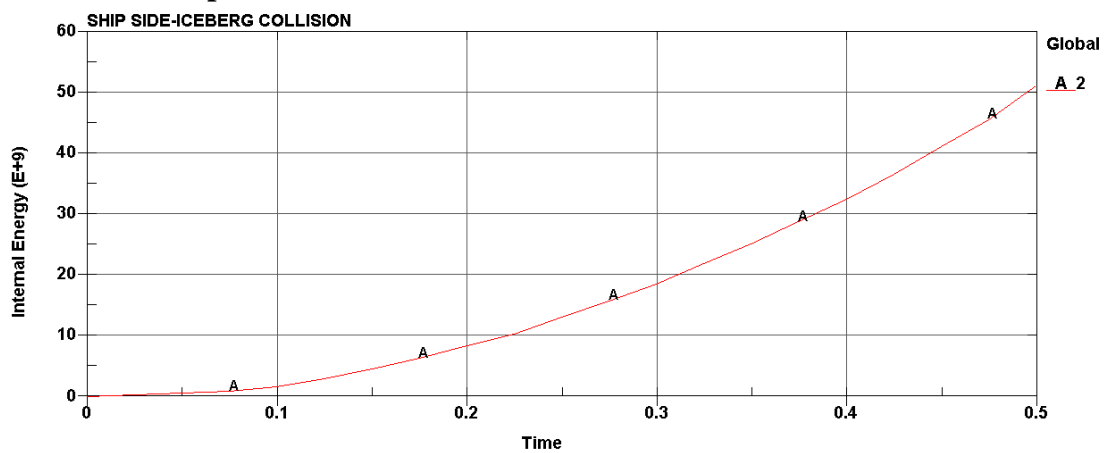
E.1.4 Collision point 4



E.1.5 Collision point 5



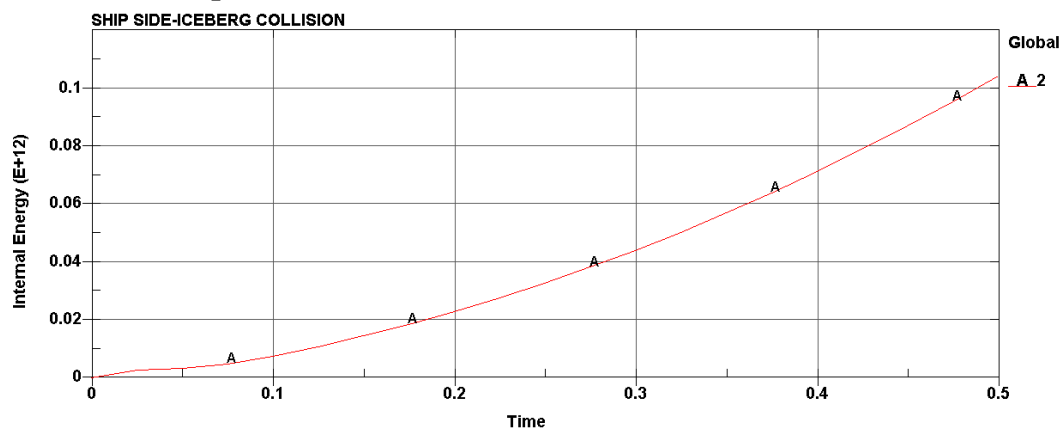
E.1.6 Collision point 6



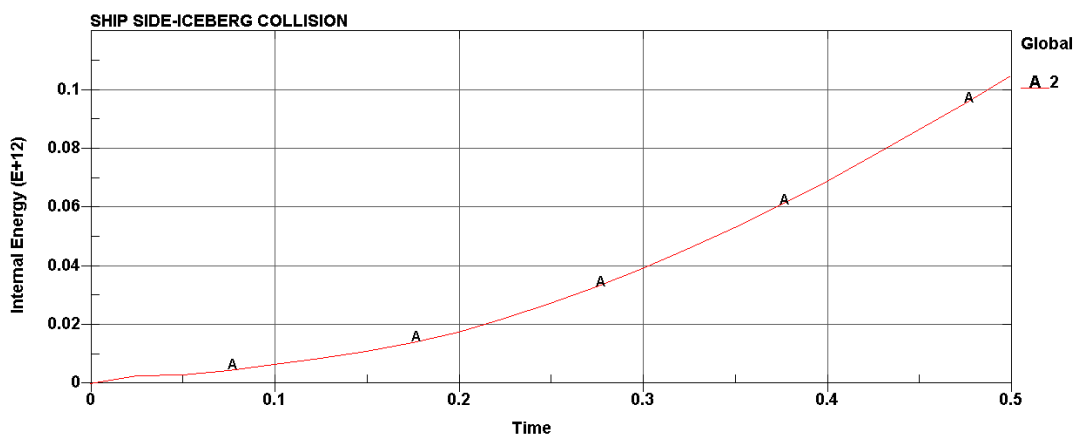


E.2 Biggest iceberg collisions

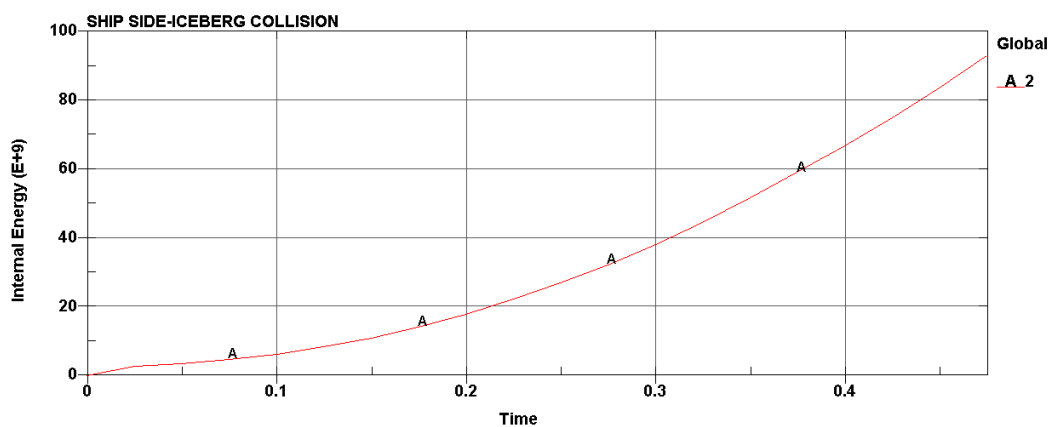
E.2.1 Collision point 1



E.2.2 Collision point 2

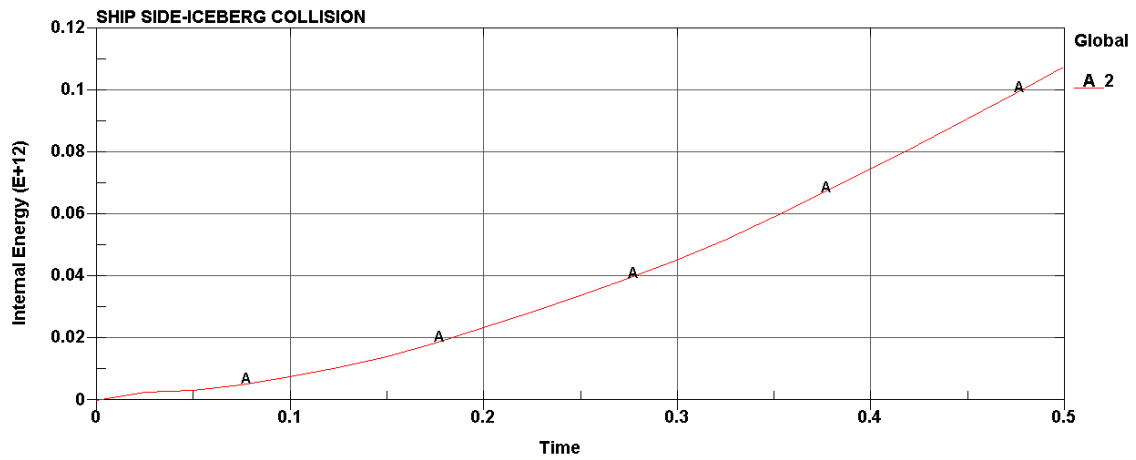


E.2.3 Collision point 3

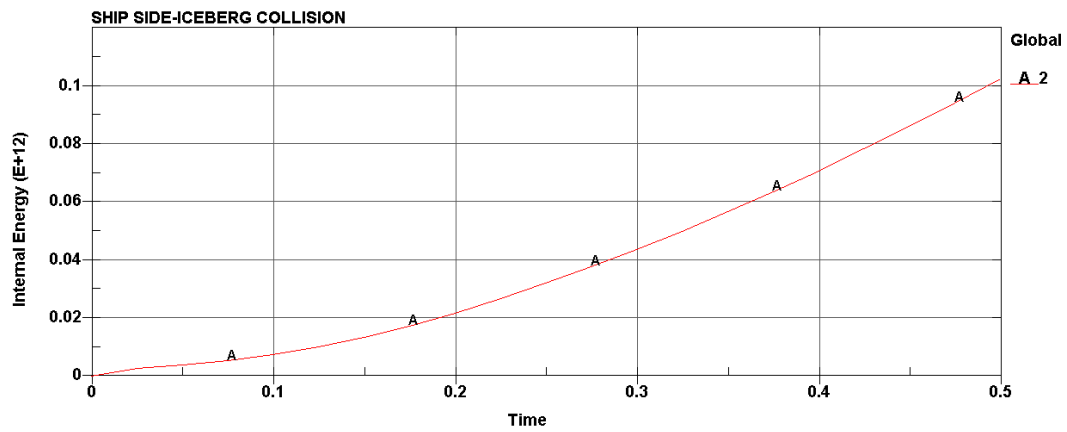




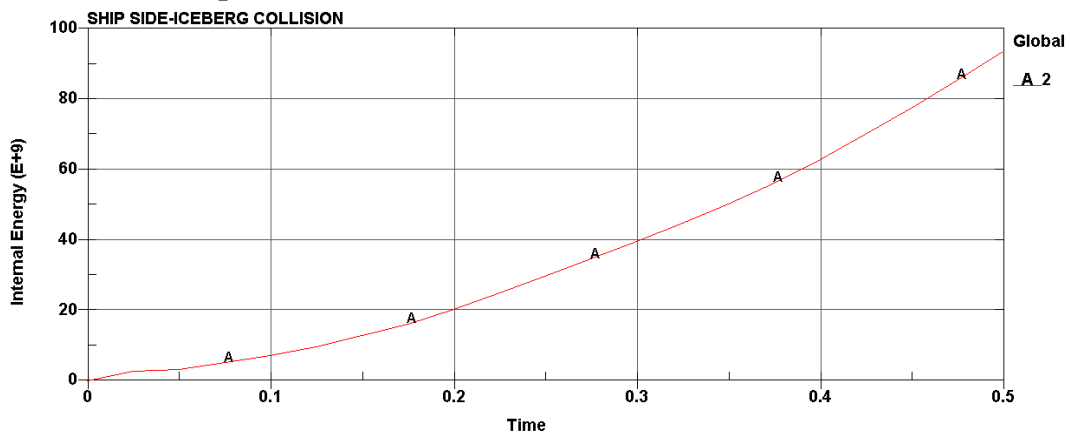
E.2.4 Collision point 5



E.2.5 Collision point 6



E.2.6 Collision point 7





F. MATLAB code

```

%% The 3D collision mechanics based on Stronge's theory
Ha=26.5;      %Ship data
La=279;
Ba=45.8;
Ta=12.00;
R=10;        %Iceberg data
h1=R/2;
dw=1025;
di=900;
Cwp=0.75;    % Coefficients
Cm=0.75;
Cb=0.75;
Mass1=157171860;
Mass2=4/3*pi*R*R*R*di;
Amx=0.05;    %Added mass, ship
Amy=2*Ta/Ba;
Amz=2/3*Ba*Cwp^2/(Ta*Cb*(1+Cwp));
Amrol=0.25;
Ampit=Ba/(Ta*(3-2*Cwp)*(3-Cwp));
Amyaw=0.21;
Bmx=0.5;     %Added mass, sphere
Bmy=0.5;
Bmz=0.5;
Bmrol=0.5;
Bmpit=0.5;
Bmyaw=0.5;
mass1=[1+Amx 0 0; 0 1+Amy 0; 0 0 1+Amz]*Mass1;    %Mass matrix included added
mass    mass
mass2=[1+Bmx 0 0; 0 1+Bmy 0; 0 0 1+Bmz]*Mass2;
rxa=(Cwp*Ba^2/(11.4*Cm)+Ha^2/12);    %Gyration radius, ship
rya=0.07*Cwp*La^2;
rza=La^2/16;
rxb=2/5*R*R;    %Gyration radius, sphere
ryb=2/5*R*R;
rzb=2/5*R*R;
%Inertia
Itrx1=[(1+Amrol)*rxa 0 0; 0 (1+Ampit)*rya 0; 0 0 (1+Amyaw)*rza]*Mass1;
Itrx2=[(1+Bmrol)*rxb 0 0; 0 (1+Bmpit)*ryb 0; 0 0 (1+Bmyaw)*rzb]*Mass2;
% gravity center of ship and iceberg under global system
shipg=[0 0 0]';
alpha=0.1; %angle between two ship's frame
gama=alpha; % water line angle
betap=0.1;
d=R;
cpg=[50.4 22.9 2]';
iceb=[0 -d 0]';
% velocity of ship and iceberg under global system
shipvg=[0 3 0]';
icevb=[0 -2 0]';
%The following codes are not checked, but assumed to give efficient answer
% calculate the relative displacement under global system
rad1g=cpg-shipg;
rad2b=iceb;
% transformation matrix between local and global system
l=sin(alpha)*cos(betap);
m=cos(alpha)*cos(betap);
n=-sin(betap);
Mab=[cos(gama) sin(gama) 0;
     -sin(gama) cos(gama) 0;

```



```
0 0 1];
Mlg=[cos(alpha) -sin(alpha) 0;
     -sin(alpha)*sin(betap) -cos(alpha)*sin(betap) -cos(betap);
     1 m n];
Mtr2=Mlg*Mab;
% calculate the rotated inertia matrix
Rtrx1=inv(Mlg*Itrx1*inv(Mlg));
Rtrx2=inv(Mtr2*Itrx2*inv(Mtr2));
mass1f=inv(Mlg*mass1*inv(Mlg));
mass2f=inv(Mtr2*mass2*inv(Mtr2));
% calculate the radius regarding to the inertia
rad1=Mlg*rad1g;
rad2=Mtr2*rad2b;
% calculate the relative velocity under local system
rvl=Mlg*shipvg-Mtr2*icevb;
% Input the reversed mass matrix
m11=(mass1f(1,1)+rad1(2)^2*Rtrx1(3,3)-
2*rad1(2)*rad1(3)*Rtrx1(2,3)+rad1(3)^2*Rtrx1(2,2))+...
(mass2f(1,1)+rad2(2)^2*Rtrx2(3,3)-
2*rad2(2)*rad2(3)*Rtrx2(2,3)+rad2(3)^2*Rtrx2(2,2));
m12=(mass1f(1,2)+mass2f(1,2))+(rad1(1)*rad1(3)*Rtrx1(2,3)-rad1(3)^2*Rtrx1(2,1)-
...
rad1(1)*rad1(2)*Rtrx1(3,3)+rad1(2)*rad1(3)*Rtrx1(3,1))+...
(rad2(1)*rad2(3)*Rtrx2(2,3)-rad2(3)^2*Rtrx2(2,1)-
rad2(1)*rad2(2)*Rtrx2(3,3)+rad2(2)*rad2(3)*Rtrx2(3,1));
m13=(mass1f(1,3)+mass2f(1,3))+(rad1(1)*rad1(2)*Rtrx1(3,2)-...
rad1(2)^2*Rtrx1(3,1)-
rad1(1)*rad1(3)*Rtrx1(2,2)+rad1(2)*rad1(3)*Rtrx1(2,1))+...
(rad2(1)*rad2(2)*Rtrx2(3,2)-rad2(2)^2*Rtrx2(3,1)-
rad2(1)*rad2(3)*Rtrx2(2,2)+rad2(2)*rad2(3)*Rtrx2(2,1));
m22=(mass1f(2,2)+rad1(1)^2*Rtrx1(3,3)-
2*rad1(1)*rad1(3)*Rtrx1(1,3)+rad1(3)^2*Rtrx1(1,1))+...
(mass2f(2,2)+rad2(1)^2*Rtrx2(3,3)-
2*rad2(1)*rad2(3)*Rtrx2(1,3)+rad2(3)^2*Rtrx2(1,1));
m23=(mass1f(2,3)+mass2f(2,3))+(rad1(3)*rad1(1)*Rtrx1(1,2)-
rad1(3)*rad1(2)*Rtrx1(1,1)-...
rad1(1)^2*Rtrx1(3,2)+rad1(1)*rad1(2)*Rtrx1(3,1))+...
(rad2(3)*rad2(1)*Rtrx2(1,2)-rad2(3)*rad2(2)*Rtrx2(1,1)-
rad2(1)^2*Rtrx2(3,2)+rad2(1)*rad2(2)*Rtrx2(3,1));
m33=(mass1f(3,3)+rad1(1)^2*Rtrx1(2,2)-
2*rad1(1)*rad1(2)*Rtrx1(1,2)+rad1(2)^2*Rtrx1(1,1))+...
(mass2f(3,3)+rad2(1)^2*Rtrx2(2,2)-
2*rad2(1)*rad2(2)*Rtrx2(1,2)+rad2(2)^2*Rtrx2(1,1));
m21=m12;
m31=m13;
m32=m23;
m=[m11,m12,m13;m12,m22,m23;m13,m23,m33];
syms dv1 dv2 dv3 dp1 dp2 dp3
rm=inv(m);
% Introducing the friction
% Dry friction colliding bodies can be representd by the Amontons-Coulomb
% law of sliding friction (Johnson, 1985).
% calculate the extreme case for stick together get the critical value miu
e=0; % restitution factor
dv1=-rvl(1);
dv2=-rvl(2);
dv3=-rvl(3)*(1+e);
dp1=subs(rm(1,1)*dv1+rm(1,2)*dv2+rm(1,3)*dv3,{dv1,dv2,dv3},{-rvl(1),-rvl(2),-
rvl(3)*(1+e)});
dp2=subs(rm(2,1)*dv1+rm(2,2)*dv2+rm(2,3)*dv3,{dv1,dv2,dv3},{-rvl(1),-rvl(2),-
rvl(3)*(1+e)});
```



```

dp3=subs(rm(3,1)*dv1+rm(3,2)*dv2+rm(3,3)*dv3,{dv1,dv2,dv3},{-rvl(1),-rvl(2),-
rvl(3)*(1+e)});
miu=sign(dp1)*sqrt(dp1^2+dp2^2)/dp3;
miu2=dp2/dp1;%n2/n1
miu0=0.15; %the input real friction
% friction matrix
flag1=1;
sm1=m11+m12*miu2+m13*sqrt(1+miu2*miu2)/miu;
sm2=m21/miu2+m22+m23*sqrt(1+miu2*miu2)/miu/miu2;
sm3=m31*miu/sqrt(1+miu2*miu2)+m32*miu*miu2/sqrt(1+miu2*miu2)+m33;
if miu0==0
    flag1=2;
    dv3=-rvl(3)*(1+e);
    dp3=dv3/m33;
    dv1=m13*dp3;
    dv2=m23*dp3;
    sm1=Inf;
    sm2=Inf;
    sm3=m33;
    dp1=0;
    dp2=0;
else
    if abs(miu)>=miu0 % sliding case
        dv3=-rvl(3)*(1+e);
        fai=atan(miu2);
        if dp2==0
            fai=0/180*pi;
        end
        flag1=2;
        sm1=m11+m12*miu2+m13*sqrt(1+miu2*miu2)/miu0;
        sm2=m21/miu2+m22+m23*sqrt(1+miu2*miu2)/miu0/miu2;
        sm3=m31*miu0/sqrt(1+miu2*miu2)+m32*miu0*miu2/sqrt(1+miu2*miu2)+m33;
        AA=[miu0*cos(fai)*1e06 -rm(1,1) -rm(1,2);
            miu0*sin(fai)*1e06 -rm(2,1) -rm(2,2);
            1e06 -rm(3,1) -rm(3,2)];
        BB=[rm(1,3)*dv3 rm(2,3)*dv3 rm(3,3)*dv3]';
        CC=AA\BB;
        dp3=CC(1,1)*1e06;
        dv1=CC(2,1);
        dv2=CC(3,1);
        dp1=miu0*cos(fai)*dp3;
        dp2=miu0*sin(fai)*dp3;
    end
end
dpp=sqrt(dp1^2+dp2^2+dp3^2);
E1=abs(1/sm1/2*dv1*(dv1+2*rvl(1)));
E2=abs(1/sm2/2*dv2*(dv2+2*rvl(2)));
if miu2==0
    E2=0;
end
E3=abs(1/sm3/2*dv3*(dv3+2*rvl(3)));
dvv=[dv1;dv2;dv3];
tt=E1+E3+E2;
disp('Total external energy:')
disp(tt)

```




G. Memory stick

- Patran files
 - I. 2D-frame
 - II. 3D tank part (3360mm)
 - III. 3D tank part (3360mm), Included mesh 250 mm
 - IV. Finished model
- LS-DYNA key files
 - I. Collision files
 - i. CollisionPoint1_5m
 - ii. CollisionPoint2_5m
 - iii. CollisionPoint3_5m
 - iv. CollisionPoint4_5m
 - v. CollisionPoint5_5m
 - vi. CollisionPoint6_5m
 - vii. CollisionPoint1_10m
 - viii. CollisionPoint2_10m
 - ix. CollisionPoint3_10m
 - x. CollisionPoint5_10m
 - xi. CollisionPoint6_10m
 - xii. CollisionPoint7_10m
 - II. Iceberg models
 - i. iceber-solid-5m-50mm
 - ii. iceber-solid-10m-100mm
 - III. Pressure-area files
 - i. Iceberg_wall_big
 - ii. Iceberg_wall_small
- Various videos from LS-Prepost
- MATLAB code for collision mechanics